Electronic Theses and Dissertations, 2004-2019

2015

Modeling Crowd Mobility and Communication in Wireless Networks

Gurkan Solmaz
University of Central Florida

University of
Central
Florida

STARS
Showcase of Text, Archives, Research & Scholarship

Modeling Crowd Mobility and Communication in Wireless Networks

by

Gürkan Solmaz
B.S. Computer Engineering, Middle East Technical University, 2010
M.S. Computer Science, University of Central Florida, 2013

A dissertation submitted in partial fulfillment of the requirements
for the degree of Doctor of Philosophy
in the Department of Computer Science
in the College of Engineering and Computer Science
at the University of Central Florida
Orlando, Florida

Fall Term
2015

Major Professor: Damla Turgut

ABSTRACT

This dissertation presents contributions to the fields of mobility modeling, wireless sensor networks (WSNs) with mobile sinks, and opportunistic communication in theme parks. The two main directions of our contributions are human mobility models and strategies for the mobile sink positioning and communication in wireless networks.

The first direction of the dissertation is related to human mobility modeling. Modeling the movement of human subjects is important to improve the performance of wireless networks with human participants and the validation of such networks through simulations. The movements in areas such as theme parks follow specific patterns that are not taken into consideration by the general purpose mobility models. We develop two types of mobility models of theme park visitors. The first model represents the typical movement of visitors as they are visiting various attractions and landmarks of the park. The second model represents the movement of the visitors as they aim to evacuate the park after a natural or man-made disaster.

The second direction focuses on the movement patterns of mobile sinks and their communication in responding to various events and incidents within the theme park. When an event occurs, the system needs to determine which mobile sink will respond to the event and its trajectory. The overall objective is to optimize the event coverage by minimizing

the time needed for the chosen mobile sink to reach the incident area. We extend this work by considering the positioning problem of mobile sinks and preservation of the connected topology. We propose a new variant of p-center problem for optimal placement and communication of the mobile sinks. We provide a solution to this problem through collaborative event coverage of the WSNs with mobile sinks. Finally, we develop a network model with opportunistic communication for tracking the evacuation of theme park visitors during disasters. This model involves people with smartphones that store and carry messages. The mobile sinks are responsible for communicating with the smartphones and reaching out to the regions of the emergent events.

ACKNOWLEDGMENTS

First and foremost, I would like to thank my advisor, Dr. Damla Turgut. Her support, encouragement, and guidance helped me a lot throughout my Ph.D. study. I would also like to thank Dr. Mostafa A. Bassiouni, Dr. Ratan K. Guha, and Dr. Brian Goldiez for serving as my committee members. I appreciate the guidance I received from Dr. Kemal Akkaya from Southern Illinois University and Dr. Ladislau Bölöni for our co-authored research papers.

A special thanks to my elder brother and only sibling Dr. Berkan Solmaz for suggesting me to start a Ph.D. in the first place and providing me the vision that helped me follow in his footsteps. I am always grateful to my parents for their endless support.

Lastly, I would like to thank my labmates Rouhollah Rahmatizadeh, Salih S. Bacanlı, Taranjeet S. Bhatia, Jun Xu, Dr. Mustafa İ. Akbaş, Saad A. Khan, Pooya Abolghasemi, Saad Arif, Sabari Nair, Edoardo Petrucci, Dr. Shameek Bhattacharjee, and Fahad A. Khan for their great friendship, collaboration, and support.

TABLE OF CONTENTS

LIST OF FIGURES

LIST OF TABLES

CHAPTER 1
INTRODUCTION

This dissertation presents contributions to the fields of mobility modeling [1], WSNs [2] with mobile sinks and opportunistic communication [3], focusing on their application in theme parks.

The first mobility model we present in this dissertation describes the movement of the visitors who visit the attractions of the theme park in an ordinary day. The model combines the non-deterministic movement decisions of the visitors with the deterministic service model of the attractions. We then model human mobility in the disaster scenarios based on the evacuation behavior of the people. In this case, we need to consider the physical obstacles and the social interactions of people which affect the pedestrian flows and the duration of the evacuation.

In the application we are considering, WSNs with mobile sinks are used to solve the event coverage problem in theme parks. The mobile sinks are implemented as electronic transportation vehicles which must reach the location where an event happened before the active time of the event passes. With a given number of mobile sinks, the positioning of the mobile sinks and the selection of a mobile sink to handle a given event affects the event coverage. We then extend this idea by considering the connectivity between the mobile sinks

during their operation. We propose a variant of the p-center problem, which we call the *communication-constrained p-center problem*, to model the distribution of the mobile sinks to the attractions.

We propose an opportunistic communication strategy for tracking the pedestrians during disasters. The network model involves human participants using smartphones to store and carry messages to the mobile sinks which track the pedestrians during their evacuation and reach emergent events when necessary.

The remainder of this chapter is organized as follows. We provide a brief introduction to mobility modeling in Section 1.1, WSNs with mobile sinks in Section 1.2, and opportunistic networks in Section 1.3. We motivate the development of the mobility models and networking approaches in Section 1.4. We present a summary of our contributions in this research domain in Section 1.5. Finally, we include the outline of the dissertation in Section 1.6.

1.1 Mobility modeling

Many sensor networks collect information about mobile targets. The ability to understand the way these targets move can help improve the sensing ability of the WSNs, and it also allows us to simulate the WSNs under realistic conditions. Although many mobility models have been proposed in the literature, most of them are generic models which do not take into account the specifics of the modeled environment. However, the humans move differently in

different environments with different goals. For a realistic model of the movement of theme park visitors we need a scenario-specific human mobility model.

Human mobility models can be classified as synthetic and trace-based models. The mobility traces of synthetic models are generated by simulations, while trace-based models are built upon real movement traces of people. Due to limited real movement data available, network simulations usually rely on synthetic models. However, a synthetic model should be tested against real mobility traces and other existing models for its validity.

1.2   Wireless Sensor Networks with Mobile Sinks

WSNs with mobile sinks can be employed for various applications such as border protection, environmental monitoring, crowd management, and animal control. They are composed of a large number of static sensor nodes and limited number of mobile sinks. The interconnection among the nodes is provided by the wireless medium. Sensor nodes are small devices with limited data processing capability, memory, transmission rate, and energy. These nodes collect information from their physical vicinities and transmit it to the mobile sinks. The transmission of data is usually done via hop-by-hop wireless communications. Mobile sinks are more capable devices in terms of communication, computation, and storage. However, mobile sinks are usually the expensive elements of the networks and they are deployed in limited numbers.

The advantages of WSNs with mobile sinks over the more traditional WSNs with a single static sink include a longer lifetime of networks and reduced data losses. Moreover, multiple mobile sinks can be used for sharing the workload and collaborative activities. However, the use of multiple sinks brings new research challenges such as mobile sink positioning, coverage, and communication among the mobile sinks. While the main goal of the mobile sinks is collecting data from sensor nodes, they can also share data and perform collaborative actions.

1.3   Opportunistic Networks

Opportunistic networks are considered as a type of wireless ad hoc networks. In these networks, data transfer occurs in a hop-by-hop manner among mobile devices during their encounters via Bluetooth or WiFi connections. The topology of these networks change frequently due to frequent addition or removal of the nodes. Moreover, data forwarding decisions during encounters have critical importance in the network performance. For instance, forwarding data in each encounter may cost the network excessive energy consumption, while limiting data transfers may prevent messages to arrive their destinations.

The opportunistic network model in this dissertation includes smartphones of the people which act as the sensor nodes of the networked system. These mobile devices store and carry messages to limited number of mobile sinks. The mobile sinks patrol among the people to collect data from the smartphones.

1.4 Motivation

Due to the increasing popularity of mobile devices, mobility modeling became an important part of networking research, as the performance of networks highly depend on the locations and movements of the human carriers of these devices. While there is a degree of non-determinism in the mobility behavior of people, it is shown that their movement decisions are also driven by their goals [4]. For instance, the daily mobility of a person who lives and works in a city may include traveling from home to the workplace in the early morning, spending hours in the office and returning home in the evening. An employee usually travels between his home and the workplace by car or public transportation. On the other hand, a student in a university campus usually walks from one classroom to another according to the scheduled classes. Thus, the mobility patterns depend on the people's aims and the nature of their environments. Theme parks have their own specific characteristics such that the movement patterns are dictated by the use of walking paths by pedestrians and dynamic changes due to movements of the visitors among attractions placed in the large but bounded areas. Therefore, scenario-specific modeling is important for the realistic representation of the theme park environment. An accurate model should take into consideration the physical environment as well as the aims of the theme park visitors. The proposed approaches and the performances of the network models in this dissertation are evaluated based on the mobility models of theme park visitors.

Networked systems are currently operational in the theme parks for various purposes including the entertainment of visitors. For instance, smart phones are used for online multiplayer games between the visitors. Moreover, opportunistic communication networks are also considered for communication in theme parks [5]. Handling emergent events is one of the major challenges in theme park environments due to inevitable problems that can occur due to hazards. Therefore, in addition to the technological security measures, theme park administrators also deploy a large number of security employees, for some parks more than a thousand, walking on foot or riding bicycles [6]. We believe that using automated networked systems and mobile sinks can decrease the sophistication in terms of communication and the large team of security personnel. Moreover, theme parks also face the risks of natural or man-made disasters. Although large theme parks have security infrastructures and large numbers of personnel, autonomous systems can provide the operators of theme parks independence from infrastructures which can be damaged in times of disasters.

While the use of wireless networks with mobile sinks offers many advantages, it also presents challenges such as adapting to dynamic changes in the environment, safety of the visitors, and the limited number of mobile sinks due to their cost. For the event coverage problem, we address the major challenges of positioning and collaboration of the mobile sinks.

1.5 Contributions

The work described in this dissertation concerns the realistic modeling of the theme park environment and the movement patterns of the visitors, and finding methods for the effective use of the mobile sinks in theme parks. Specifically, the major contributions of this dissertation are listed as follows:

- *Mobility model of theme park visitors.* We present a mobility model for typical (daily) movements of the theme park visitors [7,8]. Our model uses queuing theoretic models of the service behavior of attractions. We use fractal points and the least action principle for modeling macro mobility of the visitors. We validate our model with GPS traces collected from theme park visitors. We found that the proposed model provides a better statistical match compared to RWP and SLAW models.

- *Mobility in disaster scenarios.* We introduce a model of human mobility in theme parks for disaster scenarios [9–11] dealing with the evacuation of the visitors, physical obstacles, and social interactions. We use maps of real-world theme parks to model the physical paths and obstacles in the environment and the social force model for modeling the social interactions between visitors and the speed of the pedestrian flows. We compare the outcomes of the proposed model with several existing models as well as GPS traces and analyze the significant variations.

- *Event coverage in theme parks.* We consider a scenario where WSNs with multiple mobile sinks are used for event coverage [12, 13]. We divide the problem of event

coverage into two sub-problems: mobile sink positioning and the selection of the sink which handles a specific event. For mobile sink positioning, we propose weighted positioning according to the density of people in the attractions and adaptive sink positioning based on crowd densities of the attractions and the history of events. We select the mobile sink assigned to an event based on the shortest estimated travel time to that event. The travel times are computed by an algorithm which takes into account the length of the paths and the current density and movements of people along the roads.

- *Communication-constrained p-center problem.* For collaborative event handling, we propose a connected topology of the mobile sinks throughout the operation of the network [14]. For optimal positioning, we propose an approach building on the p-center problem. In this approach, multiple mobile sinks are positioned such that they minimize their maximum distance from the attractions, while preserving their pairwise communication links. We propose a new variant of the original p-center problem, which we call communication-constrained p-center problem and propose an exact algorithm for the p-center and p-median positioning approaches.

- *Visitor tracking with opportunistic communication.* We consider a scenario where smartphones and mobile sinks form an opportunistic as part of the disaster response during the times of disasters [15, 16]. In such situations, there may be unsafe regions in the disaster area due to the occurrence of hazards, as well as dense crowds in some roads which cause slow-downs or stuck in the pedestrian traffic. As an infrastructure-

independent alternative, the proposed networked system can replace or supplement the existing disaster response systems which might be damaged. We develop sink mobility and placement strategies for effective opportunistic communication and handling of the emergent events.

1.6   Outline

This dissertation is organized as follows.

Chapter 1 presents the problem definitions and an overview of the proposed approaches. Chapter 2 conducts a review of the literature related to human mobility analyses [17], mobility modeling, mobile elements (sinks) in wireless networks, and disaster management.

In Chapter 3, we propose a mobility model of theme park visitors. This chapter includes the detailed description of the five phases of modeling a theme park and the mobility behavior of the theme park visitors. The outcomes of the model is analyzed in detail and compared to the existing mobility models and the GPS traces of theme park visitors.

Chapter 4 describes the mobility model of theme park visitors for disaster scenarios. The use of theme park maps for modeling the roads, physical obstacles, and events are described in detail. The social interactions among the theme park visitors during evacuation times are explained and the simulation results of the model is analyzed compared to the existing mobility models.

Chapter 5 describes the event coverage problem and the proposed approaches for effective coverage. The proposed approaches are analyzed according to their event handling success. This chapter also includes the communication-constrained p-center problem and the algorithm for placing mobile sinks for optimal positioning and collaboration. The two proposed approaches, p-center positioning and p-median positioning are evaluated by comparison with two other schemes and with the placement without the communication constraint using three types of event distributions.

Chapter 6 describes tracking pedestrians and emergent events with mobile sinks and opportunistic communication during evacuation from disaster areas. Three sink mobility and placement approaches are proposed for effective communication and event handling purposes. The proposed approaches are tested against two random sink mobility model using real theme park maps and the disaster mobility model.

Chapter 7 concludes the dissertation and describes several possible extensions for future work.

CHAPTER 2
RELATED WORK

2.1   Analyses on Human Mobility

In this section, we describe the significant research and statistical analyses on human mobility which led to certain advancements in the field. We start our description with the studies related to human mobility in geographical scale. By geographical scale, we mean the people's travels in geographical distances, which includes long distance travels with airplanes, trains, cars, and other vehicles. Later, we describe the studies related to mobility in micro scale. By micro scale, we mean the human mobility in a smaller area such as a building or a shared pedestrian way, such that the speed of the person changes due to crowd dynamics, traffic congestion, social interactions, or various other reasons.

As the travels of the people are direct causes for spread of epidemic diseases around the world, the statistical analyses on human mobility have fundamental importance to society. Brockmann et al. [18] study the scaling laws of human mobility in geographical scale. While large datasets of GPS traces of human mobility are not available, these researchers analyse the mobility by observing the circulation of the bank notes around the contiguous United States. Their dataset, which is obtained from a bill-tracking system, consists of 1,033,095 tracks (reports) of 464,670 dollar bills. They consider the geographical displacements between

two consecutive reports of the same dollar bill for finding the travel distance, such that the second report's location x_2 and the first report's location x_1 are simply subtracted for finding r, which is the geographical displacement and $r = |x_2 - x_1|$ and the time t elapsed between these two points. The bank notes are originated from three cities, Seattle, Jacksonville, and New York. They observe that most bank nodes are traveled shorter distances ($r \leq 10$km) in a period of 2 weeks for consecutive reports ($t \leq 14$ days). The percentages of bank notes which traveled short distances are listed as 52.7% for Seattle, 71.4% for Jacksonville, and 57.7% for New York. On the other hand, smaller percentages of bank notes traveled longer distances ($r > 800$km). These percentages are shown as 7.8% for Seattle, 2.9% for Jacksonville , and 7.4% for New York.

By analyzing large datasets of bank note circulation, Brockmann et al. show in [18] that travel distances (flights) of people follow a power-law behavior, such that $P(\Delta r) \sim \Delta r^{-(1+\beta)}$ with the exponent value $\beta = 0.59 \pm 0.002$ (mean and standard deviation), where $P(r)$ is the probability of traveling a distance Δr in a Δt time interval. Having $\beta < 2$ corresponds to the Lévy walks [19], which is a random walk process for which step size Δr follows a power-law distribution. Lévy walk behavior shows that people mostly travel shorter distances as opposed to longer distances. The similar behavior is also observed in various animal species. For instance, Viswanathan et al. [20] observe that wandering albatrosses have the Lévy flights behavior.

González et al. [21] analyze two mobility datasets in their research. One of the datasets include trajectories of 100,000 cell phone users for six-months period of time.

100,000 anonymous users are randomly selected from more than 6 million mobile phone users. Their trajectories include the locations of cell towers to which mobile phones are connected when they send or receive text messages or phone calls. Overall, the dataset consists of more than 16 million displacement (Δr) entries. The second dataset involves 206 mobile phone users and their location in every two hours are included for one week period. The second dataset is relatively smaller (compared to the first dataset) with 10,407 entries. González et al. observe that for both datasets, the displacement values follow a truncated power-law distribution,

$$P(\Delta r) = (\Delta r + \Delta r_0)^{-\beta} exp(-\Delta r/\chi) \tag{2.1}$$

with the exponent value $\beta = 1.75 \pm 0.15$, where cutoff values are $\chi_1 = 400$km for the first dataset and $\chi_2 = 80$km for the second dataset and $\Delta r_0 = 1.5$km. Hence, they find that the trajectories follow truncated Lévy walks. They also find inherent differences (heterogeneity) in trajectories of individuals which coexist with Lévy walks.

González et al. also analyze the *gyration radiuses* in [21]. The gyration radius of a user is the total travel distance of the user for a time interval Δt. They determine the gyration radius distribution of all users in both datasets and come up with the truncated-power law equation

$$P(g) = (g + g_0)^{-\beta} exp(-g/\chi) \tag{2.2}$$

with $g_0 = 5.8$km and cutoff value $\chi = 350$.

Their results show that Lévy flights observed in [18] is a result of population heterogeneity and the individual human mobility. However, individual human mobility has a significant regularity such that a person visits the same places such as home or workplace more frequently than other places. On the other hand, bank notes always diffuse such that it is given from one person to another while this does not apply to individuals. They find that the individual trajectories can be characterized by two-dimensional probability distribution which is independent from gyration.

Song et al. [22] study the human mobility with the goal of finding if the mobility patterns are potentially predictable or not. They analyze a dataset of 50,000 cell phone users (with average call frequency $f \geq 0.5$ per hour) selected from approximately 10 million anonymous users for a period of 3 months. The dataset contains mobile phone tower trajectories as previously described. They analyze the trajectories according to the entropy characteristics. They use three metrics based on entropy: the random entropy, the temporal-uncorrelated entropy, and the actual entropy. The random entropy S^{random} is found by $S^{random} = log_2 N_i$ where N_i is the number of distinct locations (cell towers) visited by the user i. This metric characterizes the degree of predictability of the user's location if each place is visited with equal probability. Temporal-uncorrelated entropy S^{temp} is found by $S^{temp} = -\sum_{x=1}^{N_i} log_2 P_i(x)$, where $P_i(x)$ is the probability that location x is visited by the user i and it characterizes the heterogeneity of visit patterns. The actual entropy S^{actual} is given by

$$S^{actual} = -\sum_{T_i' \subset T_i} P(T_i') log_2[P(T_i')], \tag{2.3}$$

where $T_i = \{x_1, x_2, ..., x_k\}$ is the sequence of cell phone towers at which the user i is observed and $P(T_i')$ is the probability of finding a particular time-ordered subsequence T_i' in trajectory T_i. For each user i, $S_i^{random} \geq S_i^{temp} \geq S_i^{actual}$.

Based on the observation of the entropy in individual human mobility trajectories, they find the maximum predictability Π_{max} for each individual which shows the future whereabouts of the person. Π_{max} represents the fundamental limit of predictability. They find that probability $P(\Pi_{max})$ is narrowly peaked approximately at $\Pi_{max} \approx 0.93$, which implies 93% predictability and no cell phone user appears to have less than 80% predictability. While high predictability is observed in the whole dataset of 50,000 cell phone users, they also find that among these people, the ones who travel longer distances such as hundreds of kilometers on a regular basis with $g \geq 100$km, are just as predictable as the ones who have constrained movements in local environments with $g \approx 10$km. This analysis supports the previous study by González et al. [21] which suggests the regularity in the human mobility patterns. Hence, despite the spontaneity and changes in the human mobility decisions, human mobility is found to be characterized by deep-rooted regularity.

2.2 Mobility Modeling

Mobility affects the performance of network applications designed for a group of mobile users or nodes. As the usage of mobile elements in networked systems becomes popular, the effect of mobility becomes critical for various applications such as modern communication systems

of urban environments [23] and online services [24]. Considering the impact of mobility, various approaches are proposed for problems including topology control of networks [25], routing in mobile sensor networks [26], tracking in sensor networks [27–29], analysis of social networks [30, 31], disease spread simulation [32], security with autonomous agents [33], and opportunistic communication [34, 35].

Human mobility has several characteristic features, which have been observed by various measurement methods. Instances of these features are truncated power-law distributions of pause times, intercontact times (ICTs), fractal waypoints and heterogeneously defined areas of individual mobility. Rhee et al. [4, 36] show that these properties are similar to the features of Lévy walks and used these properties to design Self-similar Least Action Walk (SLAW) model. SLAW is a context based Lévy Walk model, which produces synthetic human walk traces by taking the degree of burstiness in waypoint dispersion and heavy-tail flight distribution as inputs. According to SLAW mobility model, the mobile nodes walk from one pre-defined waypoint to another. The dense regions of waypoints form the areas where the people pause and spend most of the time.

SLAW models human mobility in a general context where the waiting times at the waypoints are determined according to a power law distribution. However, for our particular theme park scenario, the waiting times must be defined according to the characteristics of the specific types of attractions. The attractions at theme parks can be combined into groups of main rides, medium-sized rides, live shows and restaurants [37]. Using the specific types, we modeled the waiting times of visitors at these attractions using queueing theoretical models.

Basically, in our model, queueing theory is integrated with the visitors' movement decisions, to create a realistic user mobility model for the theme parks.

The SLAW mobility model is used by various studies in the fields of networking and human mobility modeling. Let us describe two human mobility models which used SLAW model as the baseline: SMOOTH and MSLAW.

SMOOTH [38,39] is proposed as a realistic and simple to implement human mobility model. SMOOTH aims to provide 7 statistical features of human walks: 1) truncated power-law distribution (TPL) of flight lengths, 2) TPL of ICTs, 3) TPL of pause times, 4) human behavior of choosing popular places to visit, 5) visiting the closer places first (least-action principle), 6) non-uniform distribution of people, 7) heterogeneous division of regions of mobility for different people (moving around communities). In the model, clusters of waypoints are formed in a way that each cluster represents a community (place of movement). Clusters have unequal sizes and the cluster sizes represent the popularity of the places. For instance, in a university campus, food courts are more popular in terms of number of people visit every day, compared to places such as a specific department's building. People move in the region in groups and the region is defined as a cluster of waypoints.

For the individual's perspective, each person chooses a community according to the corresponding cluster sizes and then chooses a subset of the waypoints in the cluster to visit. These two steps can be considered as the pre-planning phases. Later, the person visits the selected waypoints via the least-action trip planning (LATP) algorithm. At each waypoint, the person's pause time is determined randomly by the power-law distribution. As opposed

to SLAW having parameters such as the hurst parameter, SMOOTH has simpler inputs so that people having no previous knowledge about the mobility models can still be able to use the model in their simulations. These inputs are listed as size of the area, number of people, number of waypoints, mobile nodes' transmission range, number of clusters, and minimum and maximum pause times. The model also expects inputs for *alpha* and *beta* parameters which are used by the LATP algorithm for choosing the next destination points and setting the pause times respectively. Furthermore, SMOOTH has the ability to imitate SLAW. Specified values for maximum sizes of a group and maximum distance of waypoints from each other correspond to ranges of hurst parameter values which are listed in a table [38]. The SMOOTH model is validated using the GPS traces collected from 5 outdoor environments and in comparison to the SLAW model with metrics such as complementary cumulative distribution functions (CCDFs) of flight lengths and ICTs and average message delays. For network simulations, SMOOTH is a good alternative human mobility model as it is easy to implement and much more realistic compared to other commonly used mobility models such as RWP, which are already proven to be unrealistic [40].

The SLAW mobility model assumes no obstacle for the human movement, such that after deciding the next destination, a person can straightly move to the next waypoint without any disturbance, so the speed and the direction does not change. Map-based SLAW (MSLAW) [41] mobility model introduces geographical restrictions to the SLAW model. The algorithm of MSLAW overall follows similar steps (e.g., fractal points generation) of the SLAW's algorithm, but these steps are modified for the purpose of including the map-based

18

geographic restrictions. For instance, waypoints are not created on top of the rivers, forests, or other inaccessible areas. MSLAW has a modified version of the LATP algorithm for deciding the next destinations. In SLAW, the distance $d(v, w)$ between two waypoints v and m was given as the Euclidean distance $(d(v, w) = \|v - w\|)$, while in the modified version, the distance is given according to the optimal route lengths. Considering the optimal route $(v_i^*)_{1 \leq i \leq j}, j \leq 2$ from v to w,, such that $v = v_1^*$ and $w = v_j^*$, the total distance of the optimal route is given as

$$d(v, w) = \sum_{i=1}^{j-1} \left\| v_i^* - v_{i+1}^* \right\|. \tag{2.4}$$

In this equation v and w are the actual waypoints which were generated in the initial fractal point generation phase. However, the points in between these two points $(v_2^*, v_3^*, ... v_{j-1}^*)$ may or may not be the waypoints, as they are only chosen as part of the optimal route for avoiding obstacles.

Set of parameters used in the MSLAW mobility model include the hurst parameter as well as the LATP distance weight parameter α, along with common mobility parameters such as the number of people, simulation time, and the size of the simulation area. Implementing MSLAW requires the similar steps of the SLAW implementations, but it is relatively harder to implement the simulation of this model compared to the SMOOTH model. MSLAW is not validated by the simulations in comparison to real-life GPS traces. However, the model is evaluated with several metrics such as ICTs, contact durations, and recontact rates against RWP, SLAW, and a map-based random mobility model RaST [42]. The mobility traces

generated by the MSLAW model seems more convenient than the traces of the SLAW model for scenarios such as human walks in the urban environments.

For the modeling of human movement in specific scenarios, a variety of mobility models have been proposed. Social force model [43] is proposed by Helbing and Johansson to represent the micro-mobility behavior of the pedestrians in crowded areas. Liu et al. [44] propose a physics-based model of skier mobility in mountainous regions by considering the physical effects of gravity and the steepness of the terrain. The goal of the model is to evaluate the effectiveness of wireless communication devices in improving avalanche safety. The Weighted Waypoint Mobility model [45] by Hsu et al. describes the pedestrian movement patterns among preferred locations on a campus. The preferred locations are predetermined in the environment and assigned "weights", which define the probability of being selected as the destination by the pedestrians. Kim et al. [46] propose a mobility model for urban wireless networks, in which the model parameters are derived from urban planning surveys and traffic engineering research. ParkSim [47] by Vukadinovic et al. is a software tool simulating the mobility of theme park visitors. The mobility model of ParkSim is driven by the possible activities of the visitors in the park. Munjal et al. [48] review the changing trends of the recently proposed mobility models used for simulations of opportunistic communication networks.

2.3 Wireless Networks with Mobile Elements

In recent years, various studies focus on the use of mobile elements in wireless networks. Mobility has significant effects on the performance of these networks and brings new research challenges for the existing problems such as data collection [49] and dissemination [50], relay node placement [51–53] path planning [54], latency [55, 56], lifetime maximization [57–60], routing [61–64], and security [65].

Most research on WSNs with mobile elements (MEs) focus on settings such that large numbers of static sensor networks distributed in a large area and limited numbers of mobile sinks move between the sensor nodes to collect data. Data collection and management, transmission scheduling of the collected data, routing, and localization are major challenges in these networks. Di Francesco et al. [66] survey data collection schemes in WSNs with MEs, while Zhu et al. [67] survey communication and data management issues in mobile WSNs. Anastasi et al. [68] investigate data delivery to one or multiple MEs in the context of sparsely deployed sensor nodes. Turgut and Bölöni [69, 70] propose heuristic approaches for the transmission scheduling problem and compare the performances of each of the proposed strategies for WSNs with multiple mobile sinks. Bölöni and Turgut [71] suggest a decision-theoretic approach for the same problem. Luo et al. [72] show the benefits of routing towards a mobile sink approach for improving lifetime of WSNs in different scenarios. Furthermore, there are studies related to other types of WSNs with MEs, where the sensor nodes are also mobile [73–75] or the sensors are mobile and the sinks are static [76,77]. There are also studies

of using WSNs with MEs in 3D environments including aerial [78–80] and underground [81] scenarios. Erol-Kantarci et al. [82] survey distributed localization techniques used in mobile underwater acoustic sensor networks.

For managing positioning and mobility of the sink nodes, various approaches are proposed in the literature. Younis and Akkaya [83] survey techniques for careful node placement strategies used in WSN for effective optimization. Vincze et al. [84] use an approach similar to our crowd density based positioning strategy, for positioning multiple sinks optimally in a sensor network based on an electrostatic model by assigning positive or negative charges to sensor nodes according to their energy level, and positive charges to the sinks. In this study, the goal is to optimize energy usage of sensor nodes in the network. Wang et al. [85] survey the mobility management methods for mobile sensor networks and compare the methods in terms of their categories and characteristic features. Melodia et al. [86] suggest a location management scheme to handle the mobility of actors with minimal energy expenditure for the sensors, based on a hybrid strategy including location updates and location prediction. Vincze et al. [87] use an adaptive approach for sink mobility in event-driven multi-hop WSNs to minimize the maximum load on sensors and prolong the lifetime of the networks. They use an intruder movement model as the event model and propose two strategies to: a) minimize the sum of event distances and b) minimize the maximum energy consumption. Wang et al. [88] propose an adaptive approach for location updates of mobile sinks in WSNs to resolve the problem of rapid energy consumption of sensor nodes increased collisions in wireless transmissions.

The use of mobile sinks in sensor networks have various advantages such as prolonging network lifetime, while it brings challenges such as finding efficient strategies of mobile sink movement and routing towards mobile sinks. Khan et al. [89] survey various data collection approaches that exploit sink mobility. They classify these approaches in three categories: namely path constrained, path unconstrained, and controlled sink mobility-based schemes. Wang et al. [90] focus on the connectivity problem of wireless sensor and ad-hoc networks and the effect of the mobility on the connectivity in k-hop clustered networks. In their study, they show that random walk mobility significantly increases connectivity while decreasing the energy consumption in k-hop clustered networks. Bi et al. [91] propose two autonomous movement approaches for single mobile sink for the purpose of increasing network lifetime. Rahmatizadeh et al. [92] use virtual coordinates and propose a routing protocol with mobile sinks for lowering energy consumption. Luo et al. [93] investigate the joint sink mobility and routing problem and propose an algorithm for solving the problem with single mobile sink and approximating with multiple mobile sinks. The same joint sink mobility and routing problem is also studied by Wang et al. [94]. They study the performance of a large dense network including one mobile sink and show that the network lifetime increases four times compared to the static network. They also propose an algorithm that provides an upper bound performance for the network lifetime. While in our study we focus on the use of mobile sinks, our main goal is to provide quality of service during disasters. In that sense, we study the network coverage and routing problem while the previous studies mostly focus on the problems of energy consumption and network lifetime.

Angelopoulos et al. [95] compare three coverage-adaptive random walks for fast sensory data collection. In Random Walk with Inertia, the mobile sink assigns probability to each directions and changes the probabilities by discovery of sensors. In Explore-and-Go Random Walk, the sink decides on moving in a straight line or changing direction based on a bias factor at each step. The last proposed walk is Curly Random Walk. In this approach, the sink traverses the network area starting from the center and expanding its mobility area by consecutive circular-like moves. Hara [96] analyzes the effects of 5 random mobility models on data availability, while Carofiglio et al. [97] use Random Direction Mobility model to provide optimal path selection for routing in mobile ad hoc networks. La [98] analyzes the inter-meeting times of the nodes of mobile networks using the generalized Hybrid Random Walk mobility model.

2.3.1 *p*-center problem

The p-center is an old problem which is NP-hard in general graphs [99]. Different versions of the p-center problem have been studied in the past to propose heuristics to solve it. Since we propose an exact algorithm, we only summarize the literature dealing with the exact solutions. For instance, Kariv and Hakimi [99, 100] are the first to define the absolute and vertex p-center and p-median network location problems and propose exact algorithms for solving these problems. Resende and Werneck [101] approach to the p-median problem by using traditional metaheuristics in order to find near-optimal solutions.

Özsoy and Pınar [102] propose an exact algorithm to solve a different version, called the capacitated vertex p-center problem. In this case, each client is labeled with a demand quantity and assignment of the p-centers is constrained. The total demand by the clients cannot exceed the capacity of the facility. A good summary of the literature for the solutions of both the capacitated and the uncapacitated p-median problems is given by Reese [103]. The connected p-center problem studied in [104] is the closest to our problem. In this problem, the p vertices should be connected on the same graph. The problem is solved with exact algorithms on trees [105], block graphs [104], and trees with forbidden vertices [106]. Our problem is different in the sense that the connectivity should be through wireless communication not physical paths.

There are other applications of the p-center problem in WSNs mostly in the context of clustering [107, 108]. In these works, the idea is to minimize the packet delay from each sensor to the sink node but there is no restriction for the connectivity of the sink nodes. Our problem is different from them in terms of its communication constraint.

2.4   Disaster Mobility and Management

There exist studies related to modeling the mobility of pedestrian crowds. Shiwakoti et al. [109] focus on the use of biological entities such as ants for empirical study to pedestrian crowds to enhance safety of pedestrians in emergency conditions. Helbing et al. [43] simulate the mobility of pedestrian crowds for the ordinary scenario and the evacuation situations.

Georgoudas et al. [110] propose an anticipative system to avoid congestions at the exit points during the evacuation of the pedestrians.

The mission critical mobility model (MCM) [111] aims to model the human mobility in the presence of obstacles for mission critical applications such as networks in times of disasters. Considering an example opportunistic network application, the nodes are carried by human participants such as firemen or policemen. MCM is a generic model, such that it is considered for all types of disaster scenarios. In the model, the destination points are chosen uniformly random by each person. In the case of no obstacle between the current point and the destination point, the person directly moves to the destination, creating a trajectory which is a straight line. In the case of having obstacles in-between, the person passes each obstacle by choosing a directly visible vertex that is closest to the final destination. The vertex location is set as the intermediate destination to pass by the obstacle. The person similarly passes multiple obstacles one by one. The movement algorithm can be considered as greedy since the person always chooses the visible vertex which is closer to the final destination, trying to minimize the total time it takes to walk. Note that the algorithm does not give the optimal shortest-path, as there are many ways of going to the same final destination, which may have shorter overall distances. However, considering the people's movement choices, people also do not always manage to choose the shortest path, instead one can claim that they mostly make greedy movement decisions for having less movement effort. The movement speed is a random value between minimum and maximum boundaries and the speed is set every time after deciding a new next destination.

MCM has the group mobility behavior, such that each group has a leader who decides the next destination for all group members. Moreover, people have different roles in the disaster area. They are considered in two roles: *emergency workers* and *medical staff*. In the MCM model, destination points are set based on the randomly generated *event* locations. For each event, there is a particular pause time, which represents the time it takes to handle the event. The events are categorized as *normal*, *serious*, or *complex* events and the group leaders do their choices based on the types of the events. For instance, groups of different types need to be involved for handling complex events. The events are handled according to First in First out (FIFO) order. The MCM model is the newer and more extensive version of the previous Human Obstacle Model (HUMO) [112], such that the model is analyzed and validated with real-life human mobility traces.

Disaster area (DA) [113, 114] mobility model is based on the two disasters that happened in Germany, which are the Wuppertal Railway Crash in 1999 and the Bruehl Roller-Coaster Fire in 2001. For the civil protection in disasters, the movements are driven by tactical reasons. For instance, a group leader for the rescue operation directs workers to move to some places. In the model, the disaster area is considered as consisting of separated regions such as the disaster incident site, casualty treatment site, transport zone, and hospital zone. The affected and injured people are considered to be found and rescued in the incident site, taken to the casualty treatment site, and moved to hospitals from the transport zone. The main characteristics of the DA model are having different roles for people, being heterogeneous area-based model, and avoiding obstacles. The group mobility behavior

is considered as a future extension to the model. The model also involves the vehicular behavior for transportation services such as ambulances. The disaster simulation area is a synthetic map considered as a static region with obstacles which are modeled with polygons. Visibility graphs are used for optimal path planning and Dijkstra's shortest path algorithm is used on top of this graph, where edges are the Euclidean distances. Each separated area (*tactical area*) has entry and exit locations. Each person is assigned to an area. Some people are considered as stationary nodes, meaning that they only move inside their assigned area. The others are considered as *transport nodes* having the ability to carry patients to the next area. In the incident zone, all people are considered as transport nodes, while in casualty treatment area there are only stationary nodes. The movements inside the areas are modeled with the RWP model [115].

There are many research studies for solving the emergency evacuation problem in city environments such as downtown areas and evacuation of buildings during disasters. Yamada [116] investigates the problem of city evacuation with a graph theoretical approach using two network flow methods. A simulation-based system for evacuation is proposed by Zou et al. [117] and six different evacuation plans for evacuation of Ocean City are simulated. Park et al. [118] propose a rule based approach to model spontaneous evacuation behavior considering a terrorist attack scenario in a complex metropolitan area. Chen and Zhan [119] compare the simultaneous and staged evacuation strategy in which vehicles are organized to evacuate according to the different sequences of the zones in the disaster area. They use an agent-based approach to model and simulate the evacuation of the vehicles. Kirchner

and Schadschneider [120] introduce a bionics approach for describing interactions of the pedestrians. They use the cellular automaton model to model the evacuation dynamics of the pedestrians from buildings. Kwon and Pitt [121] apply a dynamic traffic assignment model, "Dynasmart-P" to the evacuation problem for traffic in downtown Minneapolis, Minnesota. While the aforementioned studies focus on the metropolitan areas which involve various services and the use of vehicles, we focus on the simpler problem of evacuation of pedestrians from a relatively smaller disaster area.

Fujihara and Miwa [122] investigates the effects of opportunistic communications in evacuation times for disaster scenarios. El-Sergany et al. [123] propose a model for evacuation planning and disaster management in flood disaster scenarios. Iizuka et al. [124] propose the use of mobile devices of evacuees to form an ad hoc network and find the evacuation routes accordingly and avoid congestions. Kamiyama et al. [125] try to solve the problem of evacuation for networks that consist of a directed graphs with capacities and transit times on their arcs and propose an efficient algorithm. Helgason et al. [126] investigate the effects of the human mobility on the wireless communication performance of ad-hoc and delay-tolerant networks. Qing-Shan and Ying [127] formulate the problem of outdoor evacuation as a scheduling problem in queuing network and considers human guidance and the probability of crowd panics. Clementi et al. [128] propose using mobile ad-hoc networks (MANETs) for data flooding where nodes move independently at random and exchanges data when they are in each other's transmission range. They show that node mobility enhances the speed of information spreading even for the networks which are sparse and

disconnected. Rozner et al. [129] study the joint optimization of opportunistic routes with a model-driven optimization approach and achieve better performances compared to shortest-path routing and opportunistic routing protocols such as the conflict-graph (CG) model. Our model is unique and different than the other studies of opportunistic networks in terms of having multiple mobile sinks and pedestrians with smartphones. In this case, performance of the opportunistic network highly depends on the positioning of the mobile sinks and the pedestrian mobility.

There are many studies aiming to provide solution to the disaster management problem. Winter et al. [130] study the evacuation problem in disaster areas and propose the use of a mobile service "Get-Me-Out-Of-Here" (GOH) running on smartphones. Benefits of communication among people are observed for the evacuation scenarios in which individuals have only the local knowledge of the environment. Uddin et al. [131] propose an agent-based mobility model which models the mobility of people with different roles such as rescue workers and volunteers as well as vehicles such as police patrol cars and ambulances. They also propose the intercontact routing [132] for disruption-tolerant disaster response networks to reduce the resource overhead. Gao et al. [133] list the characteristics of disruption-tolerant networks as low node density, unpredictable mobility and lack of global knowledge and they try to optimize data access by the cooperative caching mechanism.

Ayday and Fekri [134] focus on the security problem of delay tolerant networks (DTNs), which are commonly used for disaster response, and they propose a trust mechanism to efficiently detect malicious nodes in the networks. Drugan et al. [135] investigate clustering

of dynamic networks with the help of community detection mechanisms for mission-critical application domains such as rescue and emergency services. Palmer et al. [136] develop the "RAVEN" framework for collaborative data collection by using smartphones during disaster. Another data collection system is proposed by Fujiwara et al. [137]. Their system involves the use of sensor networks and an access network for detecting damages in a disaster and sending the data to an emergency control center. Tuna et al. [138] propose a system for automatically deploying a WSN using multiple robots for the purpose of human existence detection in disaster environments. Their approach involves simultaneous deployment of the sensor nodes during the exploration of an unknown area and WSN-based communication. Our study differs from these disaster management studies as we propose using mobile sinks which can follow a determined route while there exists an uncertainty in the movement decisions of the pedestrians.

Patrix et al. [139] model mobility of agents and disaster area for crowd behavior detection. In this study, they model obstacles, dangers, and shelters as separate zones in their simulation of the disaster scenario. An agent makes movement decisions according to these zones and the movement of the other agents. A role-based mobility model is proposed by Nelson et al. [140] for disaster areas. In this model, movement patterns of objects with distinct roles such as police and civilians differ according to their various reactions to the events. Bagrow et al. [141] study collective response behavior and changes in communications of people in extreme emergency conditions such as bombing, plane crash, earthquake and power blackout. Patterson et al. [142] highlight models which focus on the effects of

communities on preparedness, response, and recovery of people from disasters. Kirchhoff et al. [143] propose link quality based routing, prioritization of control messages, and overhead reduction mechanisms for mobile wireless multi-hop networks. Their focus on the field of disaster area scenarios as the main application of this study due to the major challenges such as limited network capacity and link variability. Our model differs from the above models such that we focus on modeling human mobility in disaster areas by isolating it from other challenges such as transportation or security.

CHAPTER 3
MODELING MOVEMENT OF THEME PARK VISITORS

In this chapter, a mobility model of theme park visitors [7, 8] is introduced.

Recent advances in mobile devices enabled the increased popularity and usage of mobile applications. Urban sensing applications, where mostly smartphones are used, and wireless sensor networks with mobile sinks are examples of these applications. The realistic modeling of human movement has significant importance for the performance assessment of such mobile wireless systems.

Human mobility models simulate the movement patterns of the mobile users and they form a key component of the simulation-based performance evaluation [1]. Early mobility models relied on some type of variations of the idea of a random walk. Examples of this approach include the random waypoint (RWP) [144] and Brownian Motion [145] models. These models are only very coarse approximations of human behavior. One of the most important characteristics of human mobility is the combination of regularity and spontaneity in deciding the next destination. This behavior can also be defined as making both deterministic and nondeterministic decisions in the same time period. Considering the theme park scenario, visitors usually pre-plan their visit. They try to optimize their time on rides while minimizing the time to walk from one attraction to another. Nevertheless, when they are

in the park, they may change their decisions spontaneously depending on various factors. Random mobility models such as RWP do not provide a good match for this behavior.

Theme parks are large crowded areas with unique characteristics in terms of movement patterns of visitors, attractions in various locations and walking paths connecting the attractions. In this chapter, we present a mobility model of theme park visitors. The outputs of the model are the synthetic movement tracks, pausing locations (waiting points) and pausing times. First, the fractal points are generated by the model in order to create the pausing locations. The concentrated locations of these fractal points are defined as the meeting locations of visitors or attractions. This method decreases the number of waypoints in a map, allowing the simulation of large numbers of visitors. It also makes the mobility model more realistic since real attractions such as restaurants or rides in the environment can be simulated by their individual models. These locations are grouped into four main attraction types of theme parks: main rides (RD), medium-sized rides (M-RD), live shows (LS), and restaurants (RT). The waiting times of visitors at these attractions are modeled using queueing theory. Moreover, we define walking areas of visitors as landmarks in the theme park in order to separate the walking paths from the roads on which transportation vehicles are used.

Let us now consider how such a model is useful for wireless mobile applications. For instance, a wireless sensor network (WSN) can be deployed in a theme park for finding the fastest way to move from one location to another considering the current density of the crowds in different areas of the park ([12], [13], [14]). Such a WSN would rely on the personal

mobile devices of the visitors and can be used to offer an interactive theme park experience. Social networking applications or multi-player games can be offered to the visitors with the support of a deployed wireless system or in an ad hoc working mode. The performance of such a system would highly depend on the mobility of the users and must be evaluated by simulations before deployment.

Another class of applications would be the theme park administration. Theme park administrators must direct visitors efficiently among attractions and balance the number of visitors at each attraction. It is desirable to balance the density of the crowd in different areas of the park due to efficiency of the attractions as well as the security of the visitors. The administrators can use the mobility model to estimate the possible impact of their decisions such as the distribution of live entertainers or the arrangement of the paths for pedestrian traffic. The predictive results of the model can be used to decide the locations of security personnel. The mobility model is also used as a base for disaster simulations and emergency management applications [111].

The mobility model involves the nondeterministic macro-mobility decisions of the visitors as well as the deterministic behaviors of the attractions. The model is successful in terms of representing the social behavior of people to gather in attractions, spending time in queues, and movement decisions in terms of the least-action principle of human walks. The outcomes of the proposed model are synthetically generated mobility traces. These mobility traces are compared to the real-life theme park GPS traces and the traces of two mobility models. The mobility traces of our model have the best statistical match to the GPS traces

amongst the tested synthetic models in terms of flight length distributions, average number of waiting points, and waiting times.

The rest of the chapter is organized as follows. We provide a detailed description for our mobility model in Section 3.1. We evaluate the validity of the model in Section 3.2 and finally conclude the chapter in Section 3.3.

3.1   Human Mobility Model

In this section, we present the scenario-specific mobility model for the theme park visitors. Before describing the model, let us briefly explain the fundamental characteristics of these entertainment areas. Theme parks are large areas with one or more "themed" landmarks that consist of attractions. Visitors of a landmark plan to see a subset of these attractions by walking during their scheduled visit. SLAW [4] model provides an effective strategy in representing social contexts of common gathering places of pedestrians by fractal points and heavy-tail flights on top of these fractal points. We extend this idea for a more realistic mobility model and apply queueing models to represent the behavior and effects of different types of attractions on the mobility of theme park visitors.

3.1.1 Modeling a theme park

The modeling of a theme park consists of five main phases, which starts with the first phase of fractal points generation, and ends with the theme park model.

3.1.1.1 Fractal points

We use the term *fractal points* based on its usage in the SLAW mobility model. In our model, the fractal points are initially created in an empty area using the fractional Gaussian noise or Brownian Motion generation technique (fGn or fBm), as described by Rhee et al. [146]. A fractal point can be considered as a waypoint at the beginning. All fractal points and the area, in which these points are generated in, are used to form a landmark as described in the following phases.

It is shown that the use of fractal points and least-action trip planning on top of these self-similar points satisfy fundamental statistical features of human walk [4]. As a human behavior, people are more attracted to visit popular places. This characteristic of human mobility can be expressed using fractal points as explained in the next subsection. Fig. 3.1 demonstrates the first phase of the model in a scenario, where 1000 fractal points are generated in an area of 1000x1000 meters.
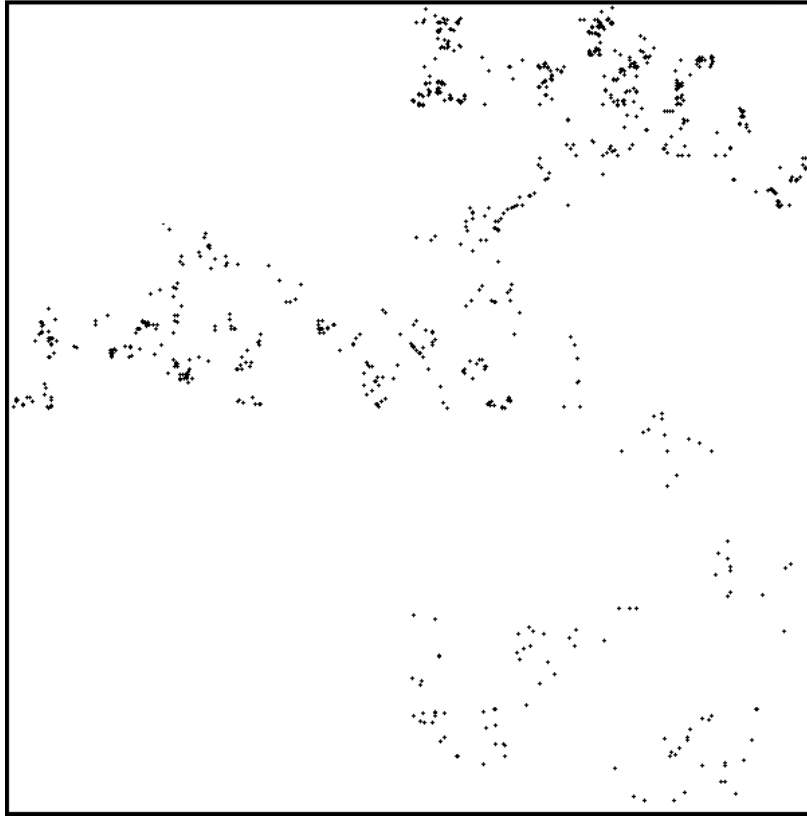
Figure 3.1: Fractal point generation phase of the model.

3.1.1.2 Clusters

After generation of the fractal points, we determine the parts of the area with highest density of the points. The goal of this phase is finding the popular areas, where people are more attracted to gather.

We use a modified version of DBScan [147] algorithm on the generated fractal points to find the attraction locations. DBScan is a density based clustering algorithm for discov-

ering clusters with noise points, which has two input parameters, epsilon Eps and minimum number of points (neighbors) $MinPts$.

The *Eps-neighborhood* of a point p, denoted by $N_{Eps}(p)$, is defined by $N_{Eps}(p) = \{q \in D | dist(p, q) \le Eps\}$, where D is the database of points. In our DBScan approach, for each point in a cluster, there are at least $MinPts$ neighbors in the *Eps-neighborhood* of that point.

In our model, DBScan algorithm is modified based on the requirements of the scenario. The input parameters include epsilon, minimum number of neighbors, number of clusters and proportion of noise points among all fractal points. The number of clusters and noise point ratio are used to specify a landmark. For instance, if there are 25 attractions in a theme park, the number of clusters becomes 25. The non-clustered point ratio is used to determine the nondeterminism in mobility empirically (e.g. 10%) or based on statistical data collected from the visitors of a theme park. The values of the minimum number of neighbors and epsilon are iteratively searched with a heuristic, which alters the values of these two parameters according to the results of the previous iteration. This heuristic is based on the fact that changing the values of these two parameters directly changes the resulting number of clusters and the non-clustered point ratio. For instance, if epsilon has a larger value and minimum number of neighbors has a smaller value, DBScan produces less number of clusters, with a smaller non-clustered point ratio.

Let us assume a landmark is required to have 10 clusters and the proportion of non-clustered points to be approximately 0.10. The initial epsilon and minimum number of

neighbors are set as 30 meters (for dimensions of 1000x1000 meters) and 8 empirically. After setting the initial values, the fractal points are scanned iteratively to set the new values for epsilon and the number of neighbors parameters. When the expected number of attractions and the expected approximate proportion of non-clustered points are achieved, the clustering of fractal points are finalized.

The clustering of the fractal points determines the areas with highest densities of fractal points. Fig. 3.2 shows an example clustering output with over 1000 fractal points in an area of 1000x1000 meters. In this example, 15 clusters are generated and marked, whereas 10% of the fractal points are not included in the clusters.
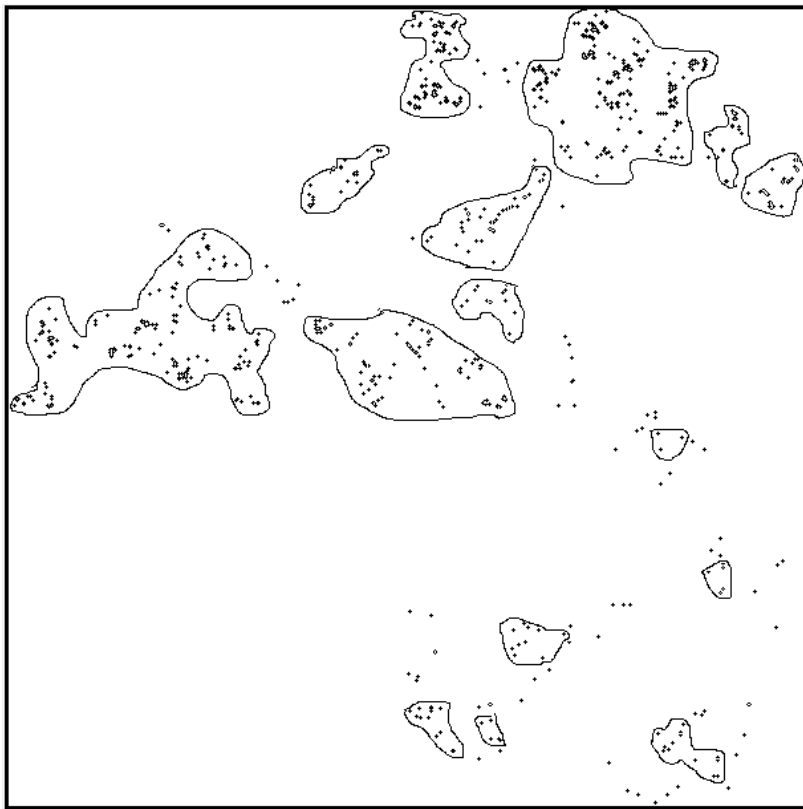
Figure 3.2: Clusters generated by DBScan over 1000 fractal points.

3.1.1.3 Attractions and noise points

The clusters as the regions with highest number of fractal points and non-clustered points are obtained from the previous step. In this phase, the most dense areas found by clustering step are marked as "attractions".

In our model, attractions are represented by queueing models. We decide on the types and the weights of the queues based on the number of fractal points and the previous work on theme park design. The weight of a queue is defined according to the number of fractal points included in its corresponding cluster. The central point of a queue is the average position of all the fractal points included in its corresponding cluster. Non-clustered fractal points are marked as "noise points". Wanhill [37] defined the attractions in a theme park by queueing models and the specified expected percentages which are given in Table 3.1.

Table 3.1: Attraction percentages

Attraction	Queue model	Percentage
Main rides (RD)	M/D/n	17%
Medium-size rides (M-RD)	M/D/n	56%
Restaurants (RT)	M/M/1	17%
Live shows (LS)	M/M/n	10%

Each attraction has a corresponding queue type according to its particular properties. $M/D/n$ queue has a constant service time, whereas $M/M/1$ and $M/M/n$ queues have

41

service times according to the exponential distribution. The number of service channels n corresponds to the amount of visitors served per service time. In our model, $M/D/n$ queue model is used for the main rides and the medium-sized rides since they have similar queue behaviors. $M/M/1$ queue model is used for restaurants and $M/M/n$ queue model is employed for live shows since restaurants and live shows have exponential service rates, while the service rates of main rides and medium-sized rides are constant.

The waiting points for the visitors in a landmark are defined by the locations of the attractions or the noise points. The attractions are clusters of fractals, whereas the noise points are non-clustered fractals. Both can be considered as the locations where the visitors spend a certain amount of time. For example, a point where a visitor stops for a while to take pictures can be considered as a noise point in the scenario.

3.1.1.4 Landmarks

Landmarks are generated as a result of the previous steps, including the generation of fractal points, density-based iterative clustering, generation of queues according to their weights, queue types, and service rates. In this phase, we form landmarks by the inclusion of visitors, which are mobile elements of a landmark. A specified number of visitors are distributed to attractions and noise points randomly. The random distribution is achieved according to the weights of attractions, and the weights of the noise points are set to 1.

A landmark is a place where there are multiple static queues, static noise points, and mobile visitors. Each landmark has two dimensions specifying its size. Fig. 3.3 shows a landmark model with initial placement of 20 visitors (mobile nodes), queues, and noise points in an area of 1000x1000 meters. In this figure, central points of the queues are represented by squares. The noise points and initially located mobile nodes are shown by small dots and circles respectively. Each queue is presented with its attraction type: main rides (RD), medium-sized rides (M-RD), live shows (LS), and restaurants (RT).
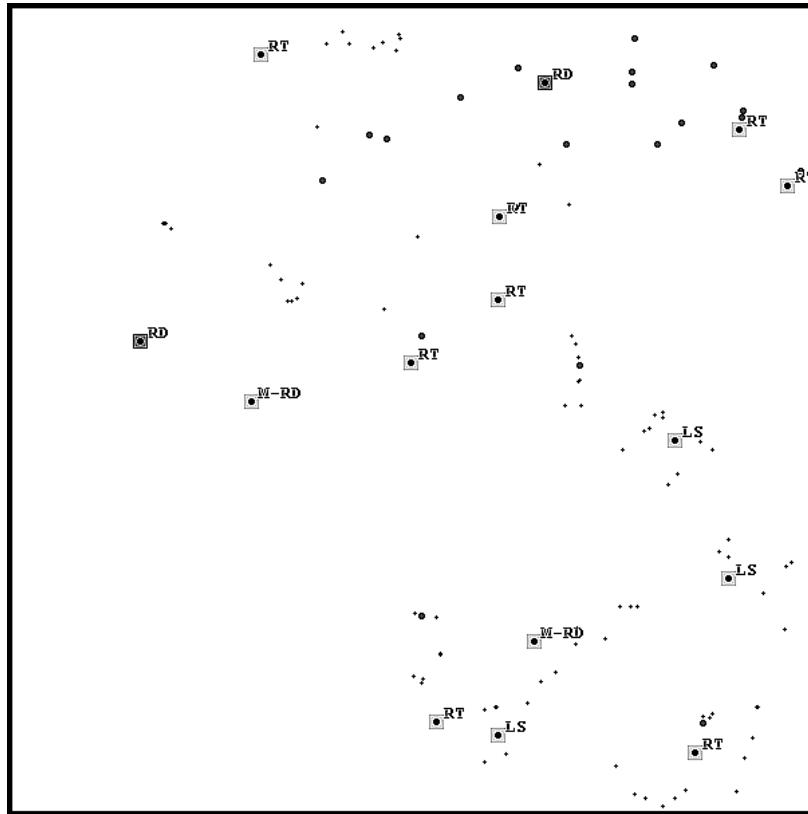
Figure 3.3: A landmark model including attractions, noise points, and initially distributed mobile nodes.

The proposed landmark model is used to model walking areas of the visitors such as the Magic Kingdom park (landmark) in the Disney World theme park by assigning the number of queues and the proportion of noise points accordingly. The landmark model separates walking areas of visitors from the areas where the vehicles are used for transportation. This differentiation is important for the realistic mobility modeling of visitors in large theme parks, where walking between various landmarks is not possible due to the long distances.

3.1.1.5   Theme park map

For modeling the theme park, we use a graph theoretical approach. The theme park map is modeled as a graph consisting of vertices and weighted non-directional edges. Each vertex in the graph represents a landmark. If there is a road between two landmarks, an edge is added with a weight corresponding to the transportation time.

Theme parks are usually large areas with transportation services among the main locations of attractions such as buses, trains and cars. Most of the theme parks are located in non-uniform 2D areas, which brings a challenge to simulate a theme park with a model assuming a uniform 2D area. By separating landmarks as vertices in a theme park graph model and adding weighted non-directional edges between the landmarks, we generalize the model of human mobility in a landmark to the human mobility in the whole theme park. The mobility model includes the landmarks and the edges between them for transportation of visitors. We do not assume that a theme park is a uniform 2D area, since it includes

geographical obstacles such as areas without pavements for pedestrians and paths or roads used for transportation. These characteristics enable our mobility model to be more realistic compared to the existing models.

Fig. 3.4 illustrates the phases of our model in a step-by-step fashion. These phases start with the generation of fractal points, density-based clustering and continues with the generation of the attractions and the noise points. The attractions, the noise points and the visitors all together form a landmark as shown in the fourth phase. In the last phase, multiple landmarks and roads are modeled with a graph.
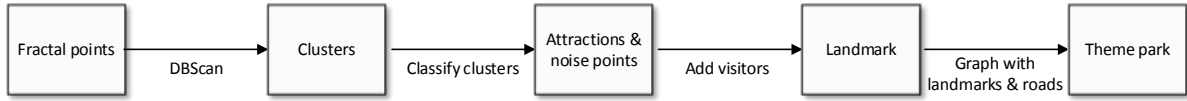
Figure 3.4: The phases of modeling a theme park.

3.1.2 Visitor model

In the model, the visitors are represented by mobile nodes. We define the states of the mobile nodes in a landmark as "initial", "inQueue", "moving", "inNoisePoint" and "removed". At the beginning of the simulation, all mobile nodes are in "initial" state. A mobile node changes its state to "inQueue" when it starts waiting in a queue. The state changes to "inNoisePoint" when the node starts waiting in a noise point. There are two different states of waiting in order to differentiate waiting in a noise point or in a queue. When a mobile

node starts changing its location to arrive to a new destination, which may be an attraction or a noise point in the landmark, it is in the "moving" state. The state of a mobile node is "removed" when the hangout time of the node passes. Fig. 3.5 shows the five states of visitors and the state transitions.

Initially, each visitor decides on the amount of time to stay in the particular landmark, which is defined as the hangout time. Hangout times of the visitors are generated by exponential distribution. Then, each visitor selects a subset from the set of all attractions at the landmark to visit. The size of the subset (the number of queues to visit) selected by a visitor is proportional to the corresponding hangout time of that visitor. If the visitor is not in "inQueue" state when the hangout time ends, the visitor leaves the landmark. In other words, the visitor arrives at an exit point of the landmark. If the visitor is waiting in a queue, (in "inQueue" state), the visitor continues to wait in the queue and leaves the landmark after being serviced. We assume every visitor has a constant speed. After attraction subset decision, the visitors move according to the least action principle among the selected attractions and noise points. The visitor marks an attraction or a noise point as visited and does not visit these points later. This principle is also used to explain how people make their walking trails in public parks.
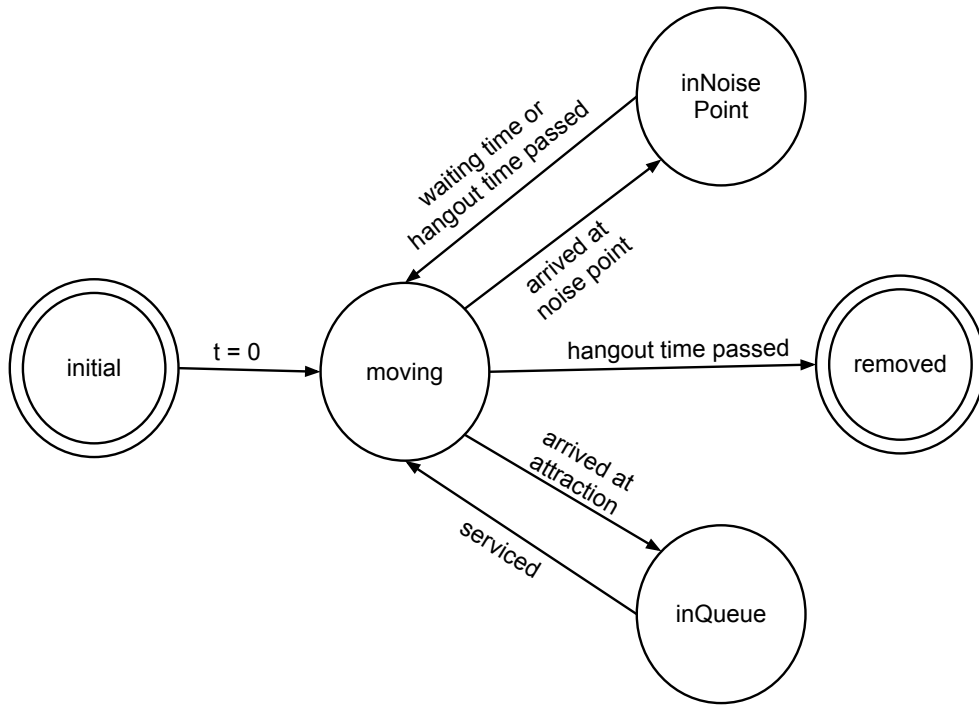
Figure 3.5: States of a visitor.

The next destinations of visitors are decided by using Algorithm 1, which is a modified version of Least Action Trip Planning (LATP) [4] algorithm. In LATP, a visitor tries to minimize the Euclidean distance traveled from a waiting point to a new waiting point (destination). The waiting points are either the attractions or the noise points in the landmark. This strategy is different than Dijkstra's Shortest Path since it does not always cause the new destination to be the nearest waiting point, where every unvisited point has a probability to be the next destination. The parameter α is used to determine this probability. The algorithm is modified to match the requirements of our mobility model.

In Algorithm 1, A is the set of attractions which are planned to be visited by the visitor, while N is the set of all noise points. W represents the set of attraction weights,

while cp is the current position of the visitor. Pr is the set of probabilities of the next destination points of the visitor. Waiting points are not identical and have varied weight values, while the weight of a noise point is always 1 and the weight of a queue (attraction) is set as the number of fractal points included in its corresponding cluster. The probabilities of the queues with larger weight values, such as main rides, are higher for selection as the new destination points. In other words, visitors are more attracted to gather in queues with larger weight values. For the calculation of Euclidean distances ($d(cp, a)$ for attractions and $d(cp, n)$ for noise points), we use the exact positions of the noise points in the landmark and the positions of the central points of queues.

At each iteration of the simulation, we check the queues to find the number of visitors serviced and the states of all visitors for possible changes. For instance, if a visitor is serviced by an attraction, the state of the visitor must change from "inQueue" to "moving".

When an attraction is selected, the visitor goes to a random sit-point inside the clustered area as the new destination position. Waiting time of a visitor in a queue depends on the number of visitors already waiting in the queue ahead of that visitor, service rate, and the number of visitors per service of the attraction. When a visitor goes to a noise point, the waiting time of the visitor is generated using the truncated Pareto distribution.

Most theme park visitors travel in groups such as families. While this model is based on individual mobility decisions, group mobility characteristics of the proposed approach or the social behaviors of the groups formed as a result of the attractions can be analyzed to improve the mobility model.

Algorithm 1 Algorithm for deciding the next destination

1: **for** each n in N **do**

2:     $Pr(n) := (\frac{1}{d(cp,n)})^\alpha$

3: **end for**

4: **for** each a in A **do**

5:     $Pr(a) := (\frac{1}{d(cp,a)})^\alpha$

6:     $Pr(a) := Pr(a) * W(a)$

7: **end for**

8: Select a point p according to probabilities Pr from the set $A \cup N$

9: **if** $p \in N$ **then**

10:     **return** Position of the noise point p

11: **else**

12:     **return** Position of a random sit-point in the queue p

13: **end if**

3.1.3 Theme park with multiple landmarks

The mobility model can be easily applied to model a complete theme park scenario. Each smaller park in a large theme park would be modeled as a landmark. For each park, real dimension lengths are used to specify the 2D rectangle area of a landmark. OpenStreetMap [148] can be used to determine the sizes of the theme parks.

In the real scenario, the number of attractions and types of those attractions are generally known; however, if this is not the case, the queue types of the attractions and the numbers specified in this chapter can potentially be used. With this approach, a portion of a theme park can be modeled as a landmark.

Each visitor in this scenario has a total hangout time, which is the amount of time to spend in the theme park. Initially, visitors decide on the parks (landmarks) to visit in an order such that the transportation (minimum weights) between them is minimized. A visitor also plans to visit particular attractions when entering a new landmark. After finishing the hanging out time in the park, the visitor goes to the next planned park through the road connecting the two parks.

Fig. 3.6 contains three main parks (landmarks) of the Disney World theme park in Orlando; namely, Epcot, Animal Kingdom and Hollywood Studios. OpenStreetMap [148] is used to illustrate the model on this map and the Magic Kingdom park is not included here for illustration purposes. In this figure, landmarks are the vertices and the lines connecting landmarks are the edges with different weights. As you can see, the landmarks have labels

L_1, L_2 and L_3, and the weights of the edges between them have labels W_1, W_2 and W_3. The landmarks can be generated according to the actual sizes of the areas of the main parks, and the weights are set with the actual transportation times. Dimensions and numbers of attractions are also set for each park. The simulation of the model is applied to the real scenario by this graph theoretical approach, which generates realistic synthetic traces of human mobility for the theme parks included in the scenario.
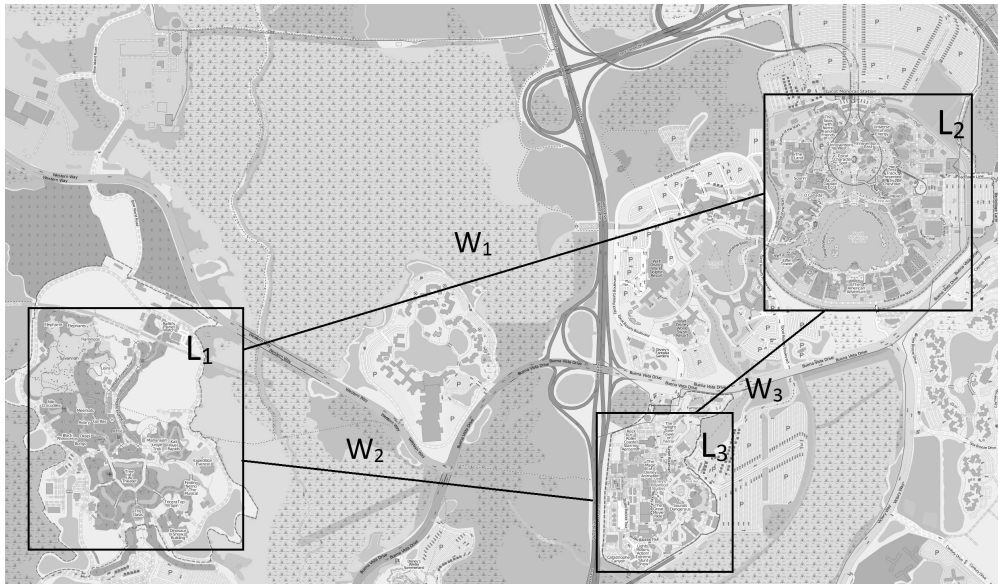
Figure 3.6: An illustration of the application of model to a real-world scenario: Disney World parks in Orlando.

3.2 Simulation Study

3.2.1 Simulation environment and metrics

In this section, the experiments are carried out to validate our mobility model in landmarks and observe the effects of the unique parameters of the model. The simulation of our model generates synthetic mobility traces of visitors in a 2D terrain. The terrain is specified by dimensions, number of attractions and the noise point ratio. Fig. 3.7 shows an output example of a simulation run with 20 mobile nodes, which is taken when simulation time is 3600 seconds.
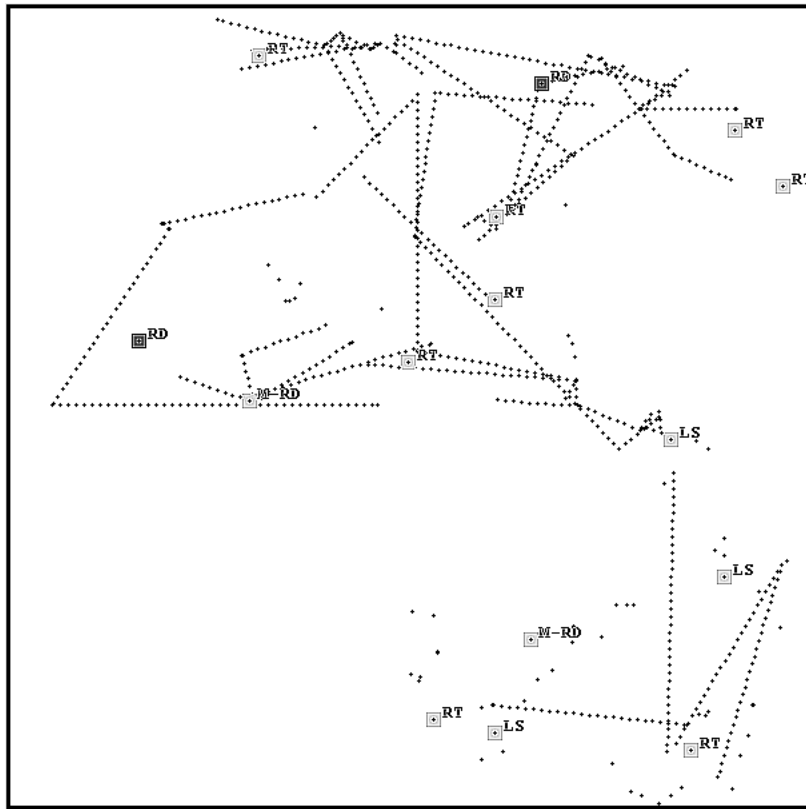
Figure 3.7: Trajectories of 20 mobile nodes after 1 hour simulation time.
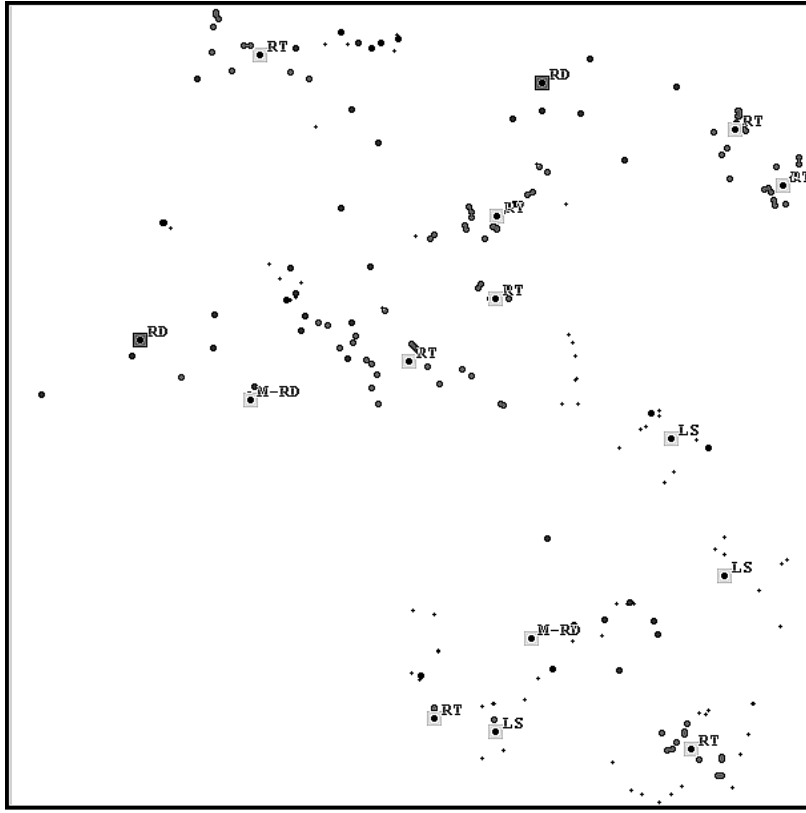
Figure 3.8: Positions of 200 mobile nodes after 1 hour simulation time.

Mobile nodes in the simulation draw their trajectory lines while moving. These trajectory lines are the consecutive points in the figure, which illustrate the movement of the mobile nodes in the landmark. The waiting points are the points of intersections of consecutive trajectory lines. The waiting points are either noise points or they are located inside the attractions. Fig. 3.8 demonstrates another simulation with 200 mobile nodes after 3600 seconds of simulation time. In this figure, by looking at the positions of the mobile nodes represented by small circles, one can observe the expected human mobility behavior to gather in common places, which are the dense regions of fractal points in the model. The

53

use of fractal points and planning trips according to the least action principle represent this social behavior.

We conducted simulations for square landmarks with dimensions of 1000x1000 meters and 2000 mobile nodes. For all experiments, total simulation time is 10 hours with a sampling time of 10 seconds. Mobile nodes have hangout times that are exponentially distributed between 2 hours and 10 hours. For a 1000x1000 landmark, we used 15 queues and approximately 10% noise point ratio. Then we changed these parameter values to observe their effects on the metrics.

We consider three metrics throughout the simulations: 1) flight length that specifies the distance between a pair of consecutive waiting points of a mobile node; 2) number of waiting points that analyzes the wait frequency of a mobile node in a time interval and; 3) waiting time of visitors that specifies the time spent by a mobile node at noise points or inside attractions.

Attractions have two parameters: (expected) service time and number of service channels that represent the number of visitors leaving the attraction per round of service. The number of service channels is set to 40 for main rides (RD = 40), 20 for medium-sized rides (M-RD = 20) and 20 for live shows (LS = 20), unless otherwise specified in the figures. The service times are 60 seconds for rides and restaurants, 120 seconds for medium-sized rides, and 300 seconds for live shows. When a mobile node reaches to an attraction, if the queue is full, the mobile node waits nearby the attraction and enters the queue afterwards.

Initially, the mobile nodes are randomly distributed to the fractal points as their start locations. We assume each mobile node has a constant speed of 1 m/s. Minimum waiting time in a noise point is 30 seconds and Pareto alpha value is empirically set to 1.5. Lee et al. [4] propose using the least-action trip planning on the waypoints of real-life traces to determine the alpha value in Algorithm 1. The same method is applied to the Disney World GPS traces. The alpha value of 3.0, resulting in the minimum error rate, is used in the simulation study. The flight length difference (error rate) is 1.94% for $\alpha = 3.0$. The error rate becomes 6.01% for $\alpha = 2.5$, 22.57% for $\alpha = 2$, and 58.22% for $\alpha = 1.5$.

3.2.2 Simulation results

We conducted simulation experiments and generated synthetic mobility traces of the theme park (TP) mobility model. The mobility traces are analyzed by comparison with 41 GPS traces from the CRAWDAD archive, which are collected from smartphones of 11 volunteers who spent their Thanksgiving or Christmas holidays in the Walt Disney World parks [149]. The average duration of the mobility traces is approximately 9 hours with a minimum of 2.2 hours and maximum of 14.3 hours. The GPS tracking logs have a sampling time of 30 seconds. We filtered out the data, assuming the visitors are traveling by transportation vehicles when they exceed their regular movement speeds during each sampling time. Moreover, we analyzed the validity of the results by comparing them with synthetic mobility traces of SLAW [4] and RWP [144] mobility model simulations. We examine fundamental charac-

teristics of mobility features, including distribution of flight lengths, average flight lengths, distribution of waiting times, and waiting rate (number of waiting points per hour) of the mobile nodes.

For SLAW and RWP, equally sized areas (1000x1000 meters) are used for the comparison with our model. For the GPS traces, we assume that a visitor is not walking if the visitor moves for more than 150m in 30 seconds sampling time, which would exceed the average speed of a person. Accordingly, the data is filtered for the time when the visitors are not walking, but possibly traveling with a bus or another vehicle in the theme park. If a mobile node is in a circular area with a radius of 10m in consecutive sampling times of 30 seconds, we assume that the mobile node is waiting in a waiting point.

3.2.2.1 Flight lengths

A flight length is the distance between two consecutive waiting points of a visitor. A waiting point is defined by an attraction or a noise point. Flight length distribution is one of the most significant characteristics of human mobility models since it reflects the scale of the diffusion. Heavy-tail flight lengths in human travels is shown as the characteristic feature of human mobility in several studies [18, 21]. The flight length distribution results also allow us to make realistic comparisons of human mobility extracted from the GPS traces with other mobility models.

In this experiment, we compared flight length distribution of the TP mobility model with the GPS traces, SLAW and RWP mobility models. The flight length distribution of the GPS traces represents the mobility decision patterns of the real theme park visitors. For instance, the probabilities of theme park visitors to travel to far destination locations (e.g., 400m) as well as their tendency to prefer moving in shorter distances (e.g., 40m) are analyzed with comparisons to the synthetic mobility traces.

The first set of experiments are conducted by using only TP model with the same parameter settings to verify that the output traces of the simulations are consistent. The flight length distributions of 3 randomly selected experiments are given in Fig. 3.9. These experiments have flight length counts between 64000 and 68000; however, all the experiments are normalized to the flight length count of 1000. Flight length distributions are consistent, have similar characteristic, and there is no significant difference between the distribution lines. The experiment shows the similar expected outcomes of the synthetic simulation of the mobility model, among different traces of the simulation model.
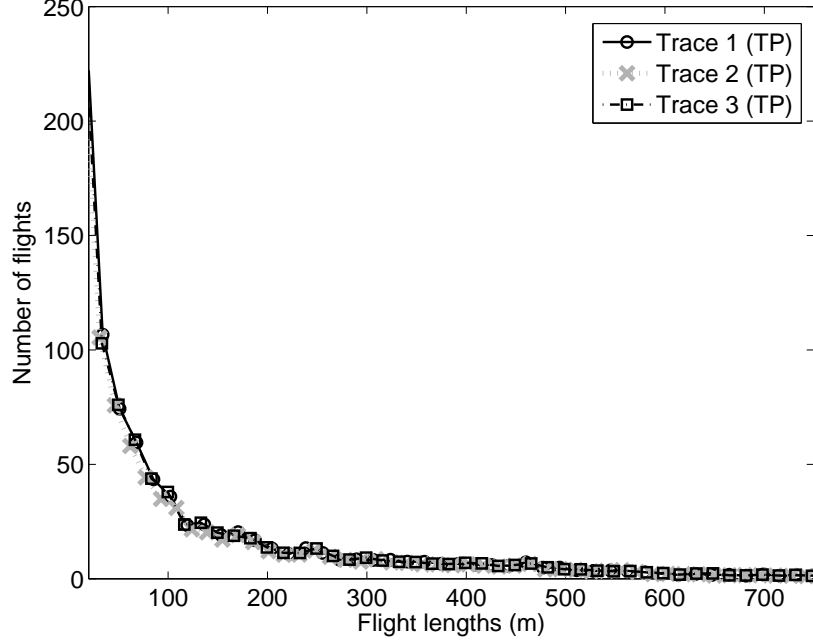
Figure 3.9: Flight length distributions of different traces of TP.

Next, flight length distribution of the simulation model is compared to the GPS traces, SLAW and RWP mobility simulation results. The normalized results of the simulations are given in Fig. 3.10. The flight length distribution of our model is closer to the GPS traces compared to SLAW or RWP mobility models. SLAW has a similar characteristic but shorter flights and RWP model has a uniform distribution. Fig. 3.10 also shows that flight length distributions of RWP model is significantly different than the GPS traces. On the other hand, TP and SLAW mobility models represent heavy-tail flight length distributions.
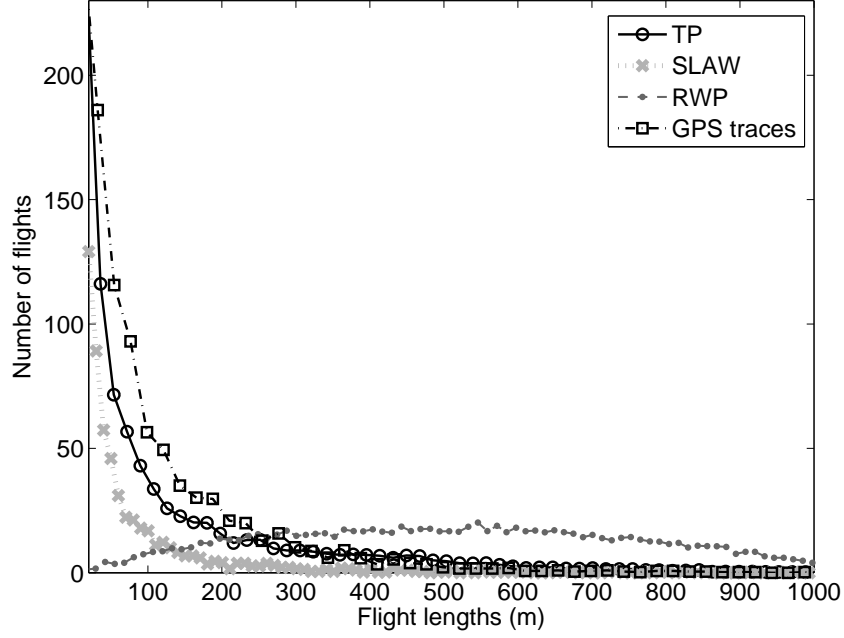
Figure 3.10: Flight length distributions of TP, SLAW, RWP, and the GPS traces.

Fig. 3.11 shows the flight length results of TP, SLAW, RWP, and the GPS traces with the confidence bounds for 3500 outputs of each trace. The average flight length of the mobility model is very close to the results of the GPS traces and the model outperforms the other mobility models. RWP has a very significant difference compared to the other three results. In the 1000x1000 terrain, RWP produced an average value of 500 meters, because of the uniform random selection of next destinations. On the other hand, the flight lengths of SLAW are significantly less than the TP model and the GPS traces. In SLAW model, consideration of all fractal points as waiting points produced shorter flights. Table 3.2 shows the mean, median and standard deviation values of the flight lengths for the mobility models and the GPS traces.
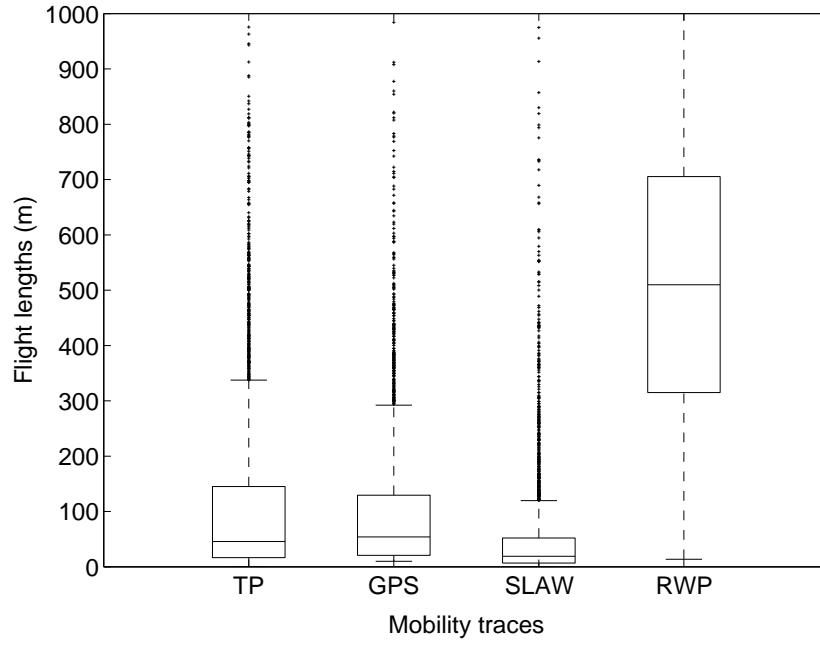
Figure 3.11: Flight lengths of TP, the GPS traces, SLAW and RWP.

Table 3.2: Flight Length Results

	Mean	Median	Standard Deviation
TP	116.6m	45.7m	163.5m
GPS	101.1m	53.9m	132.4m
SLAW	51.5m	19.0m	94.6m
RWP	500.6m	502.7m	254.1m

Additionally, we compared the TP traces to analyze the effects of different parameter values on flight lengths. The unique parameters of TP, number of attractions, noise point ratio, and number of service channels of the attractions are used for the analysis.

We start analyzing the effects of the unique parameters. Fig. 3.12 shows the normalized flight length distributions of TP model with 10, 20 and 30 attractions. We observed that even though the flight lengths do not change dramatically, compared to 10 attractions, the increased number of attractions produced shorter flights for 20 and 30 attractions as the distances between the attractions become shorter.
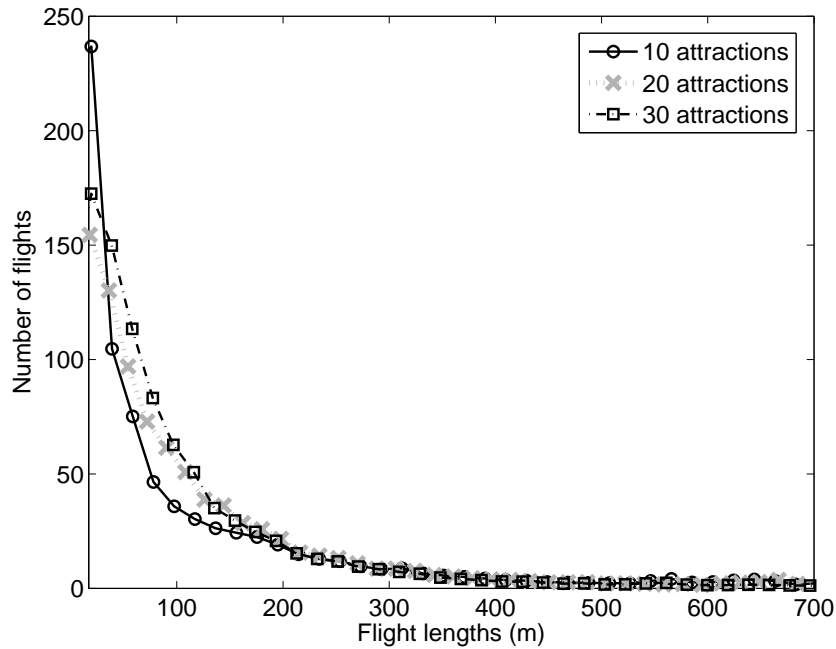
Figure 3.12: Flight length distributions of TP with 10, 20, and 30 attractions.

Noise points represent the waiting points of the visitors between the time of visiting attractions. TP model represents this behavior by giving distant noise points very small probabilities to be chosen as the next destinations, compared to the closer noise points. The effect of the ratio of non-clustered fractal points on flight lengths is shown in Fig. 3.13. In the case of no noise point (0%), the visitors always select an attraction that are distant from

each other. Therefore, 0% noise point ratio produces longer flights. The increase in the noise point ratio causes the increase in the probability of selection of a noise point. Therefore, the increase in noise point ratio shortens the flight lengths of the visitors. The noise point ratio parameter must be configured by using the GPS traces from theme parks for similar mobility traces.
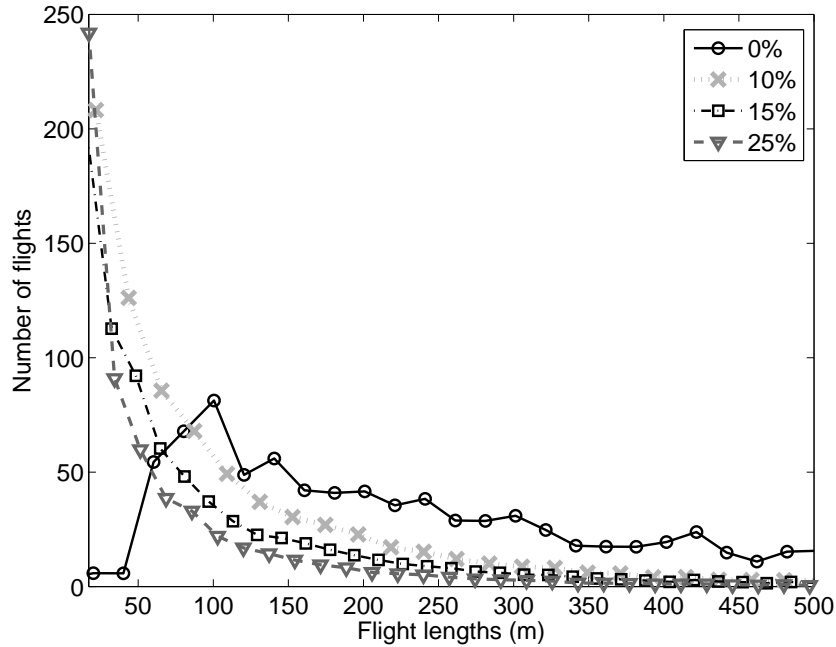
Figure 3.13: Flight length distributions of TP with 0%, 10%, 15%, and 25% noise point ratios.

Fig. 3.14 shows that there is no significant effect of the number of service channels parameter for flight length distributions. The number of service channels effects the waiting time of a visitor in the queue of an attraction, while the waiting time in attraction does not

change the selection of the next destination. RD, M-RD, and LS represents the main rides, medium-size rides and live shows respectively.
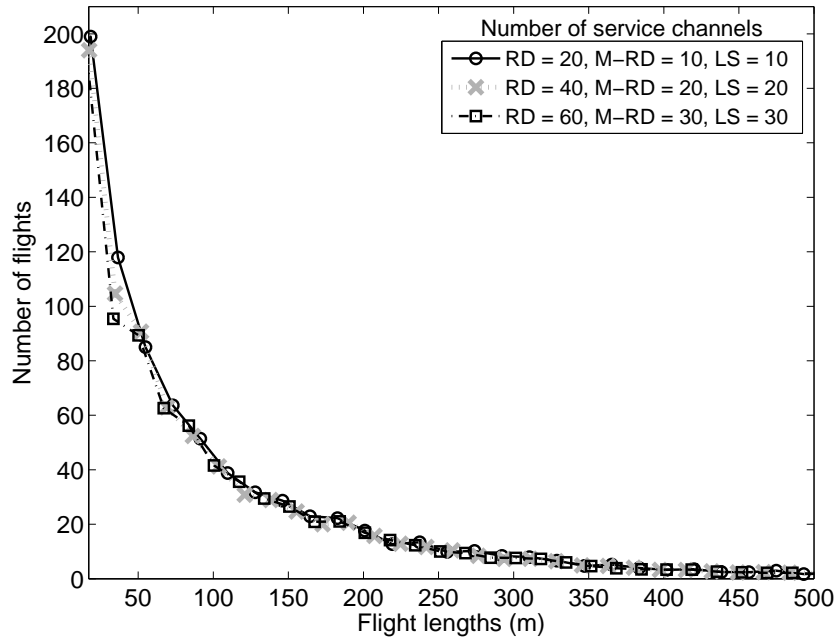
Figure 3.14: Flight length distributions of TP with 3 settings for the number of service channels. (RD = main rides, M-RD = medium-size rides, and LS = live shows)

The number of visitors in theme parks differs according to date and time. If the data for the number of visitors (population size) in different dates is available, the model can be run for each of these dates and the results would reflect the effect of variation in the number of visitors over time. In order to observe the impact of the number of visitors, we conducted simulations of the TP model with various population sizes, ranging from 500 to 10000.

The increase in the number of visitors causes spending more time on the attractions with the fixed service rates. We observe the effect of this parameter on the flight length

distributions in Fig. 3.15. While the parameter does not have a very significant impact on the results, simulations of smaller populations, such as 500, generate traces with shorter flights compared to the larger ones. This is mainly because of spending less time on the attractions. During the hangout times of the 500 visitors, they have extra time to spend in the noise points and traveling to noise points mostly produces shorter flight lengths.
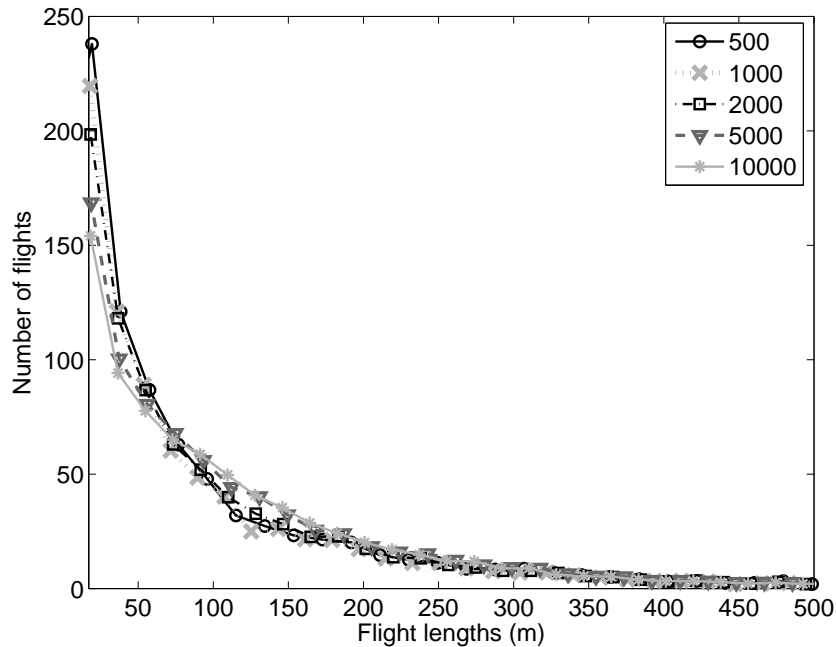
Figure 3.15: Flight length distributions of TP with 500, 1000 2000, 5000, and 10000 visitors.

3.2.2.2 Number of waiting points

In this experiment, we analyzed the number of waiting points averaged for one hour for the 3 models and the GPS traces. Average number of waiting points of the GPS traces is

approximately 10.5, which means every visitor is waiting at roughly 10 different locations in an hour on average. For SLAW mobility model, the average numbers of waiting points are close to 20 doubling the GPS traces, while it is approximately 7.5 for our simulation and 3.3 for the RWP model.

The results of the mobility traces of the models are given in Figure 3.16. Each trace set includes one trace of the models. The figure shows that TP model performs significantly better than SLAW and RWP in terms of waiting rates of the mobile nodes. RWP produces very long flights, 500 m on average, which causes longer times for reaching waiting points. In the SLAW model, on the other hand, mobile nodes move frequently between 1000 fractal points. The TP model combines the behavior of long movements between the attractions, while it allows shorter movements with a probability of visiting noise points. Therefore, the TP model is the best match for waiting frequency behavior of theme park visitors.
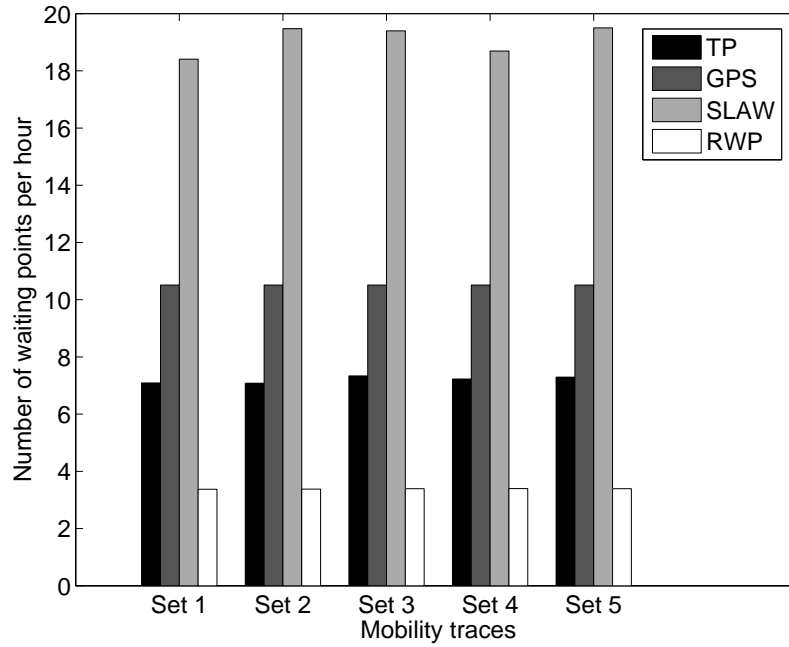
Figure 3.16: Number of waiting points per hour for TP, the GPS traces, SLAW and RWP for 5 trace sets.

Furthermore, we analyzed the effect of the parameters on the number of waiting points. In Fig. 3.17, the increase in the number of attractions slightly increases the number of waiting points since the attractions become closer to each other, the flight lengths become shorter. Thus, the visitors' ability to visit more attractions increases.
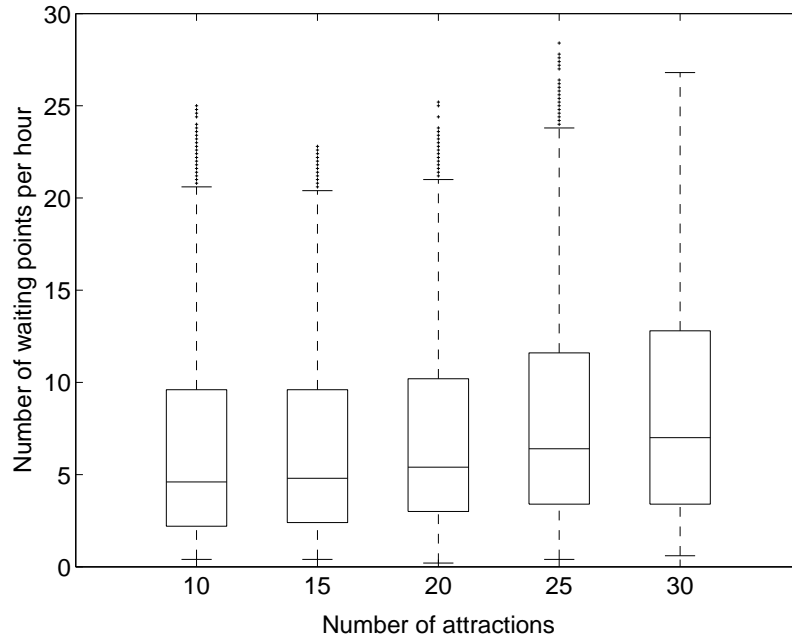
Figure 3.17: Number of waiting points per hour for TP with 10, 15, 20, 25, and 30 attractions.

Fig. 3.18 includes the results for noise point ratios ranging from 0% to 25%. The noise point ratio has a significant impact on the number of waiting points. As the ratio increases from 10% to 25%, the mean value of the number of waiting points increases approximately by 50%. On the other hand, 0% noise ratio causes the smallest mean value of the number of waiting points. Along with the longer flight lengths, the proportion of the visitors who spend time in attractions becomes higher. This causes longer waiting times in queues for the visitors.
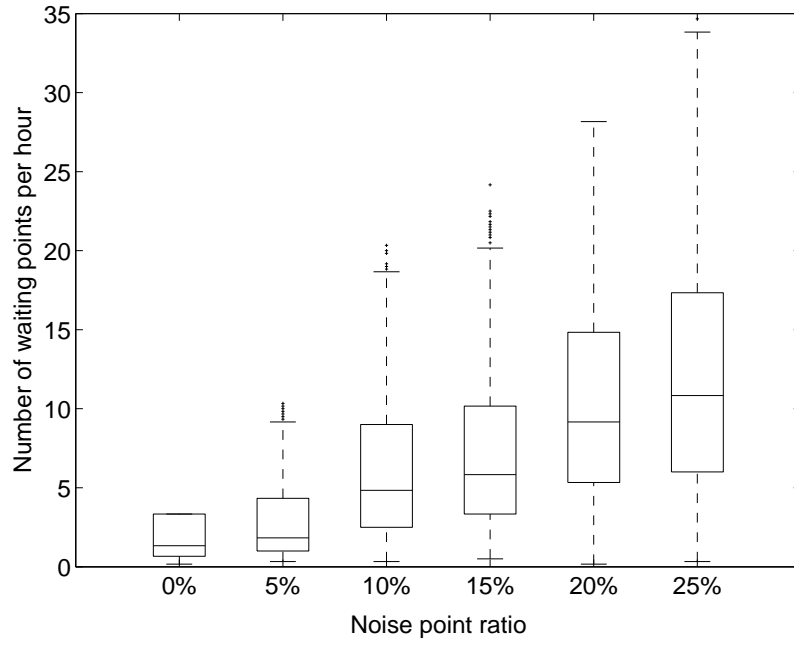
Figure 3.18: Number of waiting points per hour for TP with different noise point ratios.

As the number of visitors leaving the attractions in a round of service increases, the waiting time of the visitors in the queues of crowded attractions decreases. As shown in Fig. 3.19, the number of waiting points per hour increases. However, the effect on the number of waiting points is limited with the decrease of waiting times in the attractions. Higher numbers of service channels in attractions do not produce shorter flights.
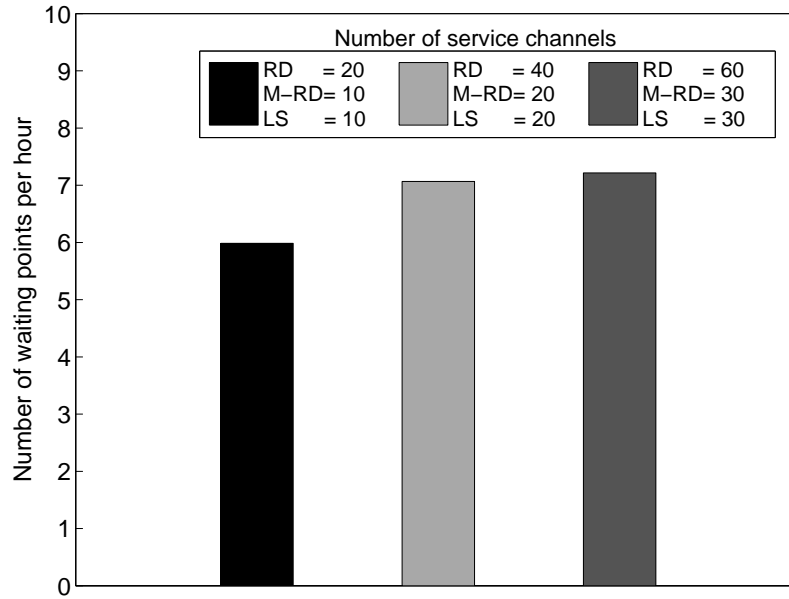
Figure 3.19: Number of waiting points per hour for TP with 3 settings of the number of service channels. (RD = main rides, M-RD = medium-size rides, and LS = live shows)

Fig. 3.20 shows the results of the average number of waiting points for the population sizes ranging from 500 to 10000. The population size changes the number of waiting points significantly because it affects the waiting times in the attractions. Average number of waiting points becomes approximately 1.5 per hour for 10000 visitors.
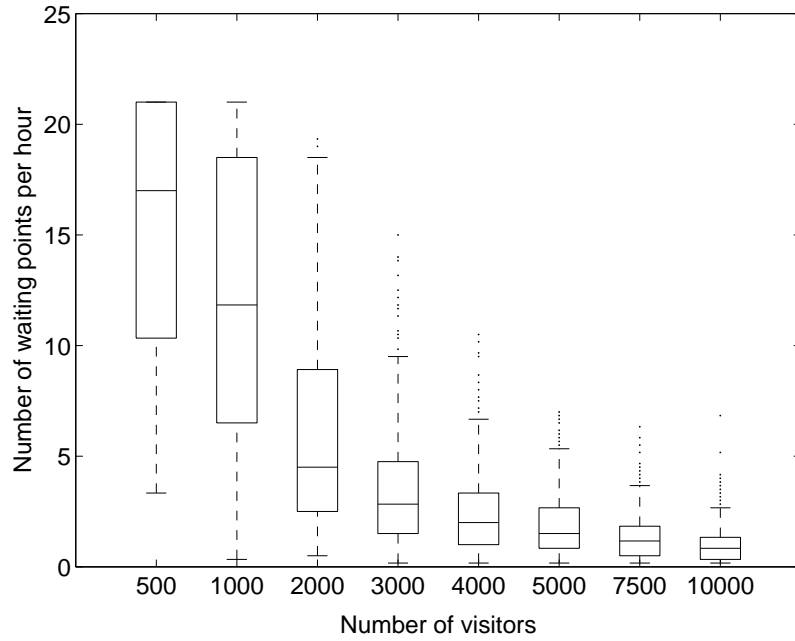
Figure 3.20: Number of waiting points per hour for TP with different numbers of visitors.

3.2.2.3 Waiting times

There are several studies on the waiting times in human walks. These studies [150, 151] show that the waiting times follow a truncated power-law distribution. While we reflect this in our model for waiting times in noise points by generating the waiting times synthetically, the waiting times in attractions are determined according to the service rates and the number of people in the queues. In this experiment, we compare waiting time distributions of TP with the GPS traces and SLAW. Due to constant waiting time of the mobile nodes, we did

not include the RWP model in this experiment. The results are normalized to 1000 waiting times.

Fig. 3.21 shows that waiting time distribution of the proposed model is similar to the GPS traces. Compared to SLAW, TP and the GPS traces have shorter waiting times. The results of the GPS traces start at 30 seconds, due to the 30 seconds sampling time. By setting noise point ratio, number of attractions, and number of service channels parameters realistically, one can obtain more accurate results to represent the real-world scenario of theme park visitors mobility.
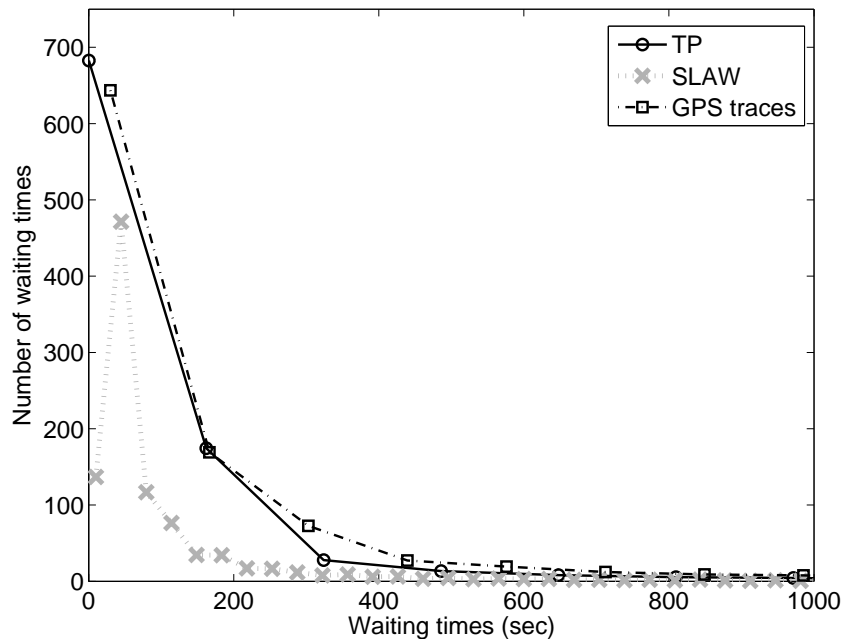
Figure 3.21: Waiting time distributions of TP, SLAW, and the GPS traces.

Fig. 3.22 shows the waiting times of the TP model with 10 to 30 attractions. We observed that the number of attractions does not have a significant effect on the waiting

times as the waiting times stay at approximately the same level. This is due to a tradeoff between visiting more attractions and having less number of people in the queues. Visiting more attractions cause longer average waiting times since the waiting times in noise points is mostly shorter. On the other hand, as the people are distributed to more attractions, fewer people wait in each queue and therefore waiting times in the queues decrease.
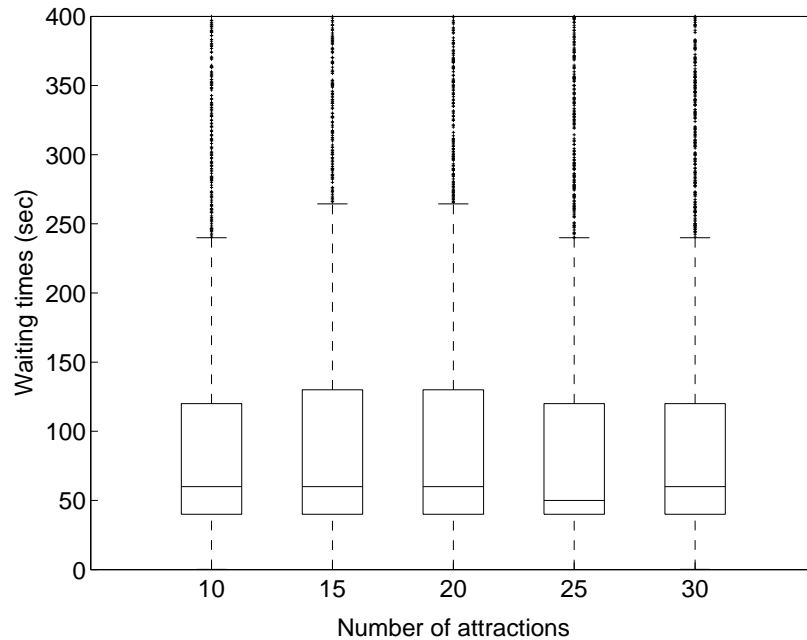
Figure 3.22: Waiting times of TP with 10, 15, 20, 25, and 30 attractions.

As shown in Fig. 3.23, noise point ratio does not have a significant effect on the waiting times, since the waiting times are mostly effected by the attractions. Still, the waiting times become slightly less because the probability of waiting in a noise point increases. Moreover, the standard deviation becomes smaller. This result shows that variation of the waiting

times at noise points is smaller than the variation at attractions. The waiting time in an attraction highly varies because of the number of people waiting in the queue.
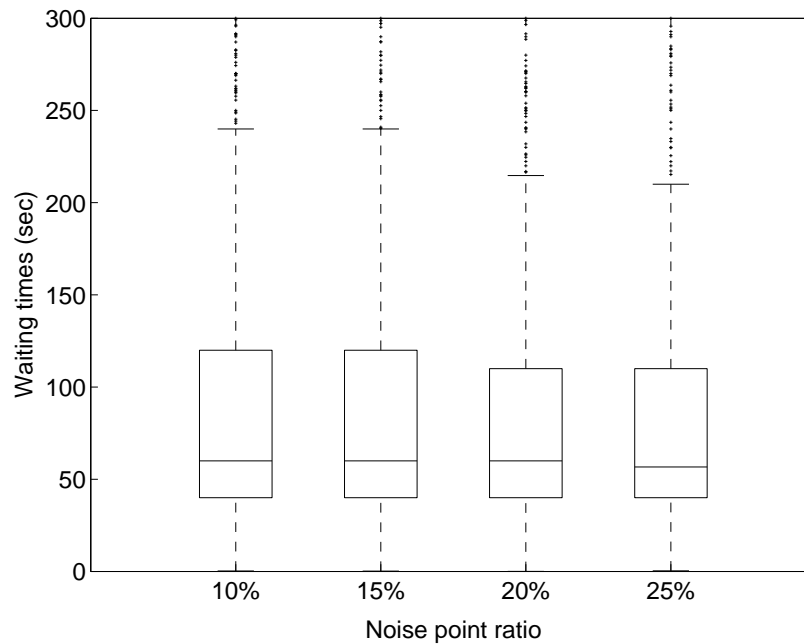
Figure 3.23: Waiting times of TP with 10%, 15%, 20%, and 25% noise point ratios.

Fig. 3.24 shows the waiting time distributions of TP model with 3 settings of the parameter, the number of service channels. Comparing the first setting which is 20, 10, and 10 for main rides, medium-sized rides, and live shows respectively, with the third setting, it can be seen that waiting times of the first setting is higher than the third one. Since the attractions serve more people with higher numbers of service channels, the waiting times at the attractions decrease. This effect becomes more significant with the decrease in the number of attractions and with the higher numbers of mobile nodes.
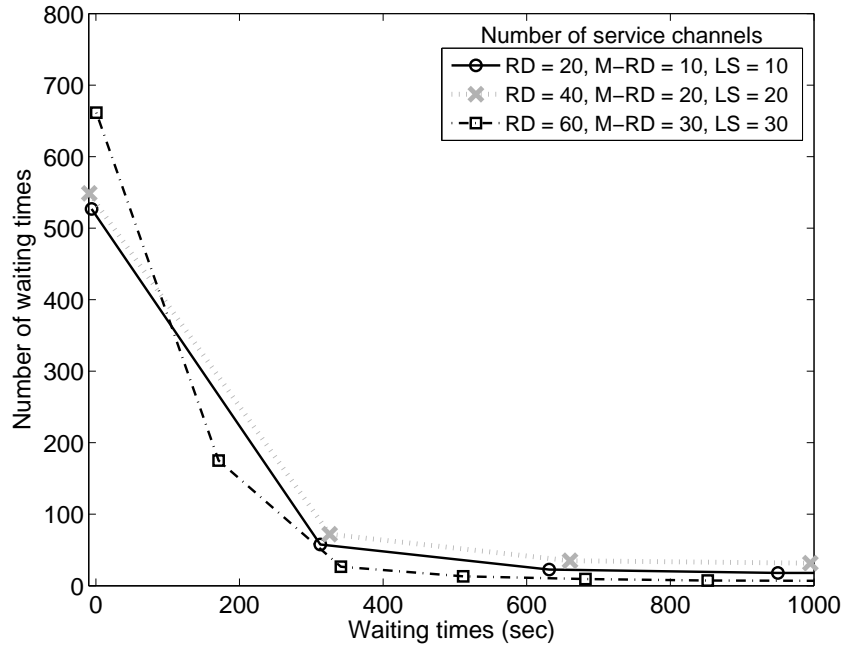
Figure 3.24: Waiting time distributions of TP with 3 settings of the number of service channels.

The waiting time distributions of our model w.r.t. the population size is shown in Fig 3.25. More people in a theme park cause longer waiting times, because of sharing the same attractions. As it can be seen in the figure, waiting times increase with the increased population sizes. While attractions do not cause significant waiting times for 500 visitors, they require on average 15 minutes and up to 2 hours waiting times for 10000 visitors. On the other hand, some attractions with less popularity may still not require longer waiting times.
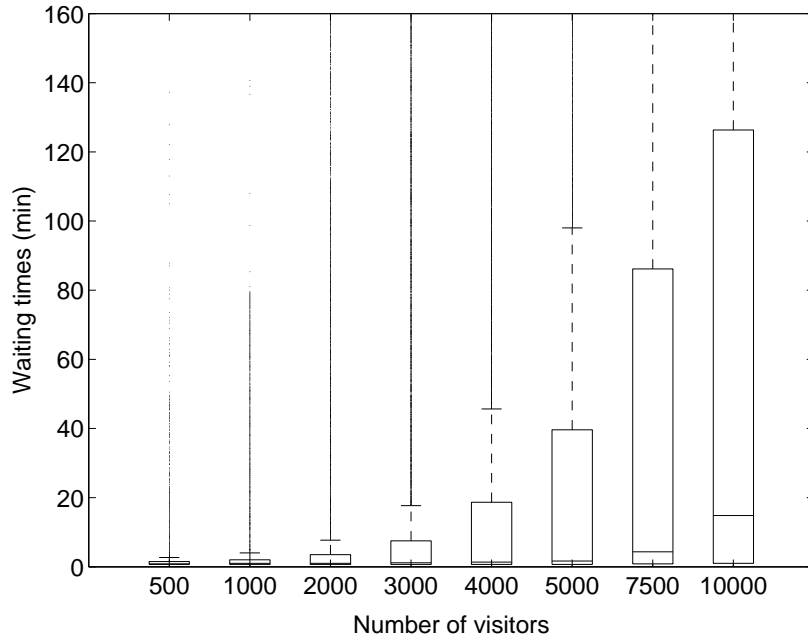
Figure 3.25: Waiting times of TP according to number of visitors from 500 to 10000.

Overall, we observed that the proposed model outperforms SLAW and RWP for the specified metrics, compared to the GPS traces. Moreover, the model gives a consistent performance. Among the tested parameters, noise point ratio is the most effective one, as it has a direct effect on the probability of selecting attractions as the next destinations. As expected, population size affects the waiting times and the average number of waiting points since more people cause increase in waiting times at the attractions.

3.3 Concluding Remarks

In this chapter, we presented a model for the movement of visitors in a theme park. In this model, we combined the nondeterministic behavior of the human mobility with the deterministic behavior of attractions in a theme park. We divided the attractions into groups of main rides, medium-sized rides, live shows and restaurants. We used queueing-theoretic models to calculate times spent by visitors at different attractions. We validated the accuracy of our model through extensive simulations using theme park statistics, the GPS traces collected in Disney World theme parks, and the data generated by simulations of other mobility models. The results show that our model provides a better match to the real-world data compared to SLAW and RWP.

We believe that an important outcome of our work is the generation of realistic mobility traces of theme park visitors for theme parks with various scales. The techniques developed in this chapter can be used to model human mobility in places which restrain people from using transportation vehicles. These places include airports, shopping malls, fairs, and festivals. For instance, in airports, travelers usually spend time and walk between the pre-determined places (hot-spots), such as check-in locations, restaurants, gates, and security check points.

By studying human mobility, we learned that the mobility behaviors of people in various environments produce significantly different movement patterns. While networks

with human participants are becoming increasingly popular, there is still a need for further research in human mobility models.

CHAPTER 4
HUMAN MOBILITY IN DISASTER AREAS

In this chapter, we propose a mobility model of theme park visitors in disaster scenarios [9–11].

Theme parks are large and crowded areas with thousands of daily visitors. Particularly, large-scale theme parks attract visitors from all over the world, and the theme park industry is one of the main contributors of their regions. While overall popularity of theme parks and the size of the industry are growing every year, the global success of theme parks is severely affected by disasters such as Hurricane Irene [152]. Considering the fact that climate change increases the risk of extreme events such as forest fires and floods [153], effect of disasters may cause damages to the regions such as Central Florida. This region has 5 of the top-10 theme parks with highest attendances in the world, while being home to various natural disasters with a history of hurricanes, floods, tornadoes, and tropical storms.

The studies on disaster recovery and opportunistic communication networks have become major research interests due to their prospective contributions on the disaster management strategies. For instance, as an impact of a disaster, communication infrastructures which are pre-deployed in the area may become unoperational. For this reason, communication systems independent from the infrastructures are taken into account in many disaster

management studies. Crowd management and evacuation of people from disaster areas are other major challenges which have theoretical and practical interests from the research community. Modeling disaster mobility in theme parks is useful for finding novel methods to solve the evacuation problem in theme parks. In addition, these methods may become the base-case for the evacuation problem of more complicated scenarios such as evacuation of people from buildings and evacuation from big cities.

We consider a wide range of disaster scenarios for theme parks. These scenarios include natural disasters such as tornado, fire, thunderstorm, hurricane, and earthquake. Moreover, we consider man-made disaster scenarios such as terrorist attacks which may threaten human lives in crowded places. While effects of these various types of disaster may differ from one another, the major goal of the operators will be safe and quick evacuation of visitors and providing them access to transportation vehicles.

We presented the model for the visitor movements in theme parks in Chapter 3 to represent daily routine mobility of theme park visitors without any consideration of the disaster scenarios. However, in our previous model and the other currently used theme park mobility models, the movement decisions of the visitors are based on visiting the attractions and exploring the park. Considering disaster scenarios, the movement decisions should be based on the security of visitors. The main goal of the theme park operation include finding easy ways to secure places and fast evacuation of the visitors from the disaster areas.

Outcomes of the simulation of the proposed model are mobility traces of theme park visitors. Since the proposed mobility model serves as a baseline, it does not take any type

of internal and external support to the theme park visitors into account. On the other hand, the effects of various possible disaster response approaches can be tested using our mobility model. Placing informative signs in strategic locations to direct the visitors to desired regions, having trained security personnel to manage crowd flows or forming visitor groups by assigning one trained person to lead each group can be considered as examples of disaster response strategies. Furthermore, autonomous robots can be used for missions such as search and rescue. Another use of our model is evaluating performances of networks resilient to disasters such as opportunistic social networks which are formed for broadcasting messages and increasing knowledge of the visitors.

In this chapter, we present the mobility of visitors in theme parks for disaster scenarios. We describe the model in detail in Section 4.1. In this section, we model theme park as a combination of roads, obstacles, lands, and red-zones using real theme park maps. To model the visitor movements, we consider the macro and micro mobility decision problems separately. We use the social force model [43] to represent the dynamics of the human motion by the social interactions. We analyze the simulation results of our model in Section 4.2 and compare it with the currently used mobility models and the GPS traces collected from theme park visitors. We conclude in Section 4.3.

4.1　Mobility Model

In this section, we present the human mobility model in theme parks for disaster scenarios. Let us first describe the characteristics of theme parks and creation process of the theme park models. Later, we will describe the mobility of the visitors in detail.

4.1.1　Characteristics of theme parks

To give a background on the problem, we first describe the fundamental characteristics of theme parks by looking from the mobility modeling perspective. Theme parks consist of attractions which are entertainment places including rides, restaurants, and places for other activities. Attractions consist of man-made structures (i.e. buildings) and they are connected to each other by roads (i.e. pedestrian ways). The roads also connect the entrance and exit points of the theme park with the attractions. They are usually used only by pedestrians, specific for theme park environment. Each road has a width which determines the capacity of the road for pedestrian flows. For instance, if a road is narrow and there are many people, the density of the people becomes large and as a result people cannot move fast enough along the road.

Theme parks are open-air areas but can also have buildings such as indoor rides, restaurants and gift shops. The area of theme parks include many physical obstacles for pedestrians. The physical obstacles include man-made and natural obstacles. People who

spend their day in theme parks have activities such as visiting rides, walking among the attractions along the roads, and eating at the restaurants.

Due to the nature of the large and crowded area, a natural or man-made disaster may have devastating effects. As a disaster response strategy, in time of a disaster, the main goal is secure and fast evacuation the visitors from the theme park. Considering an example of tornado alert in a crowded day, the visitors should leave the park to reach the transportation services located outside the park. Since there are thousands of people leaving the park, the mobility of a single pedestrian cannot be considered independent from the other people. Therefore, social interactions between the pedestrians, which may cause slowdowns in pedestrian flows, should be considered for realistic mobility modeling.

The evacuation problem of theme parks is different from other evacuation problems. For instance, in a city scenario, the main purpose is fast evacuation of the city by the effective share of streets by cars and public transportation services. Other types of evacuation scenarios focus on indoor evacuation, such as evacuation from buildings or from rooms of a building. On the other hand, the evacuation problem of theme parks includes large areas with physical obstacles and high numbers of pedestrians. As expected, the mobility of pedestrians during disasters has many differences compared with the ordinary mobility of people. Because of the aforementioned characteristics, theme parks require scenario-specific mobility modeling for evaluating performance of networks in disaster times as well as simulating and testing various evacuation strategies.

4.1.2 Theme park models

Let us now start describing the theme park model for disaster scenarios. We model the theme park as the combination of roads, obstacles, lands, and disaster events. Each road contains a set of waypoints, which are the movement points for the theme park visitors. In this case, length of a road is equal to the sum of the distances between each pair of its consecutive waypoints. The roads direct the visitors to the target locations in the map. The gates are considered as the target locations and they are placed close to the borders of the park. The gates connect the theme park with the outside world and facilities such as transportation vehicles (i.e. ambulances, fire engines).

As mentioned, attractions contain man-made buildings and other structures such as a roller-coaster. In the ordinary times, the main goal of the visitors is to visit the attractions. For the disaster scenario in which the visitors should be evacuated from the disaster area as quickly as possible, we consider the buildings as the obstacles which prevent the free movement of the visitors. Furthermore, we model the man-made structures other than the buildings in the park such as fences and walls as the obstacles. There are also natural obstacles in the environment, such as lakes, trees, forest, river, and so on. We do not focus on the evacuation problem from the buildings and assume that visitors do not spend time in the attractions after having a disaster alert.

The areas which neither include the obstacles nor the roads are classified as the lands. The lands can be used by pedestrians but they are not preferred unless there are unexpected

conditions on the available roads. For instance, when a road is unavailable due to an impact of the disaster event, the lands might be chosen instead. In some exceptional cases, lands provide shortcuts between the waypoints. Disaster areas are classified as the red-zones and represented by the circular areas reflecting the effects of the disaster. In a real scenario, one can think the red-zones as the events which damage roads or bridges, caused by an earthquake, a hurricane, a fire, a terrorist attack and so on. The red-zones have radius values which specify the damaged areas and active times. If a red-zone is in its active time and it effects an area including some portions of a road, the road is assumed to be unavailable at that particular time.
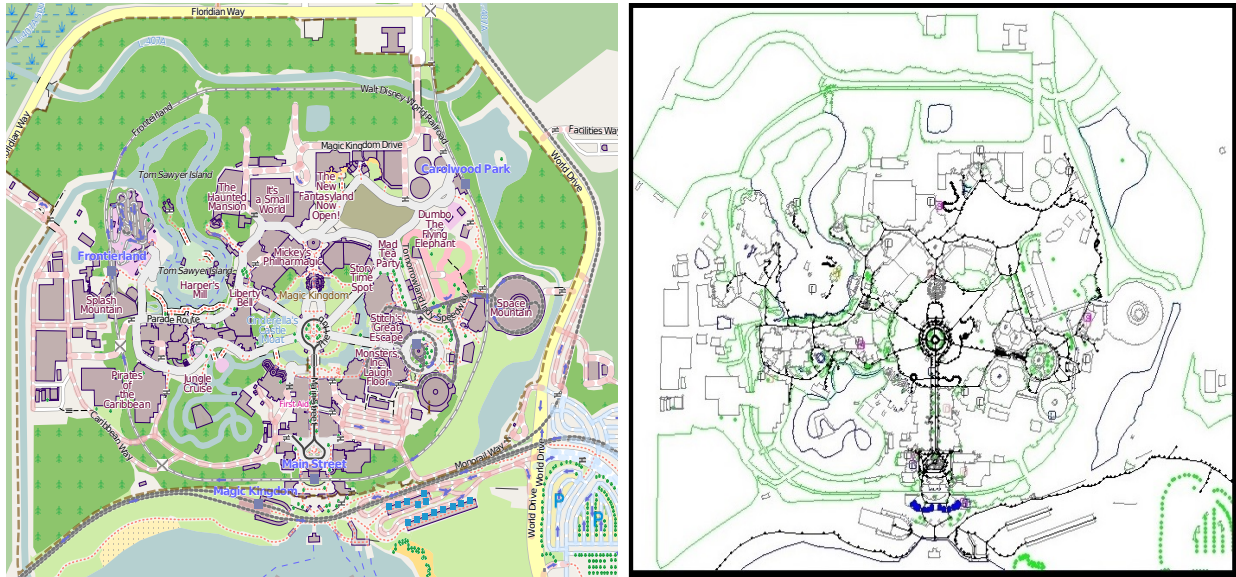
Figure 4.1: The maps of the Magic Kingdom park. Left: the map extracted from (OSM), right: the processed map with 1300 waypoints.

The model of the theme park can be created synthetically or using real maps. We choose to use OpenStreetMap (OSM) [148] to extract the real theme park maps and parse

the OSM data to generate the roads, the obstacles, the lands, and the gates. We collect the waypoints using the OSM data and connect the consecutive waypoints to create the roads. We assign width values to the roads according to their OSM types (footway, path, and pedestrian way). Fig. 4.1 and Fig. 4.2 displays examples of the real maps of the Magic Kingdom and Epcot parks from the Disney World in Orlando (left-side), and the processed version of the maps including the waypoints, the roads, the gates, and the obstacles (right-side).
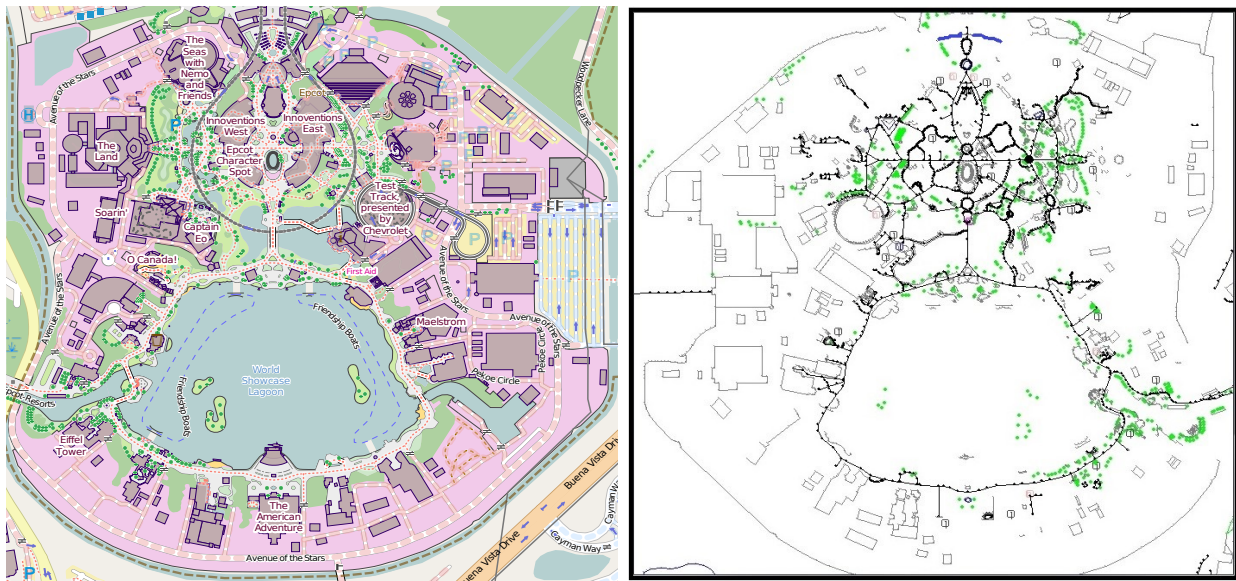
Figure 4.2: The maps of the Epcot theme park. Left: the map extracted from (OSM), right: the processed map with 2300 waypoints.

In Fig. 4.1 and Fig. 4.2, the small dots represent the waypoints, while the lines connecting the waypoints are the roads and the closed polygons are the obstacles. The model also include red-zones which are added to the model according to their active times; however, they are not included in this initial processing of the maps. The two gates can

85

be seen as the two small thick lines close to each other. The generation of the theme park models are done computationally, but it is possible to create a non-existing theme park in design stage manually and create the theme park model in the same fashion.

4.1.3   Mobility of the visitors

We describe the mobility behavior of the visitors as follows. The visitors have the local knowledge of their environments and the knowledge of the position of the gate which they are entered through. The local knowledge of the visitors is determined by the maximum visibility parameter which shows the visible distance for each visitor and the obstacles which may be located along the way. The maximum visibility parameter represents the radius of the circular visible area. The visitors are not assumed to communicate with each other and there is no broadcasting system for raising the awareness.

Initially, the visitors are randomly distributed to one of the waypoints in the theme park model. Each visitor selects an exit gate among the available exit gates in the park and mark its position as the target point. A visitor is assumed to be evacuated after reaching one of the exit gates. The visitor tries to reach the target point by moving among the waypoints. Whenever the visitor reaches a waypoint, marks it as visited. The next destination point is selected among all the visible waypoints. The visited waypoints, the waypoints positioned in a red-zone or the waypoints which are not in the visible area of the visitor are not taken into consideration as the candidates for the next destination point. The visitor selects a new

waypoint according to its distance and direction from the current position of the visitor since the visitor tries to select the destination point closer to the target.

The selection of the waypoints is constrained by the the visitors knowledge about the world, obstacles, and possible active red-zones along the way. If a visitor cannot find any waypoint as a candidate for the next destination, the new destination is selected by exploration with a random direction. The random exploration distance is a parameter which bounds the movement flexibility of the visitors in cases of the unexpected disaster events. Another parameter which effects the flexibility the most is the maximum visibility parameter. The visibility may differ according to the type and the impact of the disasters. We assume that the visibility may also differ during the disaster event by time and location of the visitor and therefore randomly set the visibility with the upper bound of maximum possible visibility throughout the simulation. We classify all the above steps of a visitor considering the global movement starting from the initial point to the target point as macro-mobility behavior of the visitors.

The speeds of the visitors differ from one to another. Basically, each visitor has a maximum speed which depends on physical attributes of the individual such as age, gender, and weight. The speed of each individual is a random value between a global minimum and global maximum speed of the visitors. The speed of a visitor varies from 0 to maximum speed. On the other hand, the global minimum value determines the slowest person's maximum speed. The maximum speed is the speed when the visitor is completely free to walk without disturbance or the obstacles. In the disaster scenario, the actual speed of a visitor is less

than the maximum speed most of the times due to the effects of the social interactions which are explained below.

Fig. 4.3 illustrates the complete theme park model generated using the map of the Epcot park in Disney World. In this figure, the visitors and the red-zones are included in the model. 20 visitors moving along the roads are represented by the triangles. The shapes of the triangles illustrate the directions and velocities of each of the visitors. The red-zones are represented by the big circles. On the left figure, the two red-zones having an intersection area appeared as an enlarged red-zone, located in the middle of the figure.
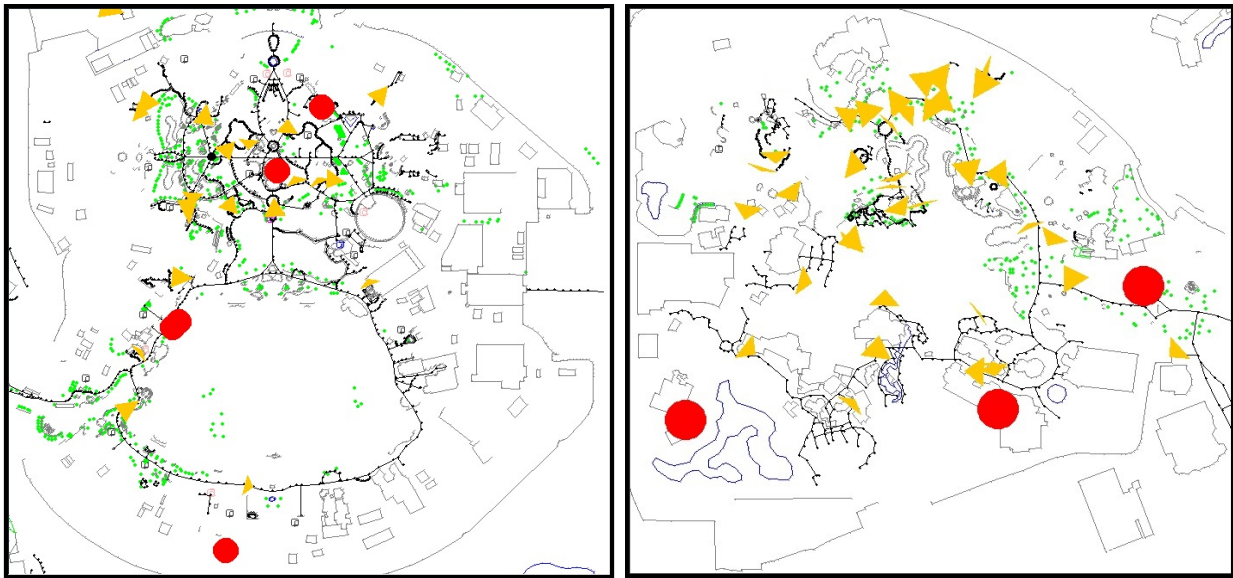
Figure 4.3: Illustrations from the mobility model. Left: Epcot simulation with 20 visitors and 5 red-zones. Right: Islands of the adventure with 40 visitors and 3 red-zones.

We consider micro-mobility as the mobility of a visitor between the two consecutive waypoints separately from the macro-mobility model and the theme park model. We use the social force model (SFM) [43] which is used by the simulators such as SimWalk and

VisSim for the micro-mobility. According to the social force concept, behavioral changes in the human motion can be explained and is actually caused by the combination of the social interactions. Using the SFM, we model the social forces on the visitors according to their social interactions with the environment. By this model, the visitors adapt their speed and direction of the movement from a waypoint to another. In SFM, the sum of the social forces is given by

$$f_\alpha(t) = \frac{1}{\tau_\alpha}(v_\alpha^0 e_\alpha^0 - v_\alpha) + \sum_{\beta(\neq\alpha)} f_{\alpha\beta}(t) + \sum_i f_{\alpha i}(t), \tag{4.1}$$

for a visitor α where τ_α denotes the relaxation time, $v_\alpha^0 e_\alpha^0$ is the desired velocity, and the sums correspond to the social forces by the other visitors (β) and the obstacles (i) respectively. The acceleration is then given by $f_\alpha(t)$ and the individual fluctuations. Assuming $f_{\alpha\beta}(t) = f(d_{\alpha\beta}(t))$, circular specification is given by

$$f(d_{\alpha\beta}) = A_\alpha e^{-d_{\alpha\beta}/B_\alpha} \frac{d_{\alpha\beta}}{\|d_{\alpha\beta}\|}, \tag{4.2}$$

where A_α, B_α denote the interaction strength and the interaction range respectively.

For the elliptical specification of the model, the circular specification formula is expressed as a gradient of an exponential decaying potential $V_{\alpha\beta}$, where elliptical interaction force via the potential is $V_{\alpha\beta}(b_{\alpha\beta}) = ABe^{-b_{\alpha\beta}/B}$. In this equation, $b_{\alpha\beta}$ is the semi-minor axis of the elliptical equipotential lines and given by

$$2b_{\alpha\beta} = \sqrt{(\|d_{\alpha\beta}\| + \|d_{\alpha\beta} - y_{\alpha\beta}\|)^2 - \|y_{\alpha\beta}\|^2}, \tag{4.3}$$

where $y_{\alpha\beta} = (v_\beta - v_\alpha)\Delta t$ and $\Delta t = 0.5s$.

$$f_{\alpha\beta} = -\nabla_{d_{\alpha\beta}} V_{\alpha\beta}(b_{\alpha\beta}) = -\frac{dV_{\alpha\beta}(b_{\alpha\beta})}{db_{\alpha\beta}} \nabla_{d_{\alpha\beta}} b_{\alpha\beta}(d_{\alpha\beta}) \tag{4.4}$$

Equation 4 gives the repulsive force and $\nabla_{d_{\alpha\beta}}$ denotes the gradient w.r.t. distance between α and β. Using chain rule, this leads to

$$f_{\alpha\beta(d_{\alpha\beta})} = A_\alpha e^{-b_{\alpha\beta}/B} \cdot \frac{\|d_{\alpha\beta}\| + \|d_{\alpha\beta} - y_{\alpha\beta}\|}{2b_{\alpha\beta}}$$
$$\cdot \frac{1}{2} \left(\frac{d_{\alpha\beta}}{\|d_{\alpha\beta}\|} + \frac{d_{\alpha\beta} - y_{\alpha\beta}}{\|d_{\alpha\beta} - y_{\alpha\beta}\|} \right). \tag{4.5}$$

Considering the angular dependence between two encountered visitors, with an angle of $\varphi_{\alpha\beta}$, the angular-dependent pre-factor $w(\varphi_{\alpha\beta})$ is given by the below equations

$$\cos(\varphi_{\alpha\beta}) = \frac{v_\alpha}{\|v_\alpha\|} \cdot \frac{-d_{\alpha\beta}}{\|d_{\alpha\beta}\|} \tag{4.6}$$

$$w(\varphi_{\alpha\beta}(t)) = \left((1 - \lambda_\alpha) \frac{1 + \cos(\varphi_{\alpha\beta})}{2} + \lambda_\alpha \right), \tag{4.7}$$

where the parameter λ_α with $0 \leq \lambda_\alpha \leq 1$ is found by evolutionary optimization as $\lambda_\alpha \approx 0.1$. The fitness of the social force model increases with the addition of the angular dependence formulation to the model.

As a consequence of SFM, the time it takes for the visitor to move to a destination point varies. The main impact of this model in the theme park scenario is that the usage of the same roads by the visitors causes an increase in the social interactions. This increase slows down the flow of the visitors along the roads. Since the theme parks are crowded areas with roads in which only pedestrian movements happen, the social force model is the best-fit

90

model to represent the crowd dynamics and the micro-mobility behavior for the evacuation of the visitors in theme parks.

We illustrate the overall mobility behavior of a visitor according to the model in Fig. 4.4. Initially, the visitor starts with setting the target location by selecting the gate point. After deciding the target location, the visitor tries to find waypoints in the visible local region and selects the best candidate if waypoints exist or sets a random point with the random exploration distance parameter. Micro-mobility phase, which is based on SFM, starts after deciding the next destination and ends whenever the visitor arrives the next destination. If the arrived location is not the target location, the movement continues by exploration of the local region, while in the case of reaching the target location, the visitors is marked as rescued.

4.2 Simulation Study

In this section, we discuss the evaluation of the mobility model. Our simulation study includes experiments and analysis from two simulations. The first is a mobility simulation in which we simulated the proposed mobility model along with other mobility models and GPS traces of theme park visitors and discussed in Subsections 4.2.1 and 4.2.2.
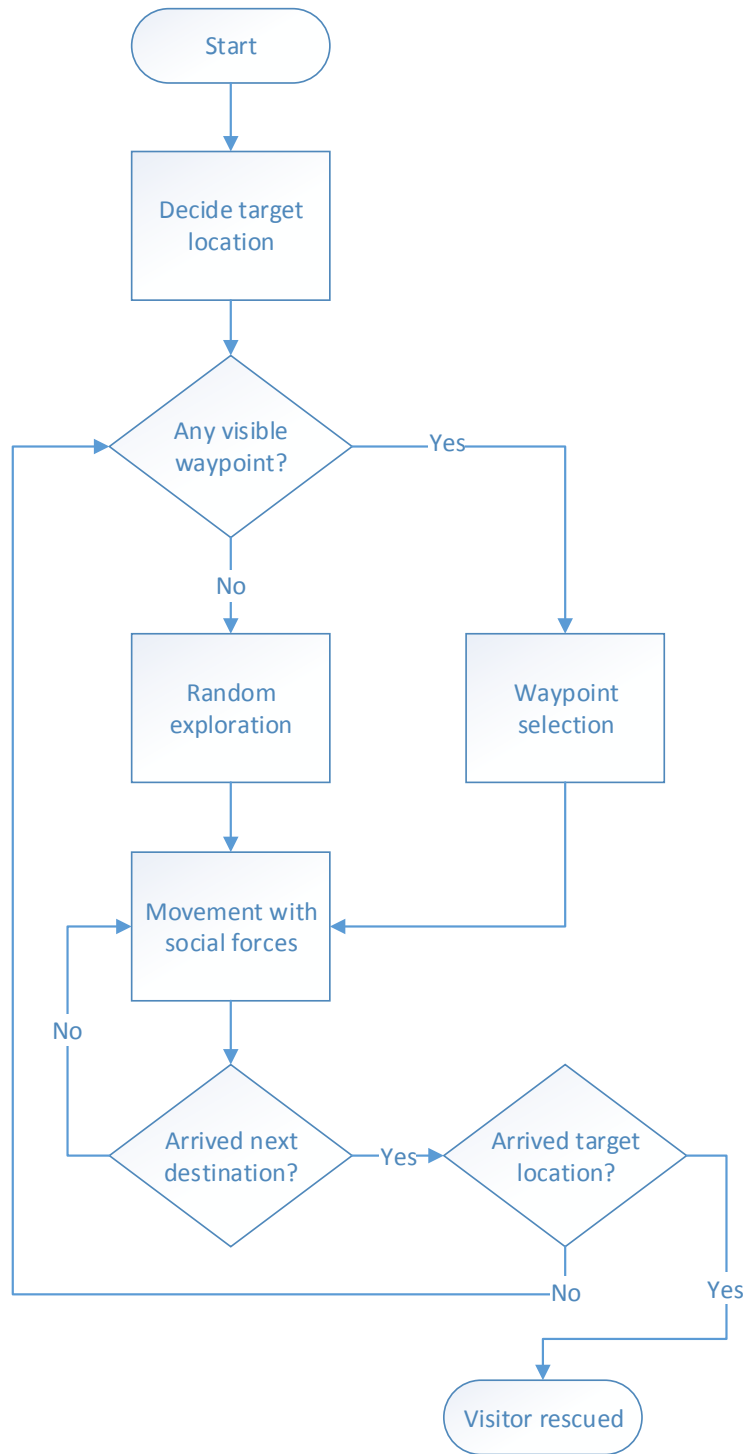
Figure 4.4: Mobility behavior of a visitor during the simulation of the model.

4.2.1 Mobility simulation setup

There are several mobility metrics used in the literature. These metrics can be classified in three types: movement-based, link-based, and network-based metrics. In the mobility simulation, we focus on the movement- and the link-based metrics. The movement-based metrics are usually extracted from analyzing individuals' movement patterns. Flight lengths, average velocity, waiting times, mean-square distances are among the movement-based metrics. The link-based metrics analyze the effects of the mobility w.r.t. the relations between the mobile nodes such as their distances from each other. Average node density, variance of node density, average pairwise distances, relative mobility are examples of the link-based metrics. The network performance-based metrics show the effects of the mobility on the performance of the networks.

The simulations of our model of theme park mobility for disaster scenarios (TP-D) are carried out to observe its characteristics. We then compare TP-D with the currently used mobility models and the 41 GPS traces from Disney World. The average duration of the mobility traces is approximately 9 hours with a minimum of 2.2 hours and maximum of 14.3 hours. The GPS tracking logs have a sampling time of 30 seconds. The traces are filtered in such a way that when a visitor is moving very fast, we assumed the visitor is in a vehicle traveling from one park to another. The remaining data is used for finding the set of flight lengths of each visitor where the flight length is defined as the distance between a pair of consecutive waypoints of a visitor.

The theme park mobility model (TP) [8] and self-similar least action human walk model (SLAW) [4] are used as realistic mobility models to simulate ordinary movement of theme park visitors. Random waypoint (RWP) model [144] is used as a generic model since it is the most commonly used mobility model in the network simulations.

Fig. 4.5 shows a snapshot from the simulation of 2000 visitors. The simulation of the model generates synthetic mobility traces of visitors in the terrain specified by the theme park map. The visitor in the theme park draws their trajectory lines while moving upon the waypoints with the goal of arriving at the gates. The dimension lengths of the maps vary from one park to another. For instance, the dimensions are close to 1000x1200 meters for Epcot and Magic Kingdom and approximately 650x750 meters for Islands of Adventure park of the Universal Studios. We used the theme park model of the Magic Kingdom in the experiments with 10000 visitors. We employ the circular specification of the SFM with the angular dependency using the same parameter values proposed in [43].

While we do not consider visitors whose escape time is more than 1000s as successfully evacuated, we include the output from all pedestrians in our averaged results such as the average evacuation times. Therefore, simulation time is empirically set to 2000s as in this duration almost all pedestrians achieve to arrive at their final destinations and consider the ones who may still stay in the disaster area as the outliers. Table 4.1 summarizes the default mobility simulation parameters and the parameters used for the SFM in the experiments.

Table 4.1: Mobility simulation parameters

simulation time	2000s
sampling time	10s
number of visitors	10000
min speed	0.0m/s
max speed	1.0m/s
number of red-zones	50
red-zone active time	1000s
red-zone radius	100m
random move distance	10m
max visibility	100m
wireless communication range	40m
SFM - interaction strength (A)	0.11 ± 0.06
SFM - interaction range (B)	0.84 ± 0.63
SFM - relaxation time (τ)	0.5s
SFM - λ	0.1
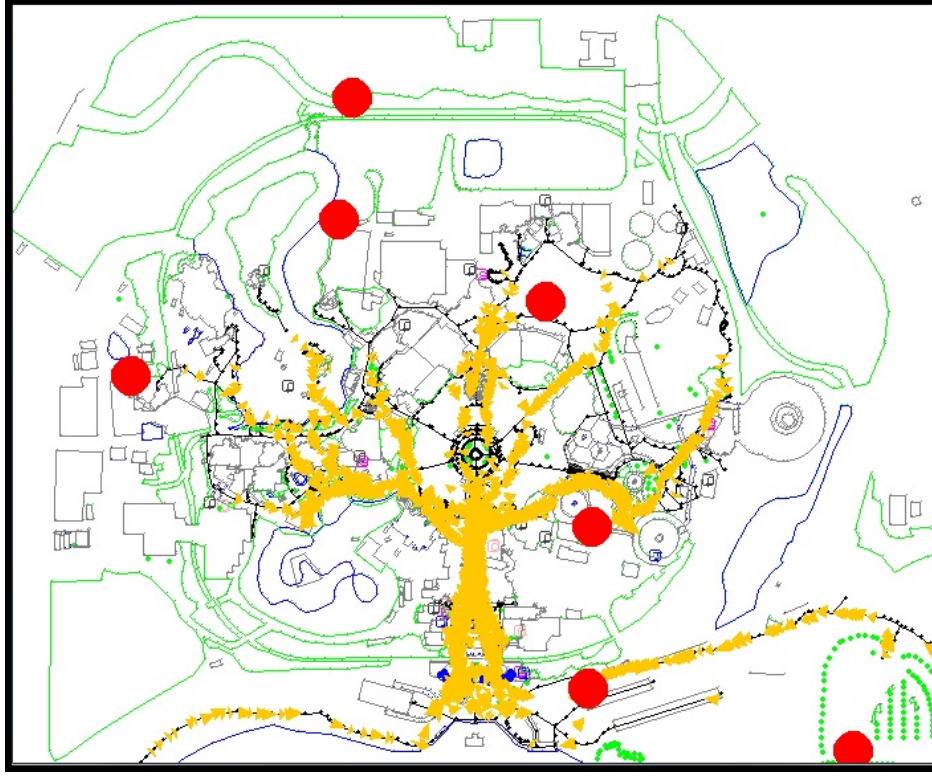
Figure 4.5: The simulation of 2000 visitors and the impact of red zones in Magic Kingdom.

4.2.2 Experimental results of the mobility model

4.2.2.1 Movement-based analysis

We start our evaluation with flight lengths metrics. A flight length is the distance between a pair of consecutive pause points of a visitor in its trajectory. Flight length distribution is one of the most commonly used metrics for human mobility models since the lengths of the movement of people and their diffusion in the system have significant effects on the performance of the mobile networks. For calculating the flight lengths, the consecutive

slowdown locations of the visitors are generated when they move less than 5m radius for more than 10s duration.

We first simulate flight length distributions of the TP-D model. We observed that the results of the simulation of the model for different simulation runs are almost identical, which shows the overall consistency of the simulation. Fig. 4.6 shows this consistency for the probability distribution function (PDF) of flight lengths among the 5 simulation runs which are randomly selected from a set of simulation runs having the same parameter settings. Moreover, Fig. 4.6 reveals that more than 50% of all flights are shorter than or equal to 50m and more than 20% are shorter than or equal to 100m. Hence, we observe a shorter flights due to frequent waiting in the pedestrian traffic caused by 10000 visitors.
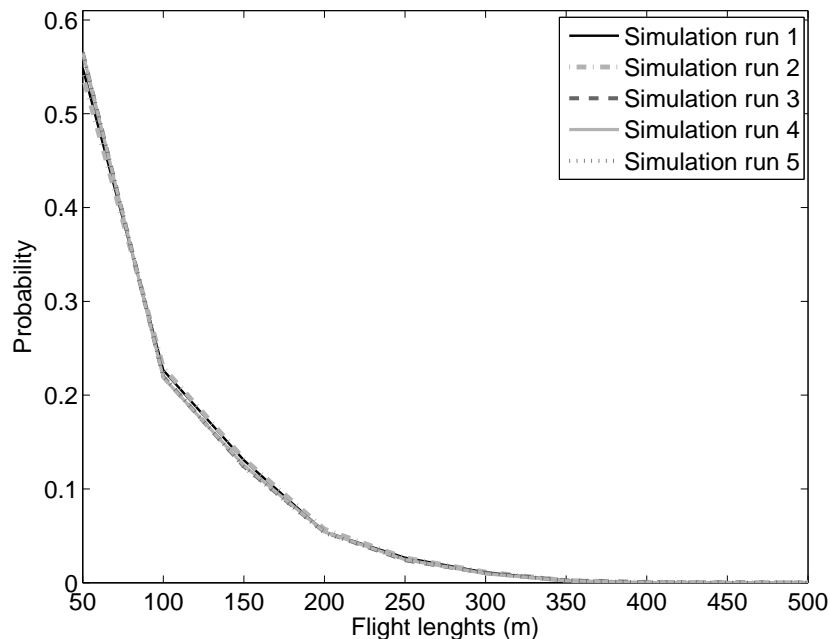
Figure 4.6: Flight lengths probability distributions of TP-D for 5 simulation runs.

We compared the flight length values of TP-D with TP, SLAW, RWP and the GPS traces. Fig. 4.7 shows PDF of flight lengths. We observed that the TP-D model produced shorter flight lengths compared to the TP model and the GPS traces. The SLAW model produced the shortest flight lengths due to the high density of fractal points used as waypoints of the simulation. However, the TP-D model produces outcomes closer to TP and the GPS traces. Being a mobility model which is specific to evacuation situation of disasters, TP-D interestingly has a similar flight length distribution. Moreover, all three models (TP-D, TP, SLAW) and the GPS traces have mostly lower than 200m flight lengths. On the other hand, RWP produces dramatically longer flight lengths with an average flight length of 500m and it can be classified as the most unrealistic model among the 4 models due to its very significant mismatch with the GPS traces.

The mean values of the flight lengths with variations are shown in Fig. 4.8. The mean flight length value and the variation of TP-D is lower than TP and the GPS traces and higher than SLAW. Considering the difference between the ordinary movement of a visitor for the model TP and the GPS traces, flight lengths vary with the choices of the visitors such as visiting an attraction or going to the nearest restaurant. On the other hand, for the disaster scenario, the visitor has the only goal of moving towards the target locations as much as possible with the traffic. Due to the lack of choices and the similar traffics in the crowd flows of different roads, the lower variability with shorter flights is an expected outcome of the TP-D model.
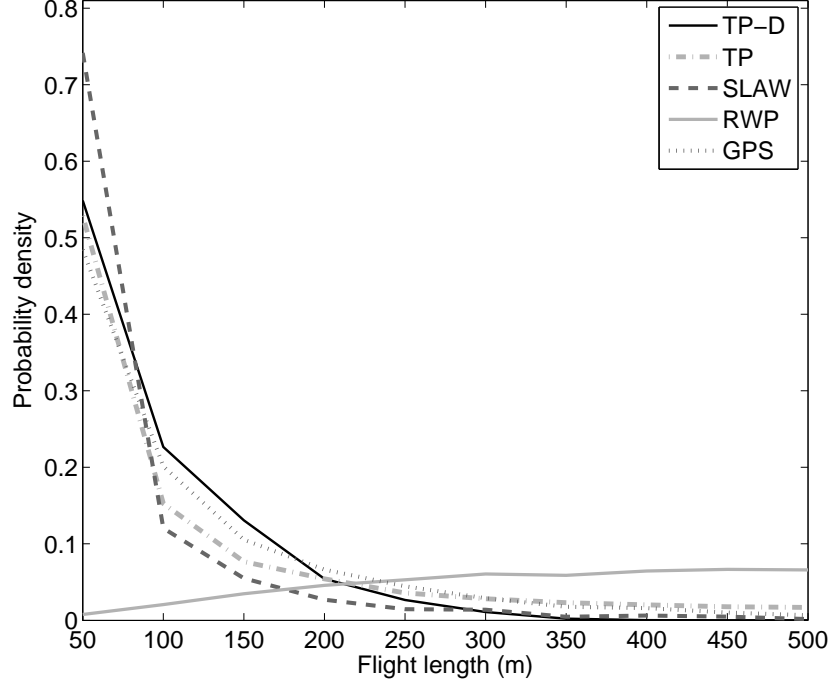
Figure 4.7: Flight length probability distributions of TP-D, TP, SLAW, RWP, and the GPS traces.

4.2.2.2 Link-based analysis

Node degree of a pedestrian is defined as the number of neighbor pedestrians. The neighbors of the pedestrian are the ones who are in the communication range with the pedestrian. In other words, two neighbors are assumed to have a wireless communication link between them if they are in the communication range of each other. Average node degrees is a link-based metric calculated as the average of the results of all pedestrians. Instead of comparing each individuals' node degrees, we observe the effects of mobility on the overall average by simulation time. Basically, a higher average node degree yields a better network

performance. We assumed a transmission range of 40m. To be fair in the comparison of average node degrees, the results are normalized to 1000 visitors in each model.
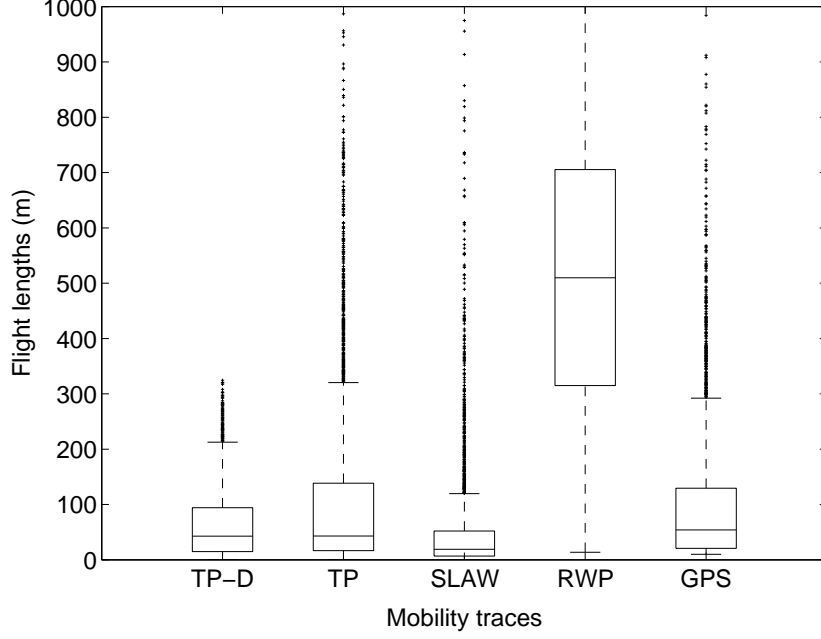
Figure 4.8: Mean values of variations of flight length results of TP-D, TP, SLAW, RWP, and the GPS traces.

Fig. 4.9 shows the average node degrees by the simulation time for TP-D, SLAW, TP, and RWP. All the mobility models generated distinct characteristic changes in node degrees w.r.t. the simulation time. TP-D has the highest average node degree along with SLAW at the initial phase since the mobile nodes are the initially distributed only on top of the roads while other models distribute the visitors to the entire area. We also see that the average node degrees stay close to the same level without a significant change, while the values may vary in short period of times. The main reason of the significant increase in node degrees

in the TP model is the gathering behavior of visitors in the attractions. In TP, visitors start waiting in the queues very close to each other and therefore we see higher average node degrees after 2000s. In TP-D, however, pedestrians travel along the roads together, which do not produce the effect of the gathering behavior. SLAW model has an initial phase of 500s and the results converges to a constant level. While the gathering behavior of SLAW is not visible for 40m communication range, it is observed for longer ranges. RWP stays constant with some variances in short times caused by the randomness.
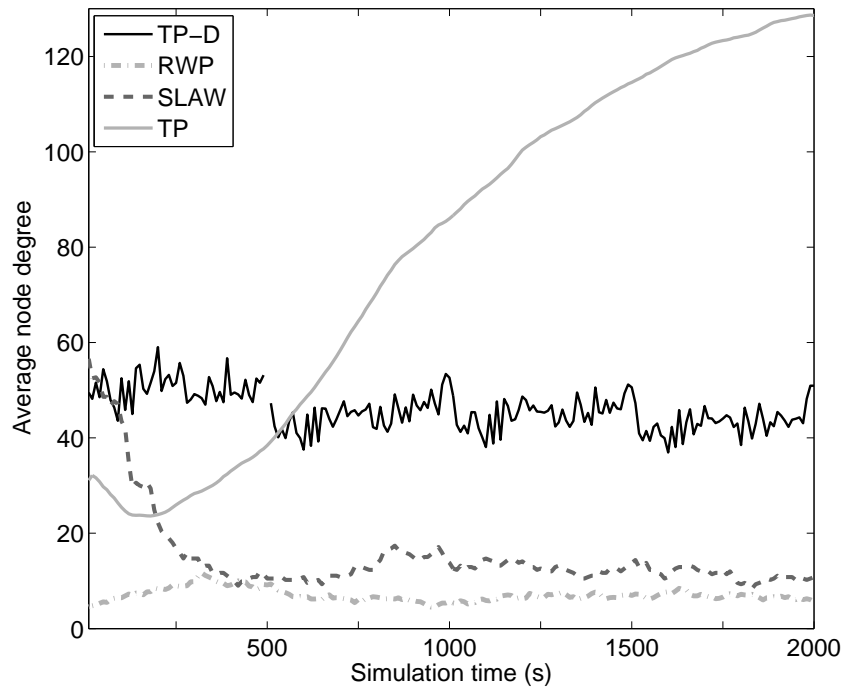
Figure 4.9: Average node degrees by simulation time for TP-D, TP, SLAW, RWP, and the GPS traces.

We analyzed the average node degrees with various transmission ranges to see the possible effects of the mobility of the visitors on the performance of networks in various simulation times. Fig. 4.10 reveals that for various transmission ranges (25m, 50m, 75m and 100m), average node degree stays consistent throughout the simulation with the fluctuations which also exist in the previous results. Moreover, as an expected overall effect of the transmission range parameter, average node degrees increased for higher transmission range values.
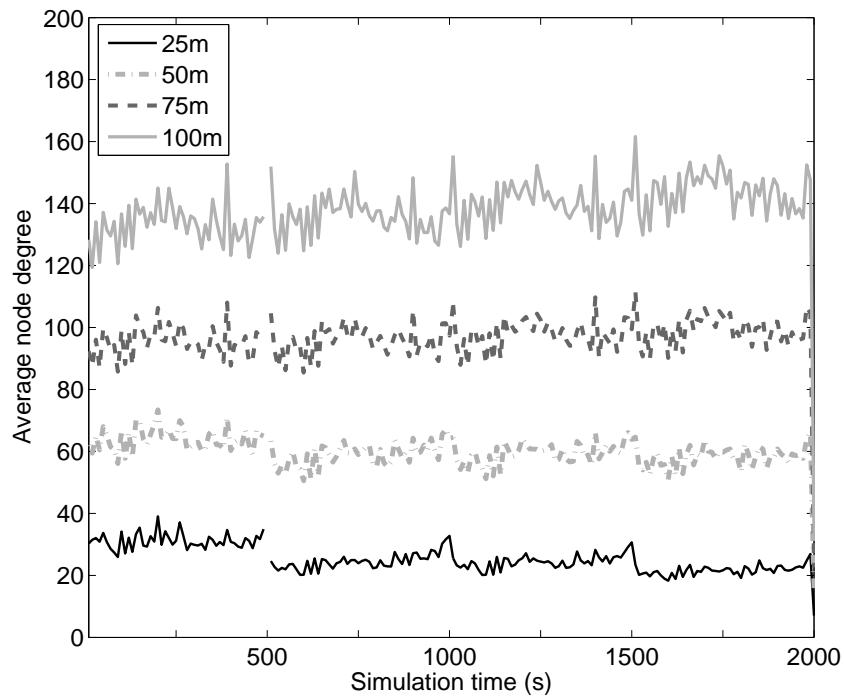
Figure 4.10: Average node degrees by simulation time for transmissions ranges 25m, 50m, 75m, and 100m.

The distances between all pairs of mobile nodes are averaged to calculate average pairwise distances. As a link-based metric, average pairwise distance helps us to evaluate the closeness of a node to another on average. This metric shows the possibility to form a new network with a desired subset of all the mobile nodes. Smaller pairwise distances are expected for better network performances. As in the average node degree results, we observed the effects of the mobility on the results by simulation times.

As it can be seen in Fig. 4.11, all the models again have distinct characteristics. TP-D has a consistency with an small overall constant decay of average pairwise distances. As also observed in the previous experiment, the pedestrians becomes closer to each other as the time passes. An interesting difference of this experiment compared to the previous one is that the significance of the change in the results of TP becomes weaker. This is because of the consideration of all people for each individual. For instance, when a visitor goes to an attraction, the pairwise distance with the other people in the same attraction becomes smaller, while the visitor's pairwise distance with all the other people in other attractions of the park may become larger. In TP-D, on the other hand, people mostly move towards the similar target locations. Furthermore, since we consider the pedestrians who reached the exit gates as removed and do not take them into consideration, the fast increase due to the gathering behavior does not exist in TP-D. After the initial phase of 500s, SLAW and RWP models reach steady-states having constant average pairwise distances with some variances due to randomness in the models.
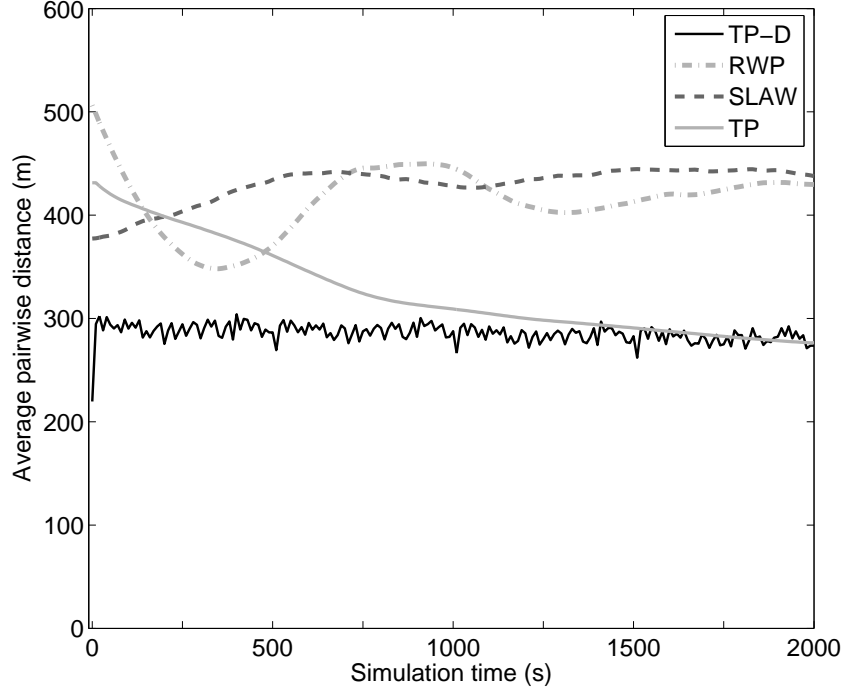
Figure 4.11: Average pairwise distances by simulation time for TP-D, TP, SLAW, RWP, and the GPS traces.

4.2.2.3 Evacuation performance

Evacuation time is the time it takes for the visitors to reach the target (exit) points from the beginning of the simulation. The results of the evacuation times are analyzed for various values of the visibility and the number of red-zones parameters. The simulations of TP, SLAW and RWP are not used for analysis, since these models do not involve the evacuation of the environment.

In order to see the impact of the local knowledge, we compare the TP-D model with various maximum visibility values. We see in Fig. 4.12 that the increase in the visibility

causes an overall decrease in evacuation times as expected. However, after the maximum visibility value of 80 meters, this effect loses its significance.
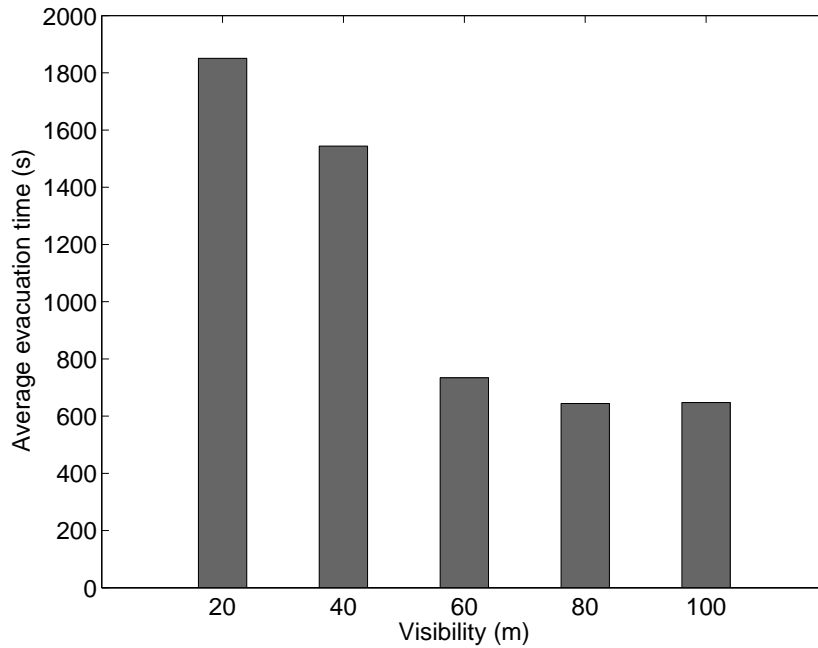
Figure 4.12: Effects of the visibility on evacuation times.

As shown in Fig. 4.13, we observed the relation between the number of red-zones and the evacuation times. The higher numbers of red-zones constantly produce the higher evacuation times, which is an expected negative effect of the red-zones. The reason behind this negative effect can be easily observed by looking at the snapshot of the visitor flows in Fig. 4.5. Among the 7 currently active red-zones which are randomly positioned, 2 of them are located in a way that they prevent the regular flow of the visitors. This impact of preventing the visitors from moving along the road and tunneling them to other ways is the reason for the increase in the average evacuation times. Since red-zones are generated

105

at random regions of the map, in some simulation runs red-zones happen to occur on top of the roads and therefore produce significantly higher evacuation times as in the 200 red-zones example shown in Fig 4.13.
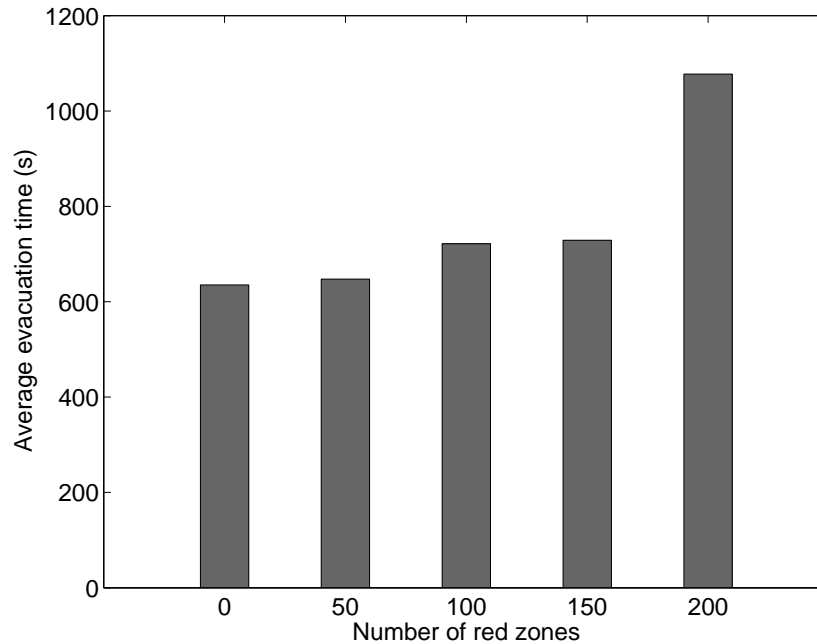
Figure 4.13: Effects of the number of red-zones on evacuation times.

We define the evacuation success ratio as the ratio of the number of visitors who were evacuated in less than a specified time limit. We assume that the visitors who could not reach the gates in the acceptable time are not successfully evacuated. We set time limit as 1000s and analyze the evacuation success ratio according to the visibility and number of red-zones parameters.

Fig. 4.14 shows the evacuation success ratios with 20, 40, 60, 80 and 100m maximum visibility. As it can be seen in the figure, increased visibility produce higher evacuation

106

success ratios. Specifically, from 20m to 40m, the success ratio increases more than two times and the maximum visibility value of 60m allows the dynamic flow of the visitors with a 75% success ratio. The significance of the increase decreases dramatically for values higher than 60m. Because of the fact that visibility plays a very important role in the evacuation time and success ratio, the parameter should be set according to the specific disaster which is simulated. While the limitation caused by various types of disasters in the vision of pedestrians is not a scope of this study, this should be further investigated for realistic simulations.
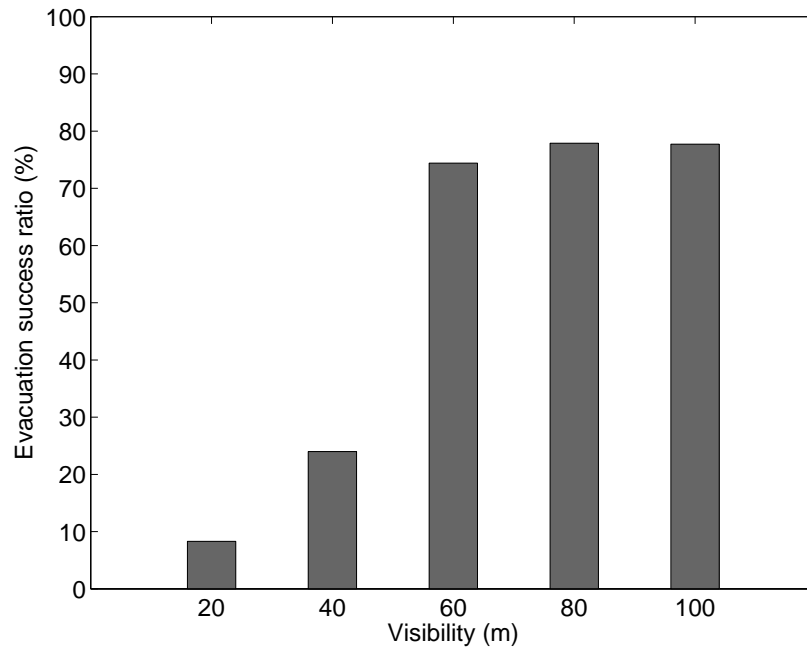
Figure 4.14: Effects of the visibility on evacuation success ratio.

Fig. 4.15 shows the evacuation success ratios with no red-zone and 50, 100, 150 and 200 red-zones. The success ratio drops from approximately 80% to 40% with 200 red-zones

compared to the 0 red-zone which is the case of no direct disaster impact in any region of the theme park. Again, due to the occurrence of the red-zones on top of the roads, 200 red-zones produced significantly lower success ratios, while 150 red-zones have more than 70% evacuation success ratio. Although the success ratio results are also based on our time limit assumption, we observed similar patterns in the results in terms of the increase in average evacuation times and decrease in the evacuation success ratios.
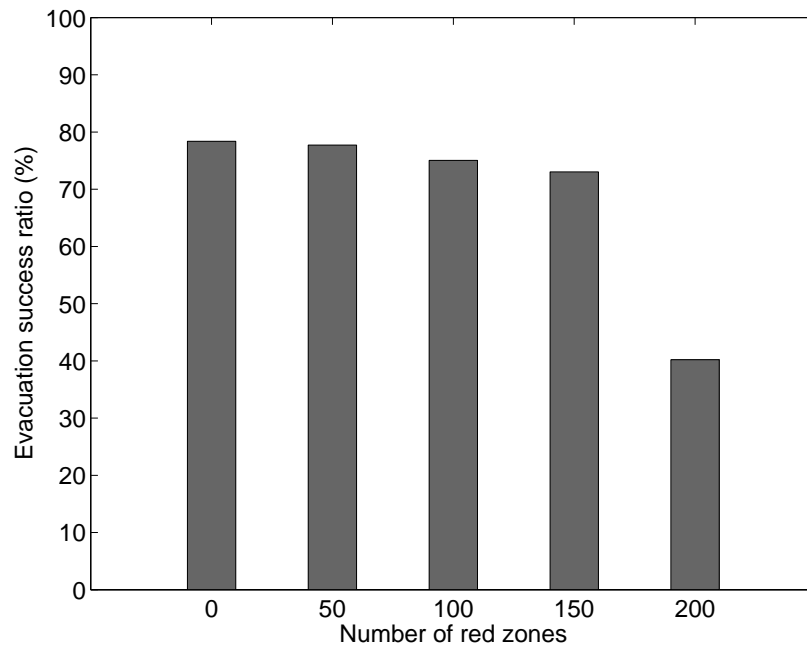
Figure 4.15: Effects of the number of red-zones on evacuation success ratio.

4.3 Concluding Remarks

In this chapter, we presented the pedestrian mobility model for disaster areas. We considered the application scenario of theme parks and proposed the theme park disaster (TP-D) mobility model. We used real theme park maps to model the environment. The mobility of theme park visitors are modeled by the theme park models and the social force model. We analyzed the outcomes of the simulation of our model in comparison with the simulations of currently used models and the GPS traces of theme park visitors.

The proposed mobility model can be used for evaluating new disaster response strategies and various network models for use in theme park environments. Moreover, the techniques used for developing our mobility model of theme park visitors can be applied for modeling human mobility in other environments such as university campuses and shopping plazas.

CHAPTER 5
EVENT COVERAGE WITH WIRELESS SENSOR NETWORKS

In this chapter, application of WSNs with mobile sinks in theme parks [12, 13] for event coverage is described in Section 5.1. Moreover, we include an extension of event coverage problem in Section 5.2 by considering a p-center approach with connected mobile sinks [14].

5.1 Optimizing Event Coverage

The operator of the theme park must be prepared to respond to events such as the operation of pickpockets, purse snatching, and disturbances caused by unruly visitors or medical emergencies. This leads to the challenge of *event coverage*: the operator must acquire information about the events and decide how to handle them. Event handling and coverage is one of the major challenges in such environments due to inevitable security and emergency problems. In addition to the technological security measures, theme parks also deploy a large number of security employees, for some parks more than a thousand, walking on foot or riding bicycles [6]. We think that using of *wireless sensor network with mobile sinks* can increase the safety of the theme parks, and it may reduce the number of personnel needed for security.

In this chapter, we describe a method for optimizing event coverage using a wireless sensor network with mobile sinks. To achieve this, the theme park operator deploys two types of nodes in the geographical area of the park. Static sensor nodes are distributed throughout the theme park, passively sense the environment and transmit their observations to the mobile sinks. Mobile sinks collect data from the nodes, and move to the location of events. In general, we assume that the mobile sinks have more powerful networking and data processing capability, and they can act as actuators, actively *resolving* the events. The movement of the mobile sinks is constrained by the capabilities of the mobility devices and the density of the visitors in various areas of the park.

We define the *event coverage problem* as the calculation of the movement of the mobile sinks for achieving an optimal coverage of events. Solutions to the event coverage problem must consider the *a priori* knowledge about the attractions and geography of the theme park and dynamic information about the movement of the visitors. Thus, the event coverage problem can be divided into two sub-problems: the positioning of the mobile sinks in the park in the absence of events and the event handling decisions of the mobile sinks.

We use the mobility model presented in Chapter 3 for visitor movement model among the attractions of the theme park. To serve as a basis of comparison, our simulations also use an alternative human mobility model, the self-similar least action walk (SLAW) [4].

5.1.1   System model

5.1.1.1   Wireless sensor network model

In the following we describe the model of a wireless sensor network with mobile sinks specifically designed to allow the operator of the theme park to efficiently and promptly handle events. The sensor network consists of two types of nodes.

Static sensor nodes are deployed throughout the theme park. Their capabilities are limited to sensing events occurring in their physical vicinity, and the transmission of their observations to the mobile sinks using hop-by-hop transmissions. The static nodes are passive observers, they cannot take actions to handle events. Sensor nodes may stay idle when there is no event or they may sense environmental data for regular monitoring purposes. We assume that static nodes are deployed uniformly and randomly in the geographical area of the theme park. In this study we focus on mobile sink positioning and the selection of the best sink for event coverage. Naturally, for a complete system, an appropriate routing protocol for WSNs with mobile sinks must be chosen [154].

Mobile sinks are nodes with the ability to receive information from the static nodes, move to the location of the events and take active steps towards handling the event. We assume that every event has an associated timeout, a window of time within which the event can be handled. If no mobile sink reached the event before the timeout, we consider that the system *missed* the event. The objective of the system is to minimize the time from the detection of an event to the time it is handled. We assume that mobile sinks have the

ability to share among each other their locations, computation results (decisions) and event information. The information is assumed to be shared directly via wireless communication between the mobile sinks whenever possible or transmission via sensor nodes between them. Moreover, we assume that the conditions of the roads and attractions in terms of the estimated traveled time and crowdedness are shared between the mobile sinks in the same way. For instance, a mobile sink computes the estimated travel time according to the conditions of the road and share this information. Note that this information can be shared by a control center which globally estimates the number of people in the attractions and roads if the mobile sinks are accessible. A possible real-world implementation of a mobile sink can be a security guard driving a personal electric transportation vehicle (e.g. Segway Patroller [155]) with a tablet computer attached to the vehicle.

Between handling events, mobile sinks must be positioned such that the handling time of future events is minimized. The number of mobile sinks deployed can change during the day (for instance, due to equipment failure or their operators taking a break). The position of the mobile sinks must be adapted to the number of currently active units.

Mobile sinks have a maximum speed determined by the technology used. Furthermore, their speed is limited by environmental obstacles, such as the density of the crowd on the paths. The mobile sinks need to plan their movement with a consideration of such slowdowns; the shortest path might not necessarily be the fastest way to reach the destination.

5.1.1.2 Event model

Let us now consider a model of the occurrence of the events in the theme park environment. We model the start times of the events through a Poisson process, while the location of an event follows one of the following three random spatial distributions:

- **Uniform random event distribution:** events occur close to one of the attractions, with all attractions having the same probability to host the next event.

- **Biased event distribution:** events are distributed according to initial probabilities of attractions, with events more often occurring at popular attractions.

- **Scenario-specific event distribution:** certain attractions have a significantly higher probability of an event to occur. This might be caused, for instance, by insufficient safety or security measures.

The distribution of events may change in time. For instance, new security and safety measures may change the distribution of the events from scenario-specific to biased event distribution. The wireless sensor network must adapt to all of the three cases using effective strategies.

5.1.1.3 Dynamic directed graph model

In the previous sections we introduced the various entities which contribute to the description of the state of the theme park augmented with a sensor network: attractions, movement paths, visitors, mobile sinks and events. In this section, we combine these in a formal model which supports the algorithms implementing the decisions of the mobile sinks. The model is implemented as a directed weighted graph. The nodes of the graphs represent the locations of the attractions, the current locations of the mobile sinks and the locations where the events happened. The edges represent available movement paths. The weights of the edges represent the time estimate for a mobile sink to travel between the nodes. For instance, to estimate the time for a mobile sink to reach an event, we need to find the shortest path from the current location of the sink to the event. In order to simplify the graph, we will not include edges which are irrelevant from the point of view of the movement of the mobile sinks (for instance, edges from the attractions and events to the mobile sink locations).

Figure 5.1 shows an example graph where $A1 \ldots A5$ are attractions, $M1$ and $M2$ are mobile sinks and $E1$ is an event. The graph is *dynamic* in the sense that some of its components depend on the current circumstances of the theme park. The attractions and their connecting links are permanent features of the graph. However, the weight of the edges connecting the attractions varies with the population of the visitors on these paths. The nodes describing the current mobile sink locations and events, as well as their edges must be generated dynamically based on the current situation.
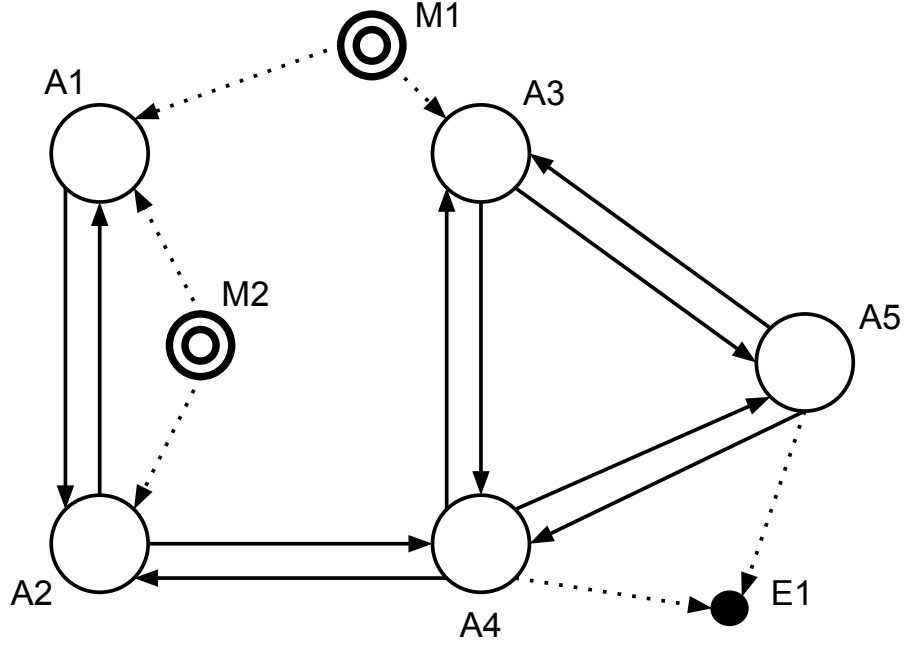
Figure 5.1: The dynamic directed graph model.

Attraction nodes are marked with the probabilities of event occurrences. The initial probability values are set according to the estimated number of visitors for each attraction. This estimation can be based on the previous observations and statistics of the attractions. In our model we use fractal points to estimate the average number of visitors in an attraction. The distribution of the fractal points corresponds to the popular areas in the theme park. The initial probability values for the attraction nodes are computed as follows:

$$P(Ai) = \frac{F(Ai)}{F(A1) + F(A2) + \ldots + F(An)}$$

where $P(Ai)$ is the probability value of an attraction Ai, $F(Ai)$ is the number of fractal points in the cluster corresponding to the attraction Ai and n is the number of attractions

116

in the landmark. The sum of the probability values of all attractions is equal to 1. Clearly, this is a rough estimate, since we do not consider some properties of the theme park model, such as the capacities of the attractions, statuses of the queues, and so on. These estimates are only used for the initial values of the attraction probabilities and they are updated dynamically. The update mechanisms for probability values are described in the following section in detail.

The most challenging part of the graph construction is the calculation of the weights, which represent estimates of the travel time of the mobile sinks on specific paths. Intuitively, if the path is empty, the mobile sink can move with its maximum speed - in our case, the 12.5 mph speed of the Segway Patroller device. However, if the mobile sink shares the road with visitors, it needs to slow down to avoid collisions. The higher the density of the visitors on the road, the more significant the slowdown. Finally, visitors moving in the same direction as the sink trigger less slowdown than visitors moving in the opposite direction - which means that the weights attached to opposite edges can be different. Thus, calculating the weights of the graph requires estimates of the density and the movement of the visitors, and information provided by the static sensor nodes.

The algorithm for calculating the weights is described in Algorithm 2. The visitor density c is the number a of visitors currently located in the road divided by the area of the road. The area of the road is equal to $d(s,t) \cdot w$ where w is the width. α is the direction difference between the sink and a visitor and $\gamma \in (0,1]$ is the constant for adjusting the effect of the direction α. The parameter β allows us to scale the impact of each visitor on

117

the speed of the mobile sink. This parameter allows us to approximate the effect of larger crowds than the ones we are effectively simulating.

Algorithm 2 Computation of the edge weights

1: s, t: Source and target nodes

2: $V(s, t)$: Set of movement directions of visitors between s and t

3: $m(s, t)$: Movement direction from the s to t

4: $d(s, t) :=$ Euclidean distance between s and t

5: $c := a/(d(s, t) \cdot w)$

6: $S :=$ Maximum mobile sink speed

7: **for** each v in $V(s, t)$ **do**

8:     $\alpha := m - v$

9:     $S := S - \beta \cdot c \cdot (S - \gamma \cdot S \cdot \cos \alpha)$

10: **end for**

11: $W := d(s, t)/S$

12: **return** Estimated travel time as the weight W

An example of the results of this algorithm are shown in Figure 5.2. In this figure, the edges drawn with dotted lines are the dynamic edges: the edges updated through the movement of the mobile sinks and the edges connecting the new event $E1$ to the closest attractions. We use an adjacency matrix to represent the graph in the implemented algorithm. Figure 5.3 shows the adjacency matrix associated with the graph in Figure 5.2 with the value x in the cells showing no edge between the two nodes.
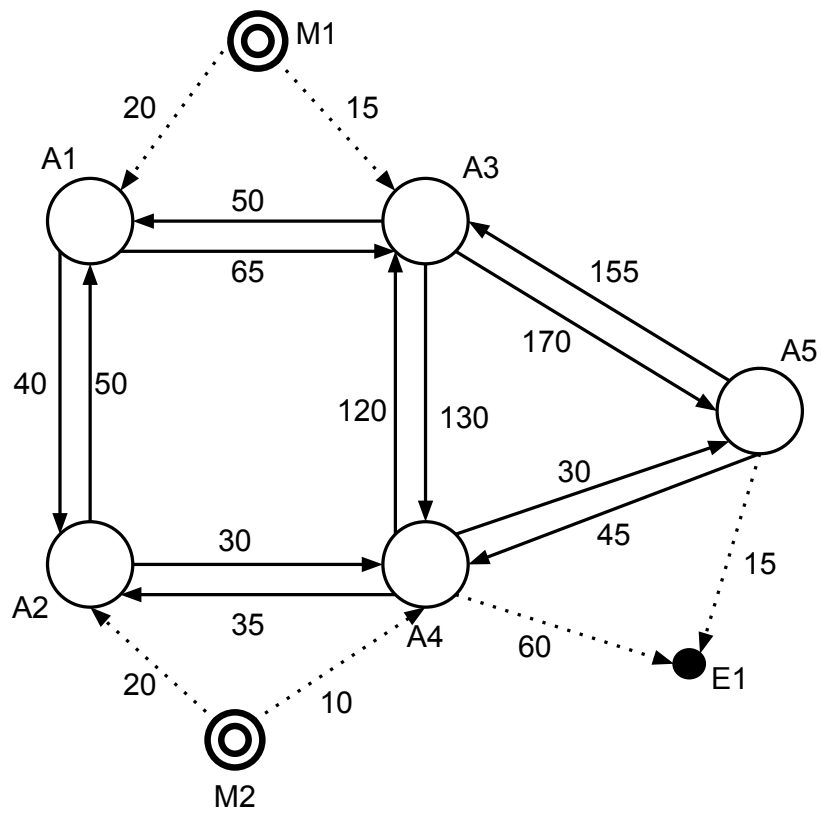
Figure 5.2: The dynamic edge weights created when an event $E1$ happens.

	A1	A2	A3	A4	A5	M1	M2	E1
A1	x	40	65	x	x	x	x	x
A2	50	x	x	30	x	x	x	x
A3	50	x	x	130	170	x	x	x
A4	x	35	120	x	30	x	x	60
A5	x	x	155	45	x	x	x	15
M1	20	x	15	x	x	x	x	x
M2	x	20	x	10	x	x	x	x
E1	x	x	x	x	x	x	x	x

Figure 5.3: The adjacency matrix with dynamic edge weight values, corresponds to the graph model in Figure 5.2.

5.1.2 Solving the event coverage problem

Solving the event coverage problem involves resolving the events occurring during the operation of the theme park as efficiently as possible. This involves two sub-problems. The mobile sink positioning problem chooses the location of the mobile sinks in the absence of any event. The goal is to distribute the mobile sinks in such a way that when events happen, there will be a sink nearby which can quickly reach the location of the event. Naturally, in order to find such a solution, we can rely on our statistical knowledge about the locations where events are likely to occur, and about the time to reach specific locations from the current location of the sink. The second sub-problem relates to the handling of events. Once an event occurred, we need to decide which mobile sink will handle the event, and which path it will follow to the location of the event.

For both sub-problems, we assume that the mobile sinks know the location of each other and the events each of them are handling. The dynamic model of the theme park, in the form of the weighted directed graph described in the previous section, is shared by all the mobile sinks.

5.1.2.1 Mobile sink positioning

We propose a mobile sink positioning algorithm which is based on estimating the probability of events happening at various locations, then assigning the mobile sinks in such a way that

they are grouped towards the most likely locations of events. Algorithm 3 shows how to update the location of the mobile sinks. We assume that the mobile sinks are stationed at attractions, $A(m)$ representing the current attraction of the mobile sink m. At each step, the mobile sink must make a decision to either stay at its current attraction, or to move to a neighboring attraction, if that attraction has a higher probability of an event to occur *and* is not already occupied by another mobile sink.

Algorithm 3 Location updates

1: M: Set of all mobile sinks

2: A: Set of all attractions

3: $O := \{\}$: Set of occupied attractions

4: **for** each m in M **do**

5:    $a \leftarrow A(m)$

6:    $N(a) :=$ The neighbor attractions of a

7:    **for** each n in $N(a)$ **do**

8:       **if** $P(n) > P(a) \wedge n \notin O$ **then**

9:          $a \leftarrow n$

10:       **end if**

11:    **end for**

12:    $A(m) \leftarrow a$

13:    $O \leftarrow O \cup a$

14: **end for**

15: **return** Updated attraction set A

This algorithm, taken as a high level framework can be customized in a number of ways. First, we can choose different definitions of the neighbors of a node: it can represent either a distance of a single edge in the graph, or it can represent all the attractions which are within a distance threshold. Another way in which the algorithm can be customized is by adapting the definition of an occupied attraction: for very high event probabilities, we can allow for more than one mobile sink to be stationed at the same attraction.

The positioning algorithm requires an estimate of the probability of future events. In the following we propose two such estimation techniques, based on different assumptions about the nature of events: a crowd density based and a hot-spot based probability estimation technique.

The **crowd density based probability estimation (CDPE)** assumes that the number of events at an attraction is proportional to the number of visitors. The number of visitors at the attraction is estimated by the sensor nodes.

CDPE assumes that each visitor contributes equally to the probability of an event. However, experience shows that certain locations are more likely to have events (possibly due to the nature of the attraction). Furthermore, events are frequently clustered into hot-spots (possibly, due to a common, but hidden cause).

The **hot-spot based probability estimation (HSPE)** takes into consideration the history of events at specific locations. The occurrence of an event increases the probability that another event will occur at the same attraction. The equation below shows the formula used for updates done after an event occurs. For each event e, the probability of an event

at attraction Ai increases if the event happened in that attraction. The magnitude of the increase is calculated by multiplying the priority of the event $\rho \in 1 \ldots 5$ with the *adaptivity value constant* δ (*e.g.* $\delta = 0.05$). It decreases for all other attractions by the same value divided by the number of other attractions $(n-1)$.

$$P(Ai) = \begin{cases} P(Ai) + \rho \cdot \delta & \text{if } e \text{ occurred in } Ai \\ P(Ai) - \dfrac{\rho \cdot \delta}{n-1} & \text{otherwise} \end{cases}$$

5.1.2.2 Event handling

The second sub-problem we are considering is that of event handling. Let us assume that the mobile sinks are positioned using one of the algorithms from the previous section, and an event $E1$ occurs. The event handling algorithm needs to decide (a) which mobile sink will handle the event and (b) which path it will follow when moving to the event's location.

We have developed two algorithms, corresponding to different levels of information available about the state of the theme park. If the information collected from the sensor nodes allow us to estimate the density and movement directions of the visitors on the paths, we can deploy the **Fastest Responder (FR)** strategy, which assigns to every event the mobile sink which can get there the fastest. To implement this, we create the dynamic graph of the current state of the node using Algorithm 2. The weight of the edges correspond to time needed to traverse them. On this time-weighted graph, we calculate the shortest path from

every mobile sink node to the event node. The mobile sink which will be assigned to the event will be the one which is at the shortest distance in this graph. Note that the fastest responder might not be the one which is physically the closest.

Figure 5.4 illustrates an example run of this algorithm. In this figure, numbers near the arrows represent the edge weights while numbers inside the graph nodes are probabilities of attractions. There are two routes, *Route 1* and *Route 2*, for the two sinks to follow. In this example, the mobile sink $M2$ is responsible for the attraction $A5$ and the other mobile sink $M1$ is responsible for $A3$ at the beginning. When the event $E1$ occurs, the mobile sink $M2$ is selected to handle the event $E1$ since the shortest path of $M2$ is 160 while the shortest path of $M1$ is 220. $M2$ follows *Route 1* to reach the event. The movement of $M2$ to handle the event, however, also triggers changes in the static positioning of the other mobile sinks. The probability of attraction $A5$ is $P(A5) = 0.35$ while the probability of $A3$ is $P(A3) = 0.15$. Therefore the mobile sink $M1$ changes its position to cover the attraction $A5$ with higher probability by following the *Route 2*, the shortest path from its current location to the attraction $A5$.

For the case when the monitoring of the movements of visitors is not possible, we use the **Closest Sink (CS)** strategy. In this strategy, the shortest path algorithm is used on a static graph, where the edge weights correspond to Euclidean distances rather than in travel times.
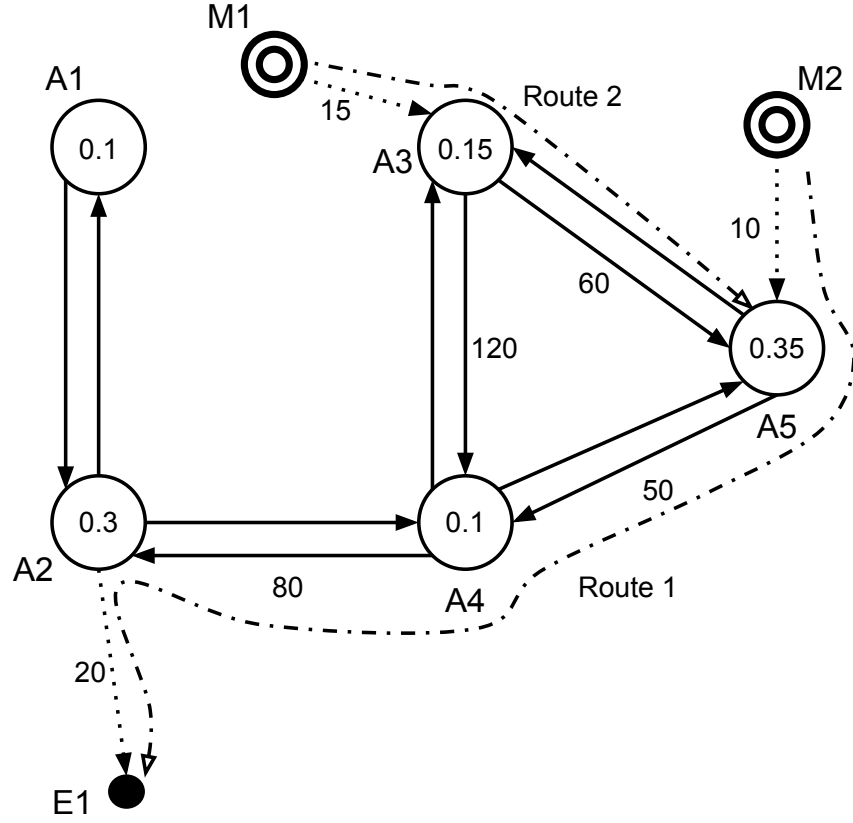
Figure 5.4: An example mobile sink selection and covering of the attractions.

5.1.3 Simulation study

5.1.3.1 Simulation setup

In the following we describe a series of simulation experiments which study the performance of the proposed event coverage algorithms.

Let us start with describing the simulation setup. We are considering a rectangular theme park of size 1000m x 1000m, with 15 geographically distributed attractions, whose locations have been determined using a fractal point model with 1000 fractal points. Between

these attractions, we created the paths in two ways: (a) by connecting all attractions with a vertex degree of 4 or higher and (b) by adding paths between random attractions until the graph density reaches 0.7.

We have considered 500 visitors who move around and visit attractions in the park. We generated two different datasets of visitor movement based on the theme park mobility model (TP) [8], and the SLAW movement model [4]. Each dataset contains trajectory files for 10 hours of mobility with a 10 seconds sampling time. The movement speed of visitors had been set to 1m/s.

The theme park contains from 1 to 20 mobile sinks with a maximum speed of 5.58 m/sec. The location update time for adaptive mobile sinks was set to 30 minutes. Sensor nodes are assumed to transmit the information of events to the mobile sinks whenever an event occurs, and mobile sinks share the current conditions of the dynamic theme park graph in the specified location update times.

Let us now discuss the generation of the events. We need to consider three aspects: the location of the events, their starting times, and their active duration. The location of the events had been created using one of the three event distribution algorithms described in Section 5.1.1.2. The arrivals of the events are modeled with a Poisson process with an average arrival rate of 30 events / hour. The active time of the events is randomly distributed in the range of 60 to 300 seconds.

Throughout the simulation scenarios, we measured two performance metrics. The *average event handling time* is the travel time for the selected mobile sink to reach an event.

This also includes situations where the sink reaches the location of the event after the event's active time expired. The *handling success ratio* is the fraction of the times the sink reaches the event before its active time expires.

5.1.3.2   Simulation results

- **Performance of CDPE**

In the first of set of experiments, we evaluated the performance of the crowd density based probability estimation (CDPE) strategy. As a comparison baseline, we used the random sink positioning (RSP) strategy, where the sinks are deployed uniformly and randomly in the theme park. The experiments considered 5 sinks. The location of the events was generated using the biased event distribution. For both positioning strategies, the fastest responder (FR) strategy was used to handle the events. The experiments were repeated with the visitor movements generated from the TP and the SLAW mobility models respectively.

Figure 5.5 shows the average event handling times for the combinations of positioning strategies and visitor mobility models. For both mobility models, the CDPE strategy clearly outperforms the RSP strategy, in average providing a 40% faster event handling time. Incidentally, the handling times are about 8% longer for the TP mobility model compared to SLAW. This difference justifies the development of theme park specific mobility models (compared to general purpose mobility models).
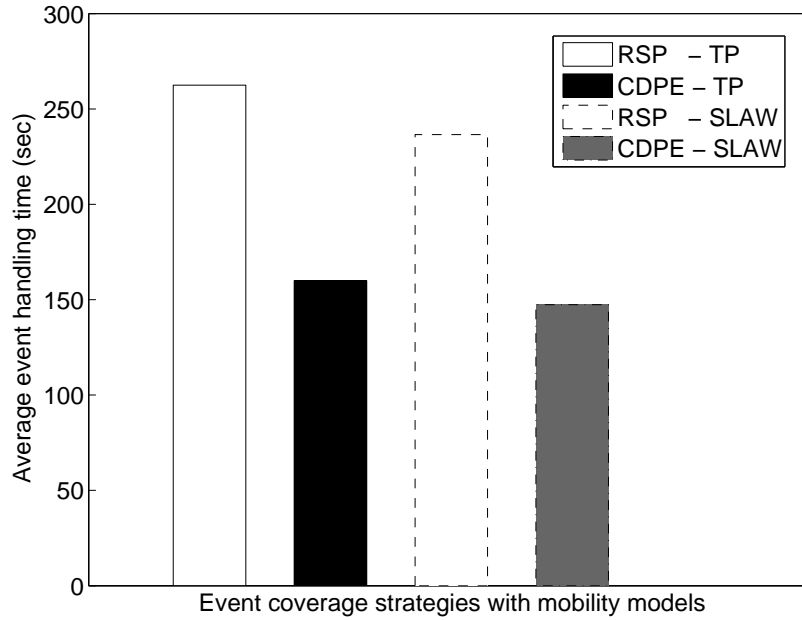
Figure 5.5: Average event handling times for CDPE vs. random sink positioning.

The faster response times of the CDPE strategy are also reflected in the higher success ratio as shown in Figure 5.6. CDPE can handle about 65% of the events within their deadlines, while RSP handles 30% for the TP mobility model and about 40% for SLAW. We notice that the binary nature of the event handling success magnifies the difference between the success ratios of RSP for the TP and SLAW models respectively.

- **Performance of HSPE**

We designed the HSPE positioning technique to handle scenarios where the events occur more frequently at certain attractions (the event hot spots). To study the performance of HSPE, we generated scenarios where three attractions are randomly selected to become hot spots. Our hypothesis is that under these circumstances, HSPE will outperform CDPE.

129
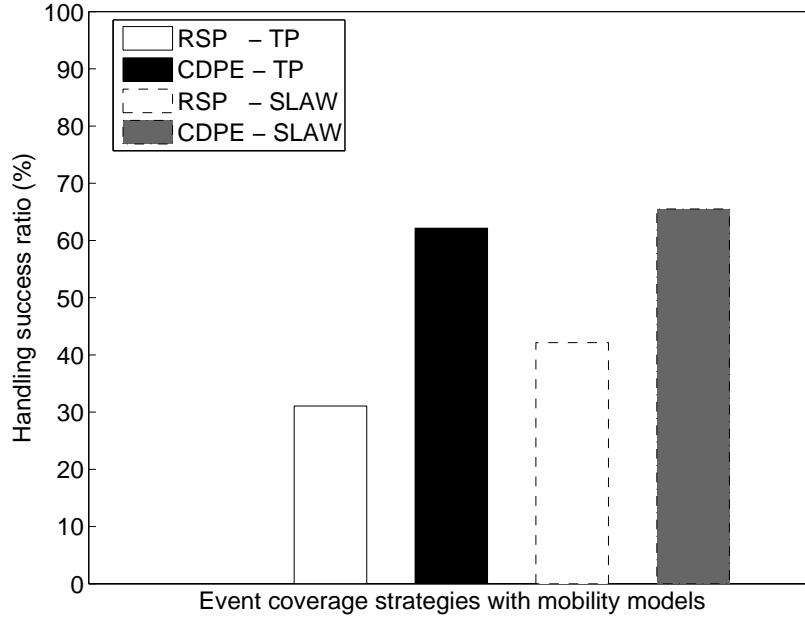
Figure 5.6: Handling success ratios for CDPE vs. random sink positioning.

The simulation was run using 3 sinks and the FR responder strategy. We repeated the simulation for both the TP and SLAW mobility models. Figures 5.7 and 5.8 show the average event handling times and handling success ratios of 500 experiments for each result. We decided to present the results using box plots to illustrate the variation of the performances. The results show that the HSPE algorithm highly outperforms CDPE in these scenarios for both performance metrics. In addition, HSPE shows very little variation in the performance. In contrast, CDPE shows a significant performance variation.
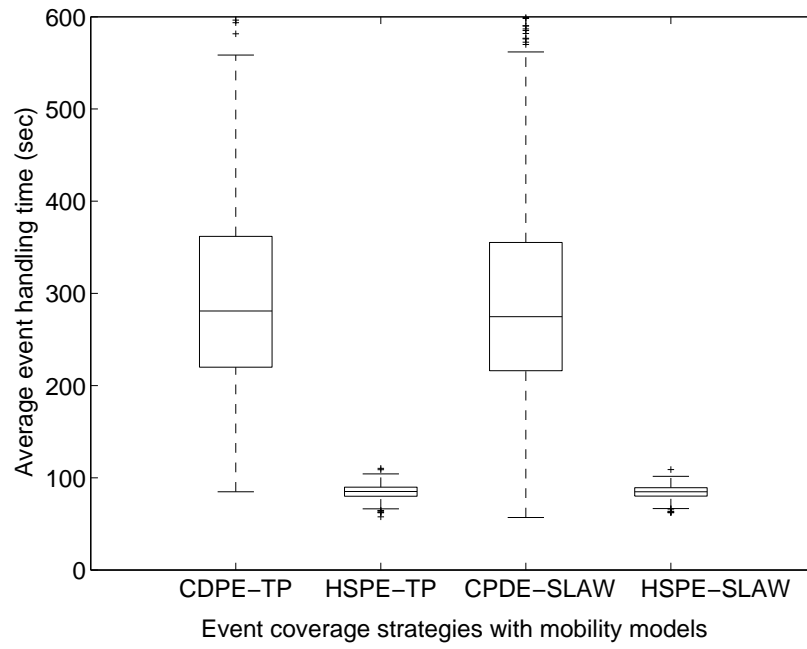
Figure 5.7: Average event handling times for sink positioning by HSPE vs. CDPE.
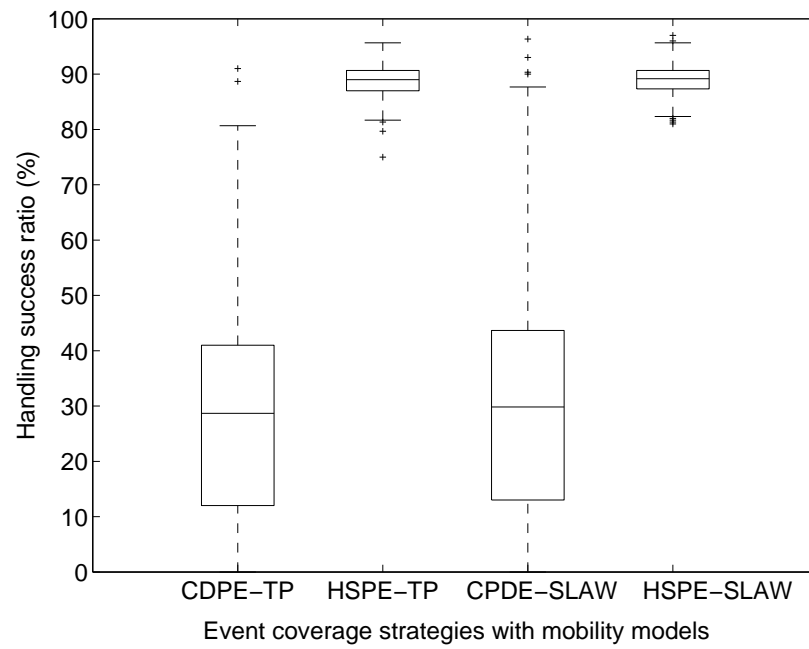
Figure 5.8: Handling success ratio for HSPE vs. CDPE positioning strategies.

The performance increase is attributable to the additional information exploited by the HSPE algorithm about historical event locations. As a note, as HSPE will behave the same as the CDPE strategy in the absence of hot spots, we recommend the use of the HSPE strategy for all deployments.

In the experiments shown in Figures 5.7 and 5.8, we considered the specific case where the number of hot spots matched the number of mobile sinks. While this might appear arbitrary, it is, in fact, a good deployment strategy to have at least as many mobile sinks as the number of hot spots.
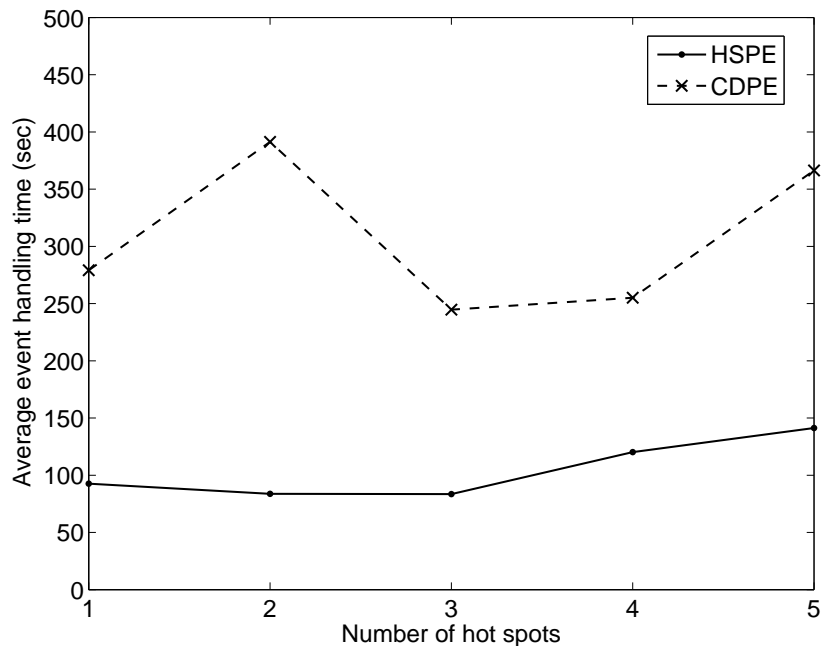
Figure 5.9: Average event handling times for HSPE vs. RSP for 1 to 5 hot spots.

In the following, we compared performance of the HSPE strategy against sink positioning by CDPE for various numbers of hot spots. 3 mobile sinks are used for handling

events created randomly from 1 to 5 hot spots. As before, we used the FR event handling strategy, and generated events with the TP mobility model.
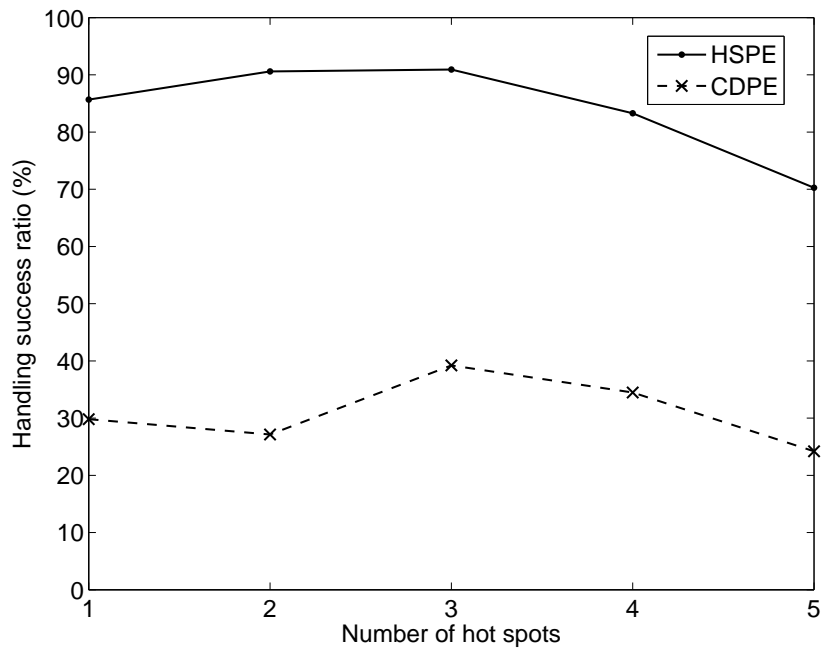
Figure 5.10: Handling success ratio for HSPE vs. CDPE for 1 to 5 hot spots.

Figure 5.9 shows the average event handling times and Figure 5.10 shows the handling success ratios for the two strategies. Overall, HSPE significantly outperforms CDPE for all the scenarios. In general, HSPE obtains its best performance when the number of sinks is equal to those of the hot spots. Once the number of hot spots exceed the number of sinks, the average event handling time increases and correspondingly, the handling success ratio decreases. CDPE on the other hand not only has a lower performance, but the performance varies with the number of hot spots significantly and without a clear pattern. The reason behind this erratic behavior is that for this scenario CDPE had simply made the wrong

134

assumptions: it assumed that the events follow the crowd distribution, while in reality, they were concentrated in hot spots.

- **Performance of CDPE and HSPE function of the number of mobile Sinks**

In general, we expect that increasing the number of mobile sinks improves the performance of the event handling, because if enough mobile sinks are spread around in the area, no matter where the event occurs, some mobile sink will be close enough to reach it fast. However, adding sinks is a significant expense, thus it is important to investigate the point where adding more mobile sinks provides minimal advantages.
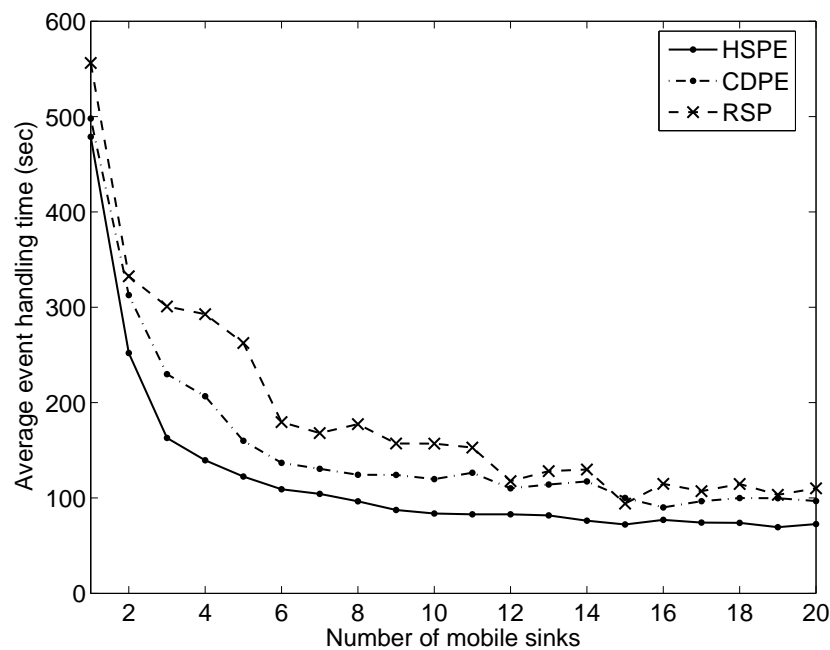
Figure 5.11: Effect of multiple mobile sinks on event handling time for the HSPE, CDPE and RSP algorithms

We have run a series of experiments using the HSPE, CDPE and RSP positioning algorithms. We used the TP mobility model and the FR strategy to handle the events. The number of mobile sinks was varied between 1 and 20. The results for the event handling time is shown in Figure 5.11 while for the handling success ratio in Figure 5.12. As expected, for all the algorithms the performance increases with the number of sinks deployed, and the increase is especially fast when moving from 1 to 2 and from then on to 3 sinks. However, the performance eventually reaches a plateau: even for the best performing HSPE algorithm, no additional increase appears to decrease the average handling time below 70 seconds, nor push the handling success ratio above 93%.
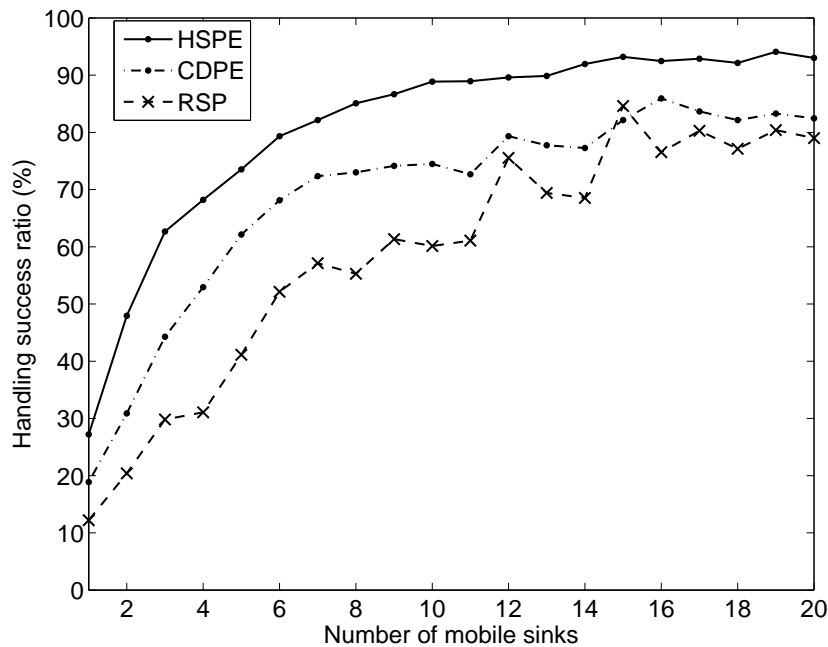
Figure 5.12: Effect of multiple mobile sinks on handling success ratio for the HSPE, CDPE and RSP algorithms

The comparative performance of the algorithms, is as expected: HSPE is the best, followed by CDPE and RSP. This holds true for all sink numbers (a single outlier aside). More important however, is the difference in the level of the plateaus. While HSPE reaches a plateau at around 93%, CDPE and RSP cannot be pushed above 80% regardless of the number of mobile sinks deployed. In fact, HSPE can achieve better performance with 6 mobile sinks, than the other algorithms would achieve with 20.

The graphs in Figures 5.11 and 5.12 can also be used for efficient allocation of human resources. It is not economically justified to add additional mobile sinks after reaching the plateau. With the assumptions we considered, for HSPE there are very few benefits to gain from adding more than 10 sinks, and none in adding more than 14. These values might change with different assumptions.

- **Performance of event handling decision strategies function of the number of mobile sinks**

In this series of experiments we studied the relative performance of various solutions to the event handling decision problem. From the two strategies we introduced, the FR (first responder) strategy requires ongoing information about the density and movement pattern of the visitors. In contrast, the CS (closest sink) strategy only requires *a priori* information about the layout of the attractions and paths of the park. As a baseline, we will use the RS (random sink) strategy, where the event is handled by a randomly assigned sink.
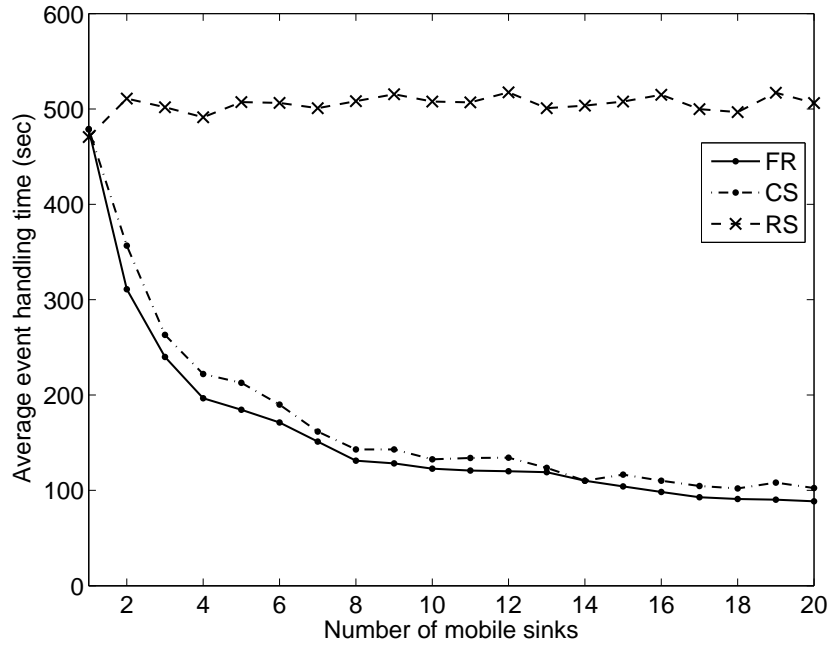
Figure 5.13: Average event handling times for fastest responder (FR), closest sink (CS) and random sink (RS) event handling strategies function of the number of sinks

All the strategies (including RS) require inter-sink coordination to avoid multiple assignments. We used CDPE for sink positioning with the number of mobile sinks varied between 1 and 20. The events are distributed according to the biased event distribution for all experiments. The results are the average of 20 experiments with different random seeds. We used the SLAW mobility model for this experiment.

Figure 5.13 shows the average event handling times and Figure 5.14 the handling success ratios. The ranking is as expected, FR performing best, followed by CS and RS. While the performance of FR and CS increase with the number of sinks, the performance of RS does not. This is justified by the fact that with more sinks, it is more likely that FR and

CS can find a sink which is close to the event. However, for RS which picks a sink randomly, the likelihood of being close or far is about the same independently of the number of sinks. While FR is consistently better than CS, their performance is relatively close: this additional benefit needs to be weighted against the expense of the crowd tracking sensor network.
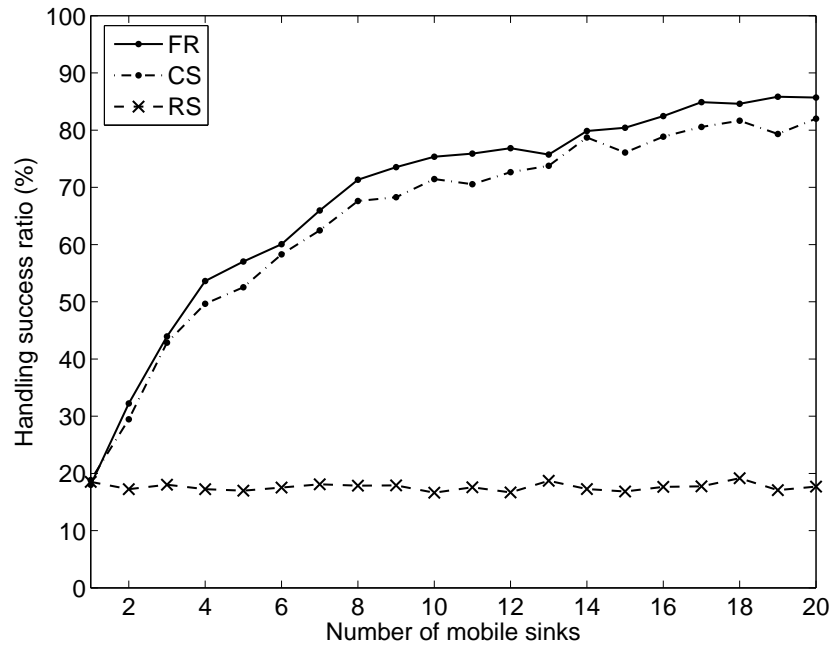
Figure 5.14: Handling success ratios for fastest responder (FR), closest sink (CS) and random sink (RS) event handling strategies function of the number of sinks

- **The impact of event distribution types**

In the last series of experiments, we study the effect of the different event distribution types outlined in Section 5.1.1.2 on the performance of the network. We used HSPE for 3 mobile sinks and the FR strategy for event handling and the TP visitor mobility model.

Figure 5.15 shows the event handling times and Figure 5.16 the handling success ratio for 5 different experiments. We find the event distribution has a very strong impact on the performance: the more random the distribution of the events, the lower the performance. The same setup which achieves 90% success rate on the scenario-specific distribution manages only 60% on the biased and about 35% at the random distribution. We conclude that stakeholders should perform careful initial studies on the distribution of events in the park, as the spatio-temporal distribution can have a critical impact on the event handling success, even if all the other parameters are the same.
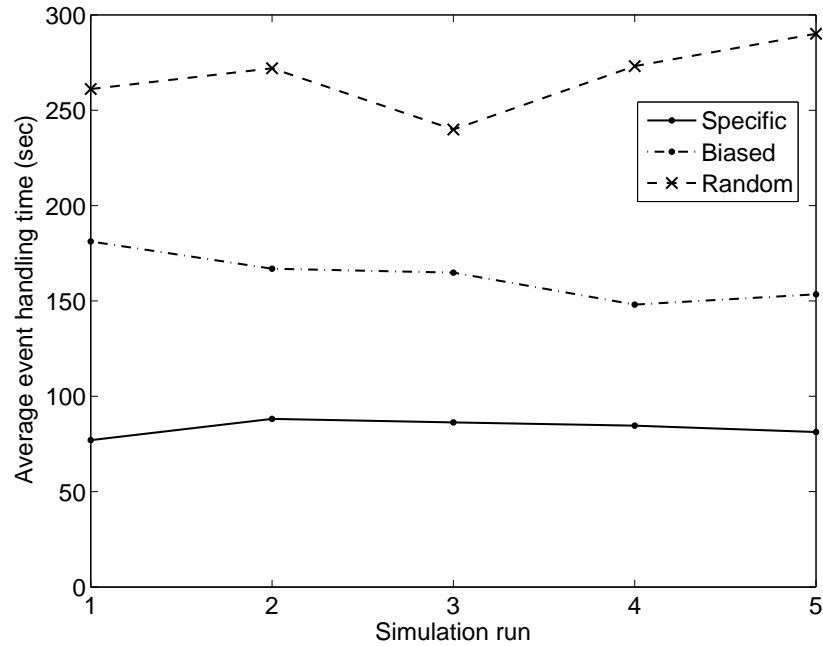
Figure 5.15: Effect of event distribution types on event handling time.
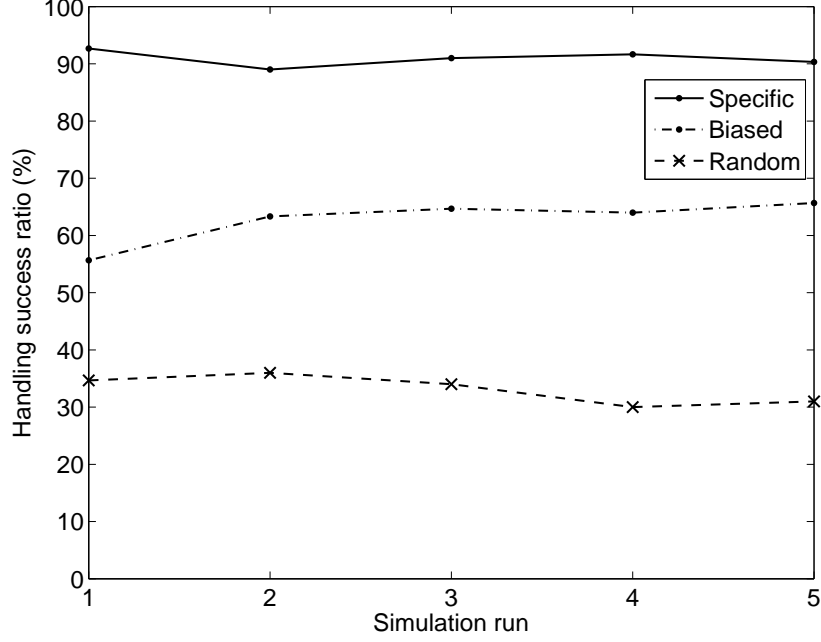
Figure 5.16: Effect of event distribution types on handling success ratio.

5.2 Communication-constrained p-Center Problem

The problem of event coverage can be modeled as a vertex p-center problem [99] which aims to minimize the maximum travel distance for each sink. Specifically, we represent the theme park with a dynamic and weighted graph. In this graph, the edges and the vertices have dynamic values that change according to the current movement and the positions of the visitors. The edges correspond to the roads and the weights of the edges are the travel times of mobile sinks on these roads. The vertices correspond to the attractions and the weights of the vertices are the event probabilities of the attractions. While the solution of vertex p-center problem produces optimal places of the mobile sinks at the attractions, the sinks

should still be able to communicate with each other to share information and request help of others if needed. In this case, there should be a connected network among the mobile sinks. This brings additional constraint to the problem which cannot be handled with the use of vertex p-center problem.

In this section, we introduce a new variant of vertex p-center problem which we call *communication-constrained p-center problem*. In this new variant, the connected sinks form wireless network which consists of a subset of the vertices. The possible locations of the mobile sinks is modeled with *connectivity graph*. We also propose an exact algorithm to solve this new problem. Our proposed algorithms has two steps: finding the connected subgraphs and placing mobile sinks to the vertices on these subgraphs such that the maximum distance from attractions to mobile sinks is minimized. The positions of the mobile sinks are updated in discrete time intervals to place the sinks either on or close to the attractions which have higher event probabilities.

We implemented and tested our approach under a variety of conditions. Compared to baselines, the proposed approaches provide reduced event handling times and increase the chance of handling events on time. In addition, the results revealed that connectivity constraint increases the event handling times, while it gives independence to the network by eliminating the need of a global monitoring infrastructure.

5.2.1 Preliminaries

5.2.1.1 Background on p-center problem

The p-center problem consists of p facilities and clients (i.e., vertices). Each client is assigned to a facility. The problem is to place the p facilities on the network in a way that the maximum distance between a client and the facility assigned to it is minimized. There are two major variants of the p-center problem: absolute and vertex p-center. In the absolute p-center problem, the facilities can be located anywhere in the network, including vertices and any points on the edges. In the vertex p-center, the facilities can be located on top of the vertices only. There is another variant called the connected vertex p-center (CpC) problem. In this case, the selected p facilities should be placed on top of the vertices and the vertices should be connected to each other via physical paths.

There are also other variants of the problem if different graph models are considered. For instance, if the vertices are weighted, then the problem is called vertex-weighted p-center; otherwise, it is called vertex-unweighted p-center problem. In case of the vertex-weighted p-center problem, the distance values are multiplied by the weight values of the vertices. The weights of the vertices are considered as the demands of the clients.

Finally, depending on the goal the p-median problem is defined that is finding the locations of p facilities on the network such that the sum of the shortest distances between the facilities and the clients is minimum. It has also two variants, the absolute and the vertex p-median problem as in the p-center problem. If the vertices are weighted, it is called

the vertex-weighted p-median problem and the vertex-unweighted p-median problem in the other case. Considering the connectivity constraint, the vertices of the p facilities must be connected and in this case it is called the connected vertex p-median problem.
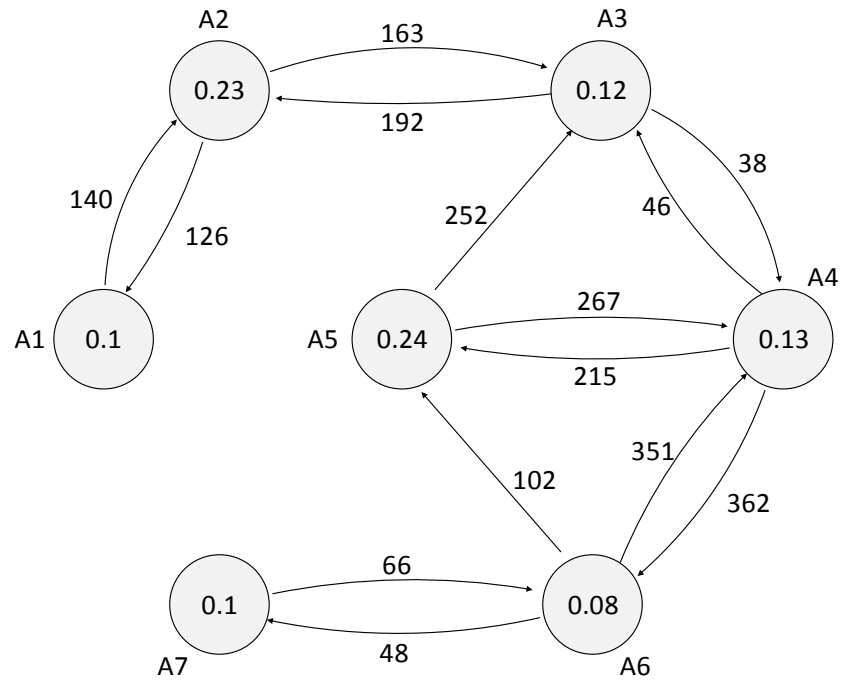
Figure 5.17: The theme park graph model.

Fig. 5.17 is another illustration of the theme park graph model, which is presented in this chapter. We consider the p-center problem based on the dynamic graph model.

5.2.2 Event coverage

5.2.2.1 Motivation

The problem of mobile sink placement can be solved by using one of the existing heuristics of the vertex p-center problem [103]. However, we have an additional constraint that needs to be satisfied. The mobile sinks should be directly connected to each other in order to share information of the events and take collaborative actions if needed. Therefore, they should always preserve a connected topology as illustrated in Fig. 5.18. In this figure, the wireless connections between the mobile sinks and an event in $A4$ are illustrated whereas the arrows represent the roads between the attractions.

Because of this additional constraint, we face with a new variant of the vertex p-center problem in which the facilities (i.e., sinks) need to communicate with each other. We call it *communication-constrained p-center problem.*

In this problem, a facility is considered as *connected* whenever it is in the transmission range of at least one other facility. As aforementioned, the original connected p-center problem forces the connectivity of the facilities through the physical paths which is different than our problem. In the new problem, even if the facilities are connected via physical paths (roads), there may not be a wireless communication among them due to limited radio range. Therefore, the solution should use two distinct graphs. The distances from facilities to clients must be computed using the theme park graph while the connectivity between the facilities must be checked with the connectivity graph.
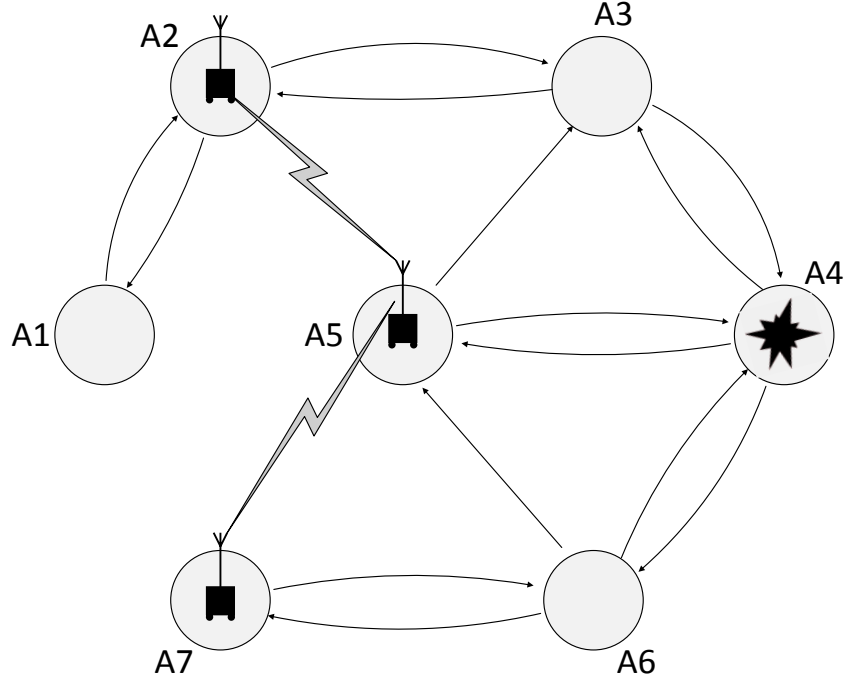
Figure 5.18: The connectivity of the mobile sinks in the attractions and an event.

5.2.2.2 Problem formulation

The formulation of the communication-constrained p-center problem is as follows. Given a connected graph G, let $V = \{v_1, v_2, \ldots, v_n\}$ be the set of its vertices. We assume that each vertex v_i has a weight value $w(v_i)$ and $w(v_i) > 0, \forall v_i \in V$ which corresponds to the demand of the vertex. $d(v_i, v_j)$ is the length of the shortest path from a vertex v_i to a vertex v_j. $D(v_i, v_j)$ is the Euclidean distance among the two vertices. There are p facilities that can be placed only on top of the vertices. The facilities should be placed on optimal p vertices, such that the maximum distance between the facilities and the vertices is minimized.

Moreover, p facilities must be connected, in a way that each facility must be located within the communication range R of at least one other facility.

The objective is to find the subset of vertices $F = \{f_1, f_2, \ldots, f_p\}$, where $F \subset V$ and $|F| = p$ to locate the facilities with the following goal:

$$\text{Min} \quad \eta(F) \quad \text{s.t.} \quad \forall\ f_i \exists\ f_j, D(f_i, f_j) \leq R$$

where

$$\eta(F) = \max_{1 \leq i \leq n} \left\{ \min_{1 \leq j \leq p} \{(w(v_i) \cdot d(f_j, v_i)\} \right\}. \tag{5.1}$$

The minimum value of $\eta(F)$ gives the optimal subset of vertices F for facility locations. For each client (vertex) v_i the minimum distance is calculated by the shortest path distance $d(f_j, v_i)$ between a facility in f_j and a client (vertex) v_i multiplied by the weight of the client $w(v_i)$.

This problem is challenging in the sense that the p-center problem is NP-hard [99]. Considering the definition of the communication-constrained p-center problem, one can easily show that the problem is NP-hard on general graphs. Assume that there exist communication paths between all pairs of vertices in graph G. In this case, the communication constraint disappears due to the fact that one can place facilities in any p locations and any selected p vertices allow the facilities to form communication paths among them. The problem of finding p vertices (finding the subset F) that minimizes the maximum distance between

the facilities and the clients on graph G becomes exactly the same as the original p-center problem [99], which is already shown as NP-hard.

5.2.2.3   Proposed approach

According to the Euclidean distances between the vertices, we consider a graph G^c, called *the connectivity graph*. The edges of the connectivity graph are created among each pair of vertices if the Euclidean distance among them is less than or equal to R. If a vertex is not in the communication range of any other vertex, we do not consider it as an element of G^c. Hence, $C = \{c_1, c_2, \ldots, c_m\}$ is the set of vertices of G^c, such that $\forall \, c_i \exists \, c_j, D(c_i, c_j) \leq R$ where $C \subset V$, $|C| = m$, $|V| = n$, and $m \leq n$.

Considering the moderate sizes of the problem in real-life context in the theme parks, we propose an exact algorithm for solving the communication-constrained p-center problem. This algorithm has two steps. In the first step, we compute the connected subgraphs with p vertices using the connectivity graph G^c. In the second step, the facilities will be placed to the vertices of these connected subgraphs using the p-center solution to minimize the maximum or total distance.

For the first step, the set of connected subgraphs $S[G^c] = \{S_1, S_2, \ldots, S_k\}$ is found which includes the candidates for the best locations of p facilities where k is the number of candidate subgraphs with $|S_i| = p, \forall S_i \in S[G^c]$.

For timely event coverage, we apply p-center problem to the connected subgraphs with p vertices using G and and compute the new positions of the mobile sinks. Depending on the goal, we can choose a different metric. For instance, if we would like to minimize the maximum distance from an attraction to the closest sink, this placement approach is referred to as *p-center positioning* (PcP). If the total distance is to be minimized, then this approach is called *p-median positioning* (PmP). We considered both of the strategies and implemented both PcP and PmP as will be detailed in Section 5.2.3.

Let the locations of vertices stored in a set F. The subset F with p vertices that minimizes the maximum (or total) weighted shortest path distance from the facilities to the clients is guaranteed to be one of the candidates since these candidates are subsets of G^c that comply with the connectivity requirement, $F \in S[G^c]$. The weighted distances from the vertices of graph G (clients) to the candidates (facilities) are computed to find the best candidate F that minimizes the maximum (total) distance to the clients. The weighted distances between the connected subsets and vertices are calculated and shown as the matrix W, such that

$$W_{S_k, v_i} = d(S_k, v_i) \cdot w(v_i)$$

where $d(S_k, v_i)$ is the minimum shortest path distance from any vertex of S_k to the vertex v_i. The pseudo-code for the algorithm is shown in Algorithm 4.

Algorithm 4 Communication-constrained p-center

1: $S[G^c]$: Connected subgraphs of G^c

2: G: Updated graph for time $t \in T$

3: Compute weighted distance matrix W using G

4: $\eta(F) := \infty$

5: Selected subgraph $F := null$

6: **for** each S_k in $S[G^c]$ **do**

7:     Max distance $m := 0$

8:     **for** each v_i in V of G **do**

9:         **if** $W_{S_k, v_i} \geq m$ **then**

10:            $m := W_{S_k, v_i}$

11:         **end if**

12:     **end for**

13:     **if** $m \leq \eta(F)$ **then**

14:         $\eta(F) := m$

15:         $F := S_k$

16:     **end if**

17: **end for**

18: **return** F

Since the weights of the edges and attractions change dynamically in the theme park, the mobile sinks have discrete location update times $t \in T$. At each update time t, one of the sinks is chosen as the *master* which runs Algorithm 4 using the new weights and assigns the new positions to the other sinks (i.e., *slave*). The assignment is done by sharing the new attraction allocation list with the sinks. Throughout the operation of the network, G^c does not change since the attractions have static locations and therefore G^c is initially provided to the *master* sink.
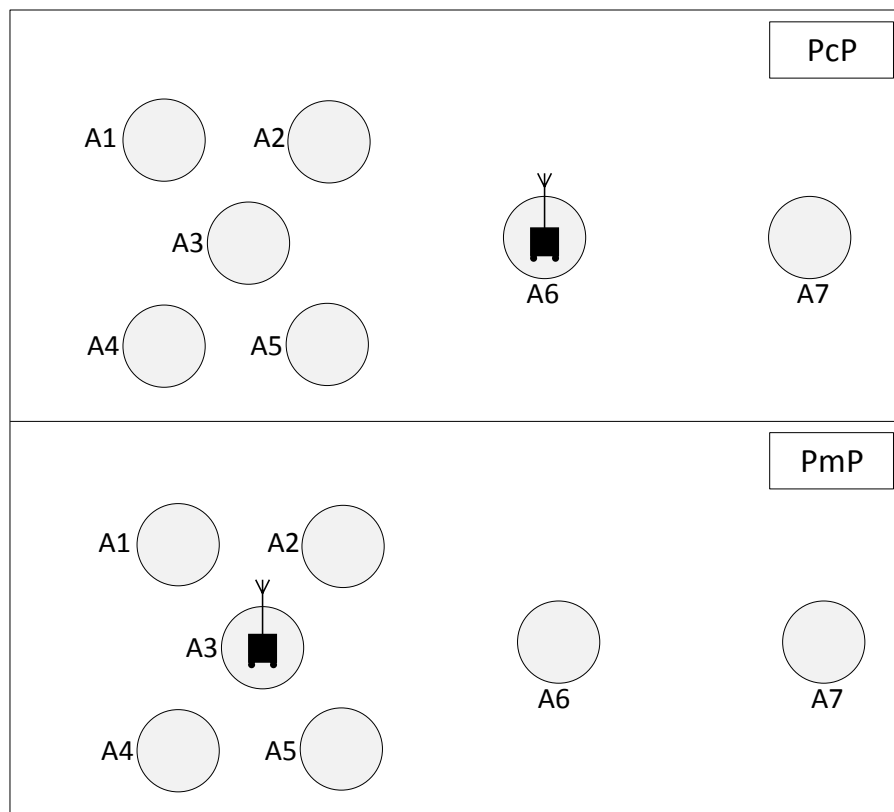
Figure 5.19: Mobile sink positioning with PcP and PmP.

Fig. 5.19 illustrates the behaviors of the PcP and PmP approaches. In this figure, we consider one mobile sink and do not illustrate the roads between the attractions for simplicity. Let us assume that the positions of the attractions represent the scaled Euclidean distances between the attractions and the event probabilities of all the attractions are equal. According to PcP, the sink needs to be placed at the attraction which is located in the middle whereas in PmP, it is placed in a location closed to most of the attractions.

5.2.2.4 Algorithm complexity

The first step of finding all connected subgraphs in a graph takes $O(enk)$ time [156], where e, n and k (i.e., $|S[G^c]|$) are the number of edges, the number of vertices of G, and the number of connected subgraphs respectively. This step is assumed to be done offline before the real-time operation of the sinks and the candidate subgraph list is provided to the *master* sink.

All weighted distances W_{S_k, v_i} are computed initially, which takes $O(n^3)$ for general graphs. The algorithm then iterates k times for each S in $S[G^c]$ and n times for each $v \in V$ of G. Hence, overall complexity of the algorithm is $O(kn)$. The efficiency of the algorithm mainly depends on k since $1 \leq k \leq C(n, p)$. In the best case, there exists only one connected subgraph with p vertices ($O(n^3)$) while in the worst-case the connectivity graph G^c is a complete graph ($k = C(n, p)$).

5.2.3   Simulation study for PcP and PmP

5.2.3.1   Simulation setup

To assess the performance of the proposed algorithm, we conducted simulations with the following settings. Initially, the attractions are generated at an empty terrain of a theme park with random event probabilities assigned as the weight values. The locations of the attractions are determined randomly and according to specified minimum and maximum Euclidean distances among attractions. The events are generated by a Poisson process. The event probabilities of all the attractions are updated according to the model described in this chapter which is based on the history of the events. We define a certain active time period for an event and once it expires, the event is assumed to end. The active times of the events are randomly generated.

The weights of the edges are initially randomly generated by using a lower bound and an upper bound. These weights are changed by a ratio at discrete update times. The speed of the mobile sinks are set to their maximum (i.e., the speed when the road is empty). While the sinks are considered as same type of vehicles with a fixed maximum speed, the speed of each sink dynamically changes during the simulation because of the slowdowns caused by movements of pedestrians on the roads.

Table 5.1: Simulation parameters for PcP and PmP

simulation time (T)	10 hours
terrain size	500 x 500 m
number of attractions (n)	15
min distance among attractions	50 m
max distance among attractions	250 m
node degree of G	4
sink update time t	30 min
sink transmission range	100 m
event probability change rate	0.01
expected number of events	100
min active time of events	200 sec
max active time of events	600 sec
edge weight change rate	0.20
max edge weight difference	400%
max mobile sink speed	1.00 m/sec

Although the mobile sinks with higher speeds handle events faster, they share the roads with the pedestrians. Therefore, their maximum speed is limited for safety of the pedestrians. The best sinks to handle events are always selected using the *shortest path* strategy. Table 5.1 summarizes the values of the parameters used in the simulation study.

5.2.3.2 Baselines and performance metrics

For positioning of the mobile sinks, four different strategies are compared. In addition to our approaches PcP and PmP, the *Weighted Positioning* (WP) and Random Positioning (RP) approaches are simulated with the scenarios in which communication constraint does (w/ CC) or does not (w/o CC) exist for the mobile sinks. In case of no communication constraint, we assume that a sink will be handling the event without any collaboration with others. This assumption relaxes the problem because the sinks are assumed to have global knowledge. Therefore, the strategies certainly produce better outcomes for w/o CC case. Knowing that forming a connected topology is necessary, we still carried out simulations for w/o CC case to observe how communication constraint affects placement and coverage performance of mobile sinks.

In WP approach, the sinks are placed at the attractions with higher event probabilities according to the vertex weight values $w(v_i)$ of graph G. Since the mobile sinks are connected, we again use $S[G^c]$ for the candidate sink positions. Among the candidates, the one which has the vertices with higher weights is chosen for sink placement. The sum of the weights

are computed for the vertices of a connected subgraph and the one with the highest sum is marked as the best candidate. In the random positioning (RP) approach, the locations for mobile sinks are selected randomly.

Throughout the simulations, we considered two performance metrics: 1) the *average event handling time* defined as the travel time for the selected mobile sink to reach an event and 2) the *success ratio*, the ratio of the times the sink reaches the event before the *active time* of the event expires.

5.2.3.3 Performance results

- **Sink positioning strategies**

We analyzed event handling times and success ratios of PcP, PmP, WP and RP under biased and random event distribution models. While the events occur at the attractions according to the event probabilities in the biased event distribution model, random model assumes them to be occurring anywhere evenly. Total of five sinks are placed in the theme park and the results of the experiments are extracted from 100 simulation runs for each setting.

The performance results for the event handling time using biased model are shown in Fig. 5.20-a. The results reveal that PcP and PmP are the winners while WP is slightly better than RP. This can be attributed to the fact that the events are generated based on weights and WP approach is the most suitable for such cases. Comparing our approaches, since we consider the average event handling time as opposed to maximum time as our metric,

PmP performs better than PcP. In particular, since the events are not evenly distributed, minimizing the total distance metric in PmP would lead to reduced average event handling times. The RP strategy is the worst in all cases since it does not take the weights of the attractions or the condition of the roads into account.

The simulations are also conducted for evaluating the performance of the approaches for the random event distribution case. The results shown in Fig. 5.20-b indicate that the best two approaches for random event distribution model are PcP and PmP. Compared to the biased case, we see that the gap between PcP and PmP is almost negligible. This is due to the fact that random events occur at any attraction independent from their weights and thus PmP's placement based on the weights does not apply here. PcP, on the other hand, places sinks in such a way that none of them stay very far away from any attractions. Due to even distribution of events at attractions, PcP and PmP perform similar. Another observation about the results is that the order of RP and WP changes. WP has slightly worse performance as opposed to RP due to its limitation for sink placement. In WP, mobile sinks always placed in attractions with higher weight values whereas in RP the sinks can be placed on any subgraph which brings flexibility. In addition, the performance gap between PcP/PmP and WP increases compared to the previous results (Fig. 5.20-a). This shows that our approaches are much suitable for events occurring by the random distribution.
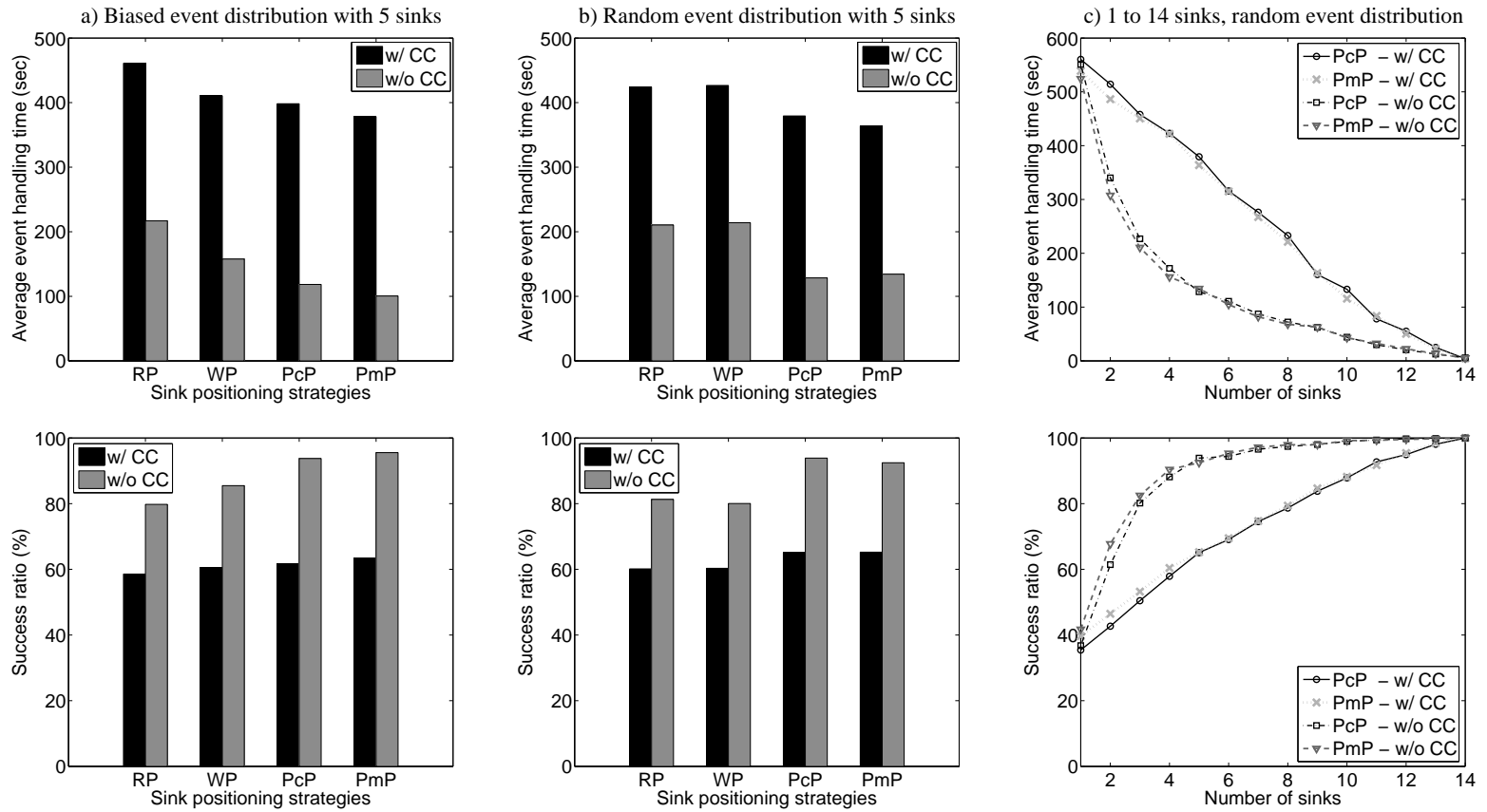
Figure 5.20: Average event handling times and success ratios for Random Positioning (RP), Weighted Positioning (WP), p-center positioning (PcP), and p-median positioning (PmP). Comparisons with a) biased event distribution b) random event distribution and c) various number of mobile sinks.

We observed that in all cases lack of communication constraint boosts the performance significantly and reduces the event handling times. This is due to the availability of more locations for the placement of sinks. Nonetheless, these experiments were performed for five sinks and with the increased number of sinks the gap could be diminished. We will perform separate experiments for such cases next.

Looking at the success ratio performance, we observe that the situation is more critical for random cases. In the biased case, the success ratios for our approaches are slightly better since in most cases the sinks were able to reach the incident locations before the active time expires (e.g., even in the middle of the event). However, for the random case, the moving time to incidents has big gaps and these gaps also affect the success ratio and causes WP and RP to miss the events.

- **Effects of the number of mobile sinks**

In the second set of experiments, we evaluated the effect of the number of mobile sinks on the event coverage performance of PcP and PmP. The experiments are conducted with mobile sinks ranging from 1 to 14. The random event distribution model is used to generate the events on top of the attractions.

As it can be observed in Fig. 5.20-c, the success ratio of PcP and PmP strategies are getting higher with the increasing number of mobile sinks. While the performance of PmP is slightly better than PcP for small numbers of sinks, the gap closes as the number of mobile sinks increases. With the increased number of sinks, both approaches can identify

sinks within the similar distances from the events and thus the event handling times do not change significantly for PcP and PmP. Again, under the unconstrained cases, PcP w/o CC and PmP w/o CC provide better results since they assume no need for a connected topology with the sinks. However, as the network becomes saturated with more sinks, the gap between the unconstrained and constrained cases is diminished. Overall, the results of the experiments suggest that either PcP or PmP can be used if a certain number of mobile sinks are already available.

5.3   Concluding Remarks

In this chapter, a WSN with mobile sinks model is proposed for event coverage in theme parks. A realistic human mobility model for theme parks (TP) is used to simulate the movement of theme park visitors. A dynamic directed graph model representing attractions, mobile sinks and dynamic events as the nodes and movement paths as the edges is proposed to model the environment. New strategies for sink positioning and event handling decision problems are introduced for the goal of event coverage. For mobile sink positioning, crowd density based probability estimation (CDPE) and hot-spot based probability estimation (HSPE) strategies are proposed. For event handling, we proposed fastest responder (FR) and closest sink (CS) strategies for both static and dynamic edge weights in the directed graph model. The success of the model and strategies are evaluated through extensive simulations of different scenarios using the TP mobility model and the SLAW model. Furthermore, it

is shown that using multiple mobile sinks has a significant advantage over using one mobile sink. We find that our model of WSN with multiple mobile sinks can be used for security and emergency applications in theme parks.

Considering the topology of connected mobile sinks, we applied a p-center approach to solve the problem on top of this model. We proposed a new variant, communication-constrained p-center problem, and an exact algorithm to solve it. Based on the algorithm, we positioned the mobile sinks and update their positions in the theme park using the proposed p-center positioning (PcP) and p-median positioning (PmP) approaches. The evaluation of the approaches w.r.t. two other baselines indicated that the event handling times of the mobile sinks reduce while success ratios significantly increase.

The techniques developed in this chapter can be adapted to many applications which require the management of security in scenarios where a large number of people are visiting waypoints in a specific geographic area. A related problem is the security in large transportation hubs such as airports and train stations.

CHAPTER 6
TRACKING PEDESTRIANS AND EMERGENT EVENTS IN DISASTER AREAS

In this chapter, we propose a novel system for tracking the evacuation of pedestrians from disaster areas [15, 16]. Let us start this chapter with a discussion about why we need such system and our approach on the problem of safe evacuation of pedestrians.

Internet has been used worldwide, offering various services which made daily lives of people easier in many ways. However, it is not a reliable communication source during disaster times as accessing the Internet services requires certain infrastructure, which may be damaged due to occurrence of hazards. While relying only on the Internet may cause people suffer in natural or man-made disasters, researchers nowadays focus on the networks that are resilient to disasters. These networks are supposed to provide and maintain acceptable levels of quality of service during disaster times, as well as accidents or faults in infrastructure in ordinary times.

As the increase in the likelihood of the more intense hazards is expected due to climate change [157], disaster resilience in networks is becoming an increasingly popular research area. Many studies nowadays focus on problems such as communication in cities which are damaged by disasters such as earthquakes or floods. These problems also apply to large areas in which the vehicle use is limited such as theme parks and campus environments.

162

Furthermore, the operators of these environments have challenges of evacuating pedestrians, rescuing wrecked people, and providing them access to ambulances or transportation services. We study the use of disaster resilient networks as a solution to communication and the safe evacuation problems in large and crowded disaster areas. Places which restrain people from using transportation vehicles such as airports, city parks (e.g., Central Park in New York city), shopping malls, fairs, and festival areas are considered in this context.

As a disaster response strategy, we propose using a networked system which includes mobile sensor nodes and a limited number of mobile sinks as described in Section 6.1. Mobile phones carried by pedestrians can be leveraged as sensor devices which communicate with each other and with mobile sinks. Mobile sinks monitor the evacuation process by patrolling in the disaster area, collecting data from the sensor nodes. They also have the goal of reaching to people who need rescue. Mobile sinks can be autonomous robots or security personnel which patrol by walk or by electronic transportation vehicles. Sensor nodes create messages when they witness people who need immediate help. They are responsible for storing and carrying the messages, sharing the messages with each other, and delivering to the mobile sinks via hop-by-hop wireless communication.

Sensor devices are carried by ordinary theme park visitors whose only goal at the time of a disaster would be safely escaping from the environment. While we do not assume any control over the visitors, we focus on the effective placement and mobility of mobile sinks in the area to gather more data from sensor nodes and find pedestrians in need of help in shorter amount of times. For efficient tracking of the pedestrians and emergent events

163

during the evacuation, we propose three approaches in Section 6.2, namely, *physical force based* (PF), *grid allocation based* (GA) and *road allocation based* (RA) approaches for mobile sink placement and mobility. PF is inspired by the natural gravitation, in a way that sensor nodes attract mobile sinks, while mobile sinks have negative impacts on each other. In GA, each sink allocates a number of grids as its own operation region. Grids are created on top of the roads in the processed theme park model. Lastly, in RA, each sink allocates one or multiple roads that are close to each other and operates on top of the allocated roads. After allocation of grids or roads, mobile sinks patrol in their allocated regions by a random movement model. The performances of the proposed approaches are evaluated in Section 6.3 with extensive opportunistic network and human mobility simulations and compared with two random mobility models for mobile sinks. We conclude the chapter in Section 6.4.

6.1 Network Model

We propose a network model with sensor nodes and mobile sinks for the purpose of efficient tracking of the pedestrians and the emergent events during the disasters. In the rest of this section, we define the roles of the sensor nodes, mobile sinks and the routing protocol respectively.

6.1.1 Sensor nodes

Sensor nodes represent mobile devices carried by theme park visitors. The sensing of an emergent event can be automatically done by the devices (e.g., by sensing sounds) or messages can be explicitly created by the users' input to their smartphones. Marking the location of a person in need of help is an example of an emergent event. Whenever an emergent event is sensed, a message including location and the sensing time is prepared and stored in buffer of the sensor node. The sensor node then carries data and sends the messages on its buffer to other sensor nodes or to a mobile sink by wireless communication. Sensor nodes are assumed to have limited capacities in terms of energy, storage, and transmission power.

6.1.2 Mobile sinks

Mobile sink nodes represent either mobile autonomous robots or security personnel carrying mobile devices. The mobile sinks patrol in the theme park and collect data from the sensor nodes. When they receive a message with a new unknown emergent event, they move to the region of the event. Mobile sink nodes are more powerful devices with enhanced computation and communication capabilities, storage and energy resources, while they exist in limited numbers.

6.1.3   Routing protocol

The message delivery to mobile sinks is done via hop-by-hop wireless transmissions. The epidemic routing protocol [158] is used with minor modifications regarding to the purpose of our model. Epidemic routing is a commonly used protocol for opportunistic social networks and it is mainly developed for mobile wireless networks considering missions such as disaster recovery or military deployment.

In epidemic routing, whenever a pair of nodes come up being in the transmission range of each other, they create a new session in which one of them acts as the initiator and the other acts as replier. The session consists of three phases. In the first phase, the initiator initiates a session by sending a summary vector of *Message IDs* located in its buffer. In the second phase, the replier compares its own vector and the received (initiator's) vector, then requests messages by sending the difference vector, which is the vector of *Message IDs* of message that do not exist in its buffer. In the third phase, initiator sends the messages missing in replier's buffer and finally closes the session.

Figure 6.1 illustrates two different sessions and the type of message transmissions during opportunistic communication between the two sensor nodes P_1, P_2 and the mobile sink *Sink A*. In this figure, the two sensor nodes are placed inside the transmission range of the mobile sink. However, at this time only one sensor node has an open session with the mobile sink. Concurrently, P_1 and P_2 has a session in which P_1 requests messages. Therefore, the sensor node P_2 acts as the initiator and P_2 acts as the replier. In the second session,

Sink A acts as the replier and P_1 acts as the initiator. In the epidemic routing protocol, there are three types of transmissions between the initiator and the replier, which we call *initiation*, *request*, and *messages* respectively. *Initiation* contains the summary vector of *Message IDs* which are located in the initiator's buffer. *Request* contains the difference vector and in the last transmission (*Messages*) initiator sends the messages which are requested by the replier.
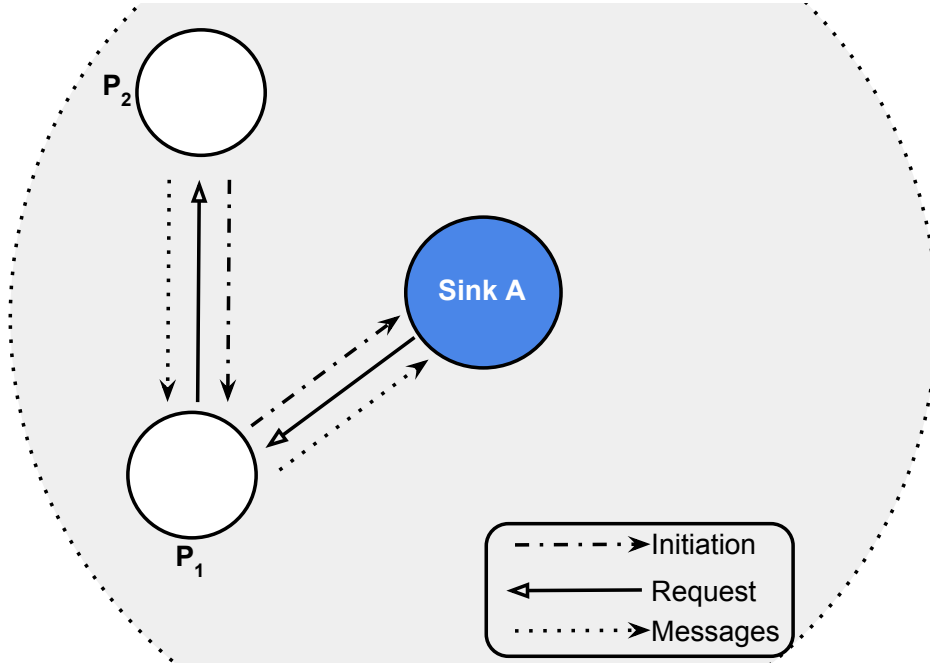
Figure 6.1: Opportunistic message transfers between *Sink A* and sensor nodes P_1 and P_2.

In our model, sensors act as either initiator or replier while mobile sinks always act as repliers, since their responsibility is to gather data from sensors. Moreover, after a pair of sensor nodes successfully finish a session, they wait for a specific time period before initiating a new session. This duration can be specified empirically and according to the density of the sensor nodes and their speeds at that time. For instance, if sensors stuck and wait in a

road for long time due to high crowd densities, the time period can be adjusted to prevent unnecessary communication overhead which leads to energy consumption.

6.2 Sink Placement and Mobility

6.2.1 Initial placement

Let us start this section by describing the initial placement process of the mobile sinks. The process starts with the creation of a grid layout on the theme park model. The grids are specified with relatively small sizes (e.g., 50x50m) in comparison to relatively larger disaster area (e.g., 1000x1000m). The small-sized grids are located only on top of the roads. In other words, obstacles and lands are excluded during the process of grid creation as we assume that the mobile sinks do not have the ability to patrol on top of the obstacles or lands. Grid creation process starts with the generation of 2D quasi-random points. Number of the generated points is equal to the number of mobile sinks. This generation is repeated iteratively and at each iteration, the sum of pairwise distances between the quasi-random points are computed. We keep the set of quasi-random points with the highest distance sum. Since this computation is handled offline before the start of the operation of mobile sinks, it does not cost an overhead to system. Therefore, the iteration can be repeated many times in order to have the best result.

The best set of quasi-random points are marked as the *base points*. For each grid, the closest base point is selected and the grid is marked with the index of this base point. Figure 6.2 illustrates creation of the grids on the roads, which are assigned to 10 base points. The creation of grids and the assignment is the base for initial mobile sink distribution. Mobile sinks are represented as the blue ring-shaped nodes.
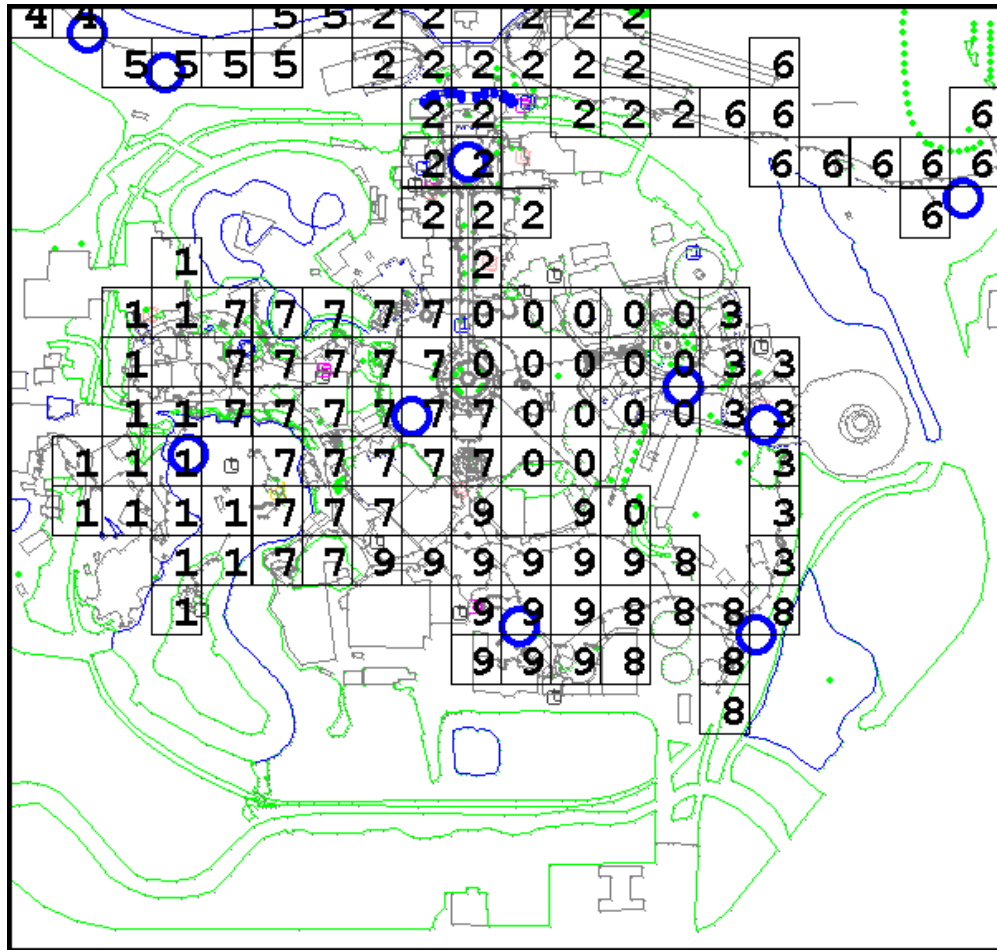
Figure 6.2: Grid allocation based placement of 10 mobile sinks.

As shown in the figure, each mobile sink is placed on a random point, which is one of the waypoints in the grids with corresponding index. The main purpose is to distribute

the sinks in a way that they share the workload of the entire disaster area while they are all located on top of the roads to start their patrolling duty.

The pseudocode for the initial placement of mobile sinks is given in Algorithm 5. First, the quasi-random points are iteratively generated (lines [4-20]). Later, grids are assigned to the base point indices, such that each grid is assigned to a base point index bp. At the end, each base point index bp has a set of grids $GridSet(bp)$ (lines [21-29]). After the assignment is finished, each mobile sink m_i is placed on top of a waypoint which is selected randomly among all waypoints contained by the particular grid set (lines [30-37]).

The initial placement procedure is conducted only once before the mobile sinks start their operation. The initial placement can be used as a common procedure for various mobile sink mobility models. On the other hand, the movement decisions of the mobile sinks during their operation varies according to choice of the mobility model.

Algorithm 5 Initial placement of mobile sinks

1: $B := \{\}$ ▷ Set of base points
2: $G := \{g_1, g_2, ..., g_T\}$ ▷ Set of grids
3: $M := \{m_1, m_2, .., m_K\}$ ▷ Set of sinks
4: $MinSum \leftarrow \infty$
5: **for** $i := 1$ to N **do**
6:     $Q := \{p_1, p_2, ..., p_M\}$ ▷ Set of points
7:     $Sum \leftarrow 0$
8:     **for** $j := 1$ to K **do**
9:         **for** $k := 1$ to K **do**
10:             **if** $j \neq k$ **then**
11:                 $D \leftarrow Distance(p_j, p_k)$
12:                 $Sum \leftarrow Sum + D$
13:             **end if**
14:         **end for**
15:     **end for**
16:     **if** $MinSum > Sum$ **then**
17:         $MinSum \leftarrow Sum$
18:         $B \leftarrow M$
19:     **end if**
20: **end for**
21: **for** $i := 1$ to T **do**
22:     $MinDist \leftarrow \infty$
23:     **for** $j := 1$ to K **do**
24:         **if** $D_{ij} < MinDist$ **then**
25:             $bp \leftarrow p_j$ ▷ Base point index
26:         **end if**
27:     **end for**
28:     $GridSet(bp) \leftarrow GridSet(bp) \cup \{g_i\}$
29: **end for**
30: $W \leftarrow \{\}$
31: **for** $i := 1$ to M **do**
32:     **for** each $g \in GridSet(p_i)$ **do**
33:         $W \leftarrow W \cup WaypointSet(g)$
34:     **end for**
35:     Select a random $w \in W$
36:     $InitPosition(m_i) \leftarrow w$
37: **end for**

6.2.2 Sink mobility

Let us now describe the mobility models for the mobile sinks.

6.2.2.1 Physical force based sink mobility (PF)

In PF, the main goal of the sink mobility is tracking people and following them along during the evacuation process. Inspired by Newton's law of universal gravitation, each pedestrian assumed to have a unit mass which attracts the mobile sinks, while distances cause less attractions. A mobile sink which detected a group of people tends to follow the group as long as it does not encounter with another larger group or other mobile sinks on the way.

In order to prevent each other to intercept, the mobile sinks also have masses which are larger than the unit mass and the mobile sink masses cause inverse forces in the opposite direction. The sink mass is equal to the division of the number of active pedestrians by the number of mobile sinks. Each mobile sink computes a physical force vector based on the positions of people and the other mobile sinks and moves along the direction of the physical force vector.

Figure 6.3 illustrates the movement direction of the $Sink$ A after encountering with pedestrians P_1 and P_2 with unit masses and $Sink$ B with a higher mass producing the strongest physical force among the three forces $\vec{F}_1, \vec{F}_2$ and $\vec{F}_B$. In this case, $Sink$ A moves in the direction of the vector $\vec{V}_A$, which is the sum of the three physical force vectors.

Having n pedestrians and m mobile sinks with masses 1 and M respectively, the physical force movement vector $\vec{V}_a$ on the $Sink\ A$ is calculated as follows:

$$\vec{V}_a = \alpha \cdot \left(\sum_{i=1}^{n} \vec{F}_i - \sum_{j=1}^{m} \vec{F'}_j \right) \quad s.t. \ \ j \neq a \tag{6.1}$$

where

$$\left| \vec{F}_i \right| = G \cdot \frac{M \cdot 1}{d^2}, \tag{6.2}$$

$$\left| \vec{F'}_j \right| = \lambda \cdot G \cdot \frac{M \cdot M}{d^2}. \tag{6.3}$$

λ is an empirical constant value, which defines the impact of the sink mass $M = \frac{n}{m}$ and the gravity constant G. α is the constant which adjusts the magnitude of the sum vector $\vec{V}_a$. The value of n changes during the operation according to the number of people in the environment at that time. Overall complexity of the computation for each mobile sink is $O(n+m)$. For simplicity, this computation can be done by the mobile sink only considering the pedestrians and the mobile sinks in its visible area by ignoring other masses which have longer distances (d) that cause negligible forces.
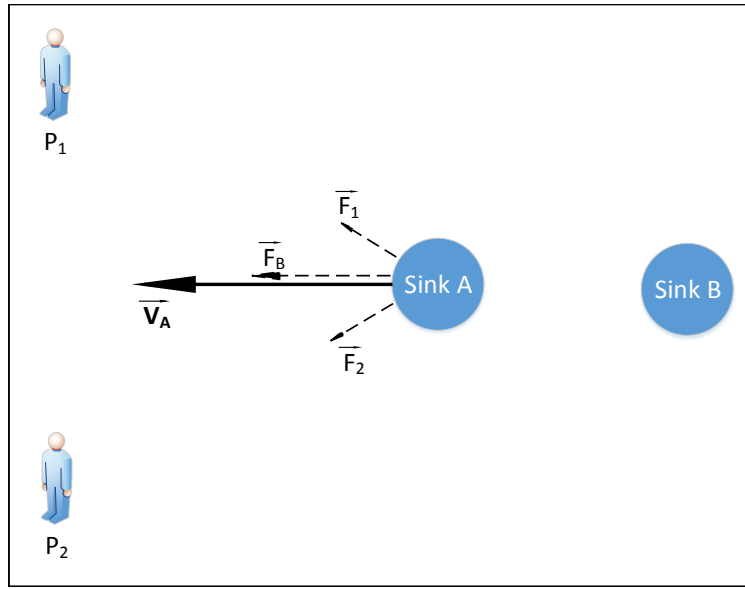
Figure 6.3: The physical forces and movement vector of $Sink\ A$ along with pedestrians P_1, P_2 and $Sink\ B$.

6.2.2.2 Grid allocation based sink mobility (GA)

In this approach, each mobile sink allocates a set of grids according to the grid indices which were found in the initial grid creation phase. Basically, the grids in Fig. 6.2 are used for allocation in a way that each sink is responsible for the grids with a particular number. For instance the grids which are marked as 1 are assigned to the first mobile sink, while the grids with mark 2 are assigned to the second sink, and so on. During the operation, each sink patrols in its allocated grids. The sink chooses a random waypoint as the next destination point among the waypoints which are place on top of the set of the allocated grids. After reaching to the next destination, the sink decides another next destination and updates in

the same fashion. This mobility model aims to divide the workload of the disaster area evenly on the patrolling mobile sinks, while they are not intercepting on each other's region.

Algorithm 6 includes the pseudocode for the sink mobility with GA. After the initial placement, the current positions are set as the initials (lines [2-4]). Throughout the operation of the mobile sinks, the movement decisions are made in discrete time intervals. Whenever the mobile sink reaches a next destination, it updates its next destination with a random waypoint selected in the waypoint set of the particular base point index $WaypointSet(p_i)$ (lines [5-16]). If the mobile sink has not reached its next destination, it continues its movement towards the next destination $NextDest(m_i)$ (lines [17-19]).

While this procedure handles the patrolling duty of the mobile sinks, the mobile sink will move towards an event in the case of emergency. In the time of an emergency event, $NextDest(m_i)$ of the mobile sink is set as the location of the event, which is received from the sensor nodes.

Algorithm 6 Sink mobility with GA

1: $M \leftarrow \{m_1, m_2, ..., m_M\}$ ▷ Set of mobile sinks

2: **for** $i := 1$ to M **do**

3:    $CurrPos(m_i) \leftarrow InitPosition(m_i)$

4: **end for**

5: **for** $t := 0$ to T **do**

6:    **for** $i := 1$ to M **do**

7:       **if** $NextDest(m_i) = CurrPos(m_i)$ **then**

8:          $N := SizeOf(GridSet(p_i))$

9:          **for** $j := 1$ to N **do**

10:            $W := \{\}$

11:            **for** each $g \in GridSet(p_i)$ **do**

12:               $W \leftarrow W \cup WaypointSet(g)$

13:            **end for**

14:            Select a random $w \in W$

15:            $NextDest(m_i) \leftarrow w$

16:          **end for**

17:       **else**

18:          Move towards $NextDest(m_i)$

19:       **end if**

20:    **end for**

21: **end for**

6.2.2.3 Road allocation based sink mobility (RA)

In the road allocation based sink mobility (RA) approach, each sink allocates one or multiple roads and patrols only these roads during its operation. The allocation is based on the grids and the waypoints in each road. Multiple grid indices may contain waypoints in the same road. In this case, the number of waypoints that corresponds to each grid index is calculated and compared. The best grid index with most number of waypoints marks the road with its index, which will be then used for allocation by the mobile sinks. The main purpose of using grids for road allocation is the goal of allocating the closer roads by the same sink instead of the sink having roads in different regions. Initial placement of RA is different than the previous two approaches, because after sinks finish allocating the roads, each sink chooses a random waypoint among the waypoints in its allocated roads. During the operation, mobile sinks iteratively decide their new destinations by randomly choosing random waypoints in their allocated roads whenever they reach a destination.

Figure 6.4 illustrates the allocation of the roads to the mobile sinks $m_1, m_2, ..., m_9$ in the Magic Kingdom park. Each road is assigned to a mobile sink while a mobile sink may or may not allocate multiple roads. The RA approach guarantees the mobile sinks to operate in separate regions from each other such that at any time of the operation, multiple mobile sinks cannot be patrolling on the same roads. RA can be seen as an alternative way of balancing the workload of the disaster area among the mobile sinks.
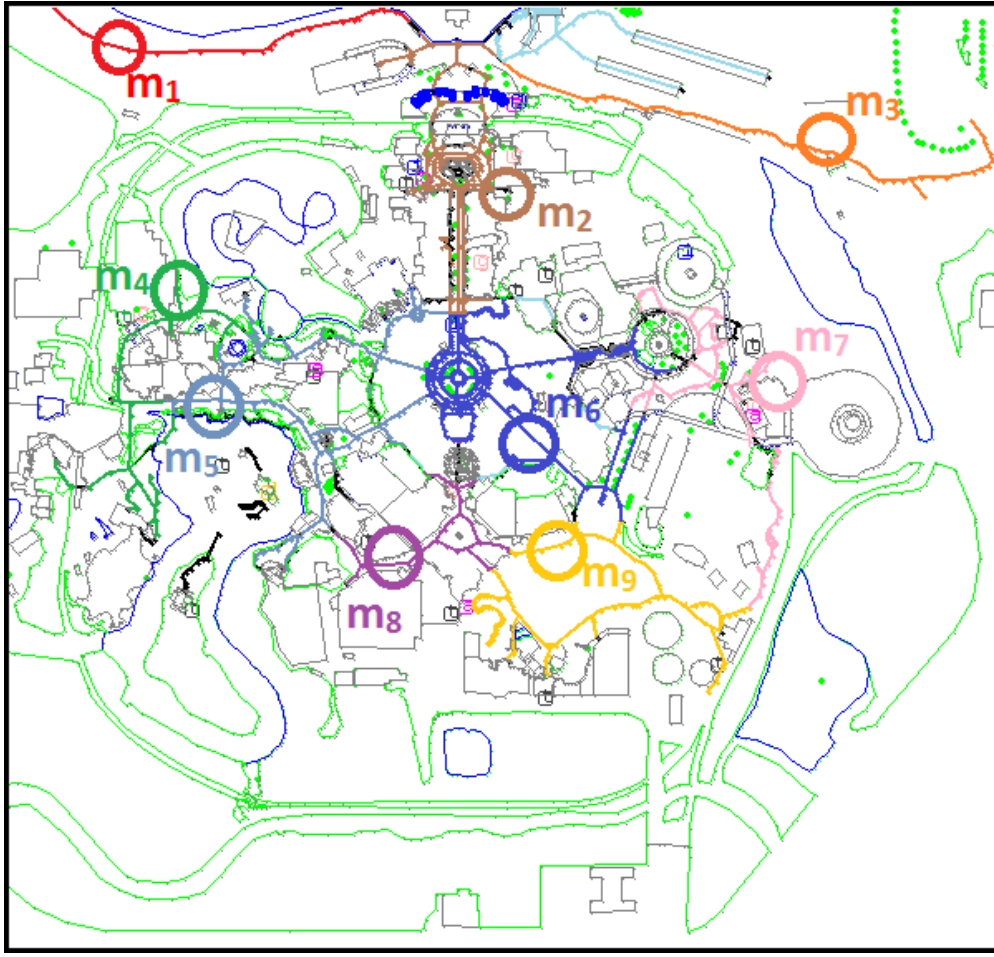
Figure 6.4: Road allocation to 9 mobile sinks $M := \{m_1, m_2, ..., m_9\}$.

Initial placement of RA is implemented by Algorithm 7. In this algorithm, each road is assigned to a base point index bp according to the number of waypoints included by the grids with particular base point indices. The corresponding road is assigned to a bp with most number of waypoints (lines [4-19]). Later, each mobile sink is placed on top of a waypoint. The waypoint is selected randomly among all waypoints of the set of roads of each base point index (line[20-27]).

While the initial placement of RA is different than the initial placement of GA, mobility decisions of RA during the operation follow a similar pattern with GA. The only difference between them is that with GA a mobile sink updates the next destination by selecting a random waypoint among all waypoints in the corresponding grid set. In RA, however, the random waypoint is selected among the waypoints in the road set. For some cases such as a case where most people stuck in a particular region, RA and GA may produce unbalanced workloads on the mobile sinks, as some of the mobile sinks do not encounter with many sensor nodes. PF, however, overcomes this extreme case as people's locations attract mobile sinks.

Algorithm 7 Initial placement of RA

1: $R \leftarrow \{r_1, r_2, ..., r_K\}$ ▷ Set of roads

2: $B \leftarrow \{b_1, b_2, ..., b_M\}$ ▷ Set of base points

3: $M \leftarrow \{m_1, m_2, ..., m_M\}$ ▷ Set of sinks

4: **for** $i := 0$ to K **do**

5:    $MaxSize \leftarrow 0$

6:    $bp \leftarrow null$ ▷ Selected base point index

7:    **for** $j := 0$ to M **do**

8:       $W := \{\}$

9:       **for** each $g \in GridSet(b_j)$ **do**

10:          $W \leftarrow W \cup WaypointSet(g)$

11:       **end for**

12:       $W \leftarrow W \cap WaypointSet(r_i)$

13:       **if** $W \neq \{\}$ and $SizeOf(W) >$ $MaxSize$ **then**

14:          $MaxSize \leftarrow SizeOf(W)$

15:          $bp = j$

16:       **end if**

17:    **end for**

18:    $RoadSet(bp) \leftarrow RoadSet(bp) \cup r_i$

19: **end for**

20: $W \leftarrow \{\}$

21: **for** $i := 1$ to M **do**

22:    **for** each $r \in RoadSet(b_i)$ **do**

23:       $W \leftarrow W \cup WaypointSet(r)$

24:    **end for**

25:    Select a random $w \in W$

26:    $InitPos(m_i) \leftarrow w$

27: **end for**

6.3   Simulation Study

6.3.1   Simulation environment

We analyze the proposed network model and the sink mobility models PF, GA, and RA through simulations of the opportunistic network with mobile sinks. The simulation experiments are conducted for the Magic Kingdom park. We include two sink mobility models for comparisons, which are called "random target location" (RTL) and "random waypoint distribution" (RWD) models. In RTL, each mobile sink chooses any random target location on the map, then sets the closest waypoint to the target location as the sink's next destination. In RWD, each mobile sink chooses a waypoint randomly among all waypoints and sets it as the next destination. RWD favors the popular roads because popular roads tend to include more waypoints than other roads.

Various metrics can be used for evaluating the effect of the mobility models and the network performance. These metrics can be classified into two types: *Link-based* and *network coverage* metrics. Link-based metrics include intercontact times, recontact rate, minimum hop counts, message delays, and number of transmissions. Network coverage metrics include number of detected sensors, rescue success ratio, and average distance to detected event. We include performance results related to intercontact times, recontact rate, number of detected sensors, number of transmissions and rescue success ratio.

We evaluate the success of the opportunistic network with 1-10 mobile sinks and transmission ranges of 10, 20, 50 and 100m. Evaluation of each setting is based on 50

simulation runs. Each simulation run generates at least about 2000 message transmissions among sensor nodes or from sensor nodes to mobile sinks, while the number of transmissions to mobile sinks varies by the sink mobility model and parameters such as the number of mobile sinks. All nodes in the network communicate with the epidemic routing protocol [158]. We assume that after two sensor nodes close a session, they wait for a cut off time empirically set as 1 min before opening a new session.

Table 6.1 includes the list of the simulation parameters. Parameters related to the human mobility and the social force model can be found in Table 6.2. Disasters tend to have effects on the random locations of the area during the simulation time. In this simulation study, instead of creating artificial disaster zones, we marked the pedestrians which are effected due to the effects of disasters.

Table 6.1: Simulation parameters

simulation time	2000 s
sampling time	2.0 s
disaster area size ($\approx$)	800x800 m
number of sensor nodes	200
sensing range	20 m
sensor message storage capacity	100
transmission probability	0.9
grid width/height	50 m
number of effected people	20
rescue failure time	600 s
sink relative mass constant(λ)	0.5
physical force impact factor α	20.0
sink max speed	1 m/s
pedestrian max speed	1 m/s
pedestrian visibility	50 m

Table 6.2: Human mobility parameters

number of pedestrians	1000
min speed	0.5m/s
max speed	2.5m/s
number of red-zones	20
red-zone active time	500s
red-zone radius	50m
random move distance	10m
visibility	50m
SFM - interaction strength (A)	0.11 ± 0.06
SFM - interaction range (B)	0.84 ± 0.63
SFM - relaxation time (τ)	0.5s
SFM - λ	0.1

6.3.2 Performance results

6.3.2.1 Intercontact times

Intercontact time is defined as the duration between two consecutive encounters of a mobile sink with a sensor node. Intercontact times metric is commonly used for evaluating the performance of mobile opportunistic social networks. We analyze intercontact times of PF, GA, RA, RTL and RWD with 5 mobile sinks placed in the disaster area and 25m transmission range.
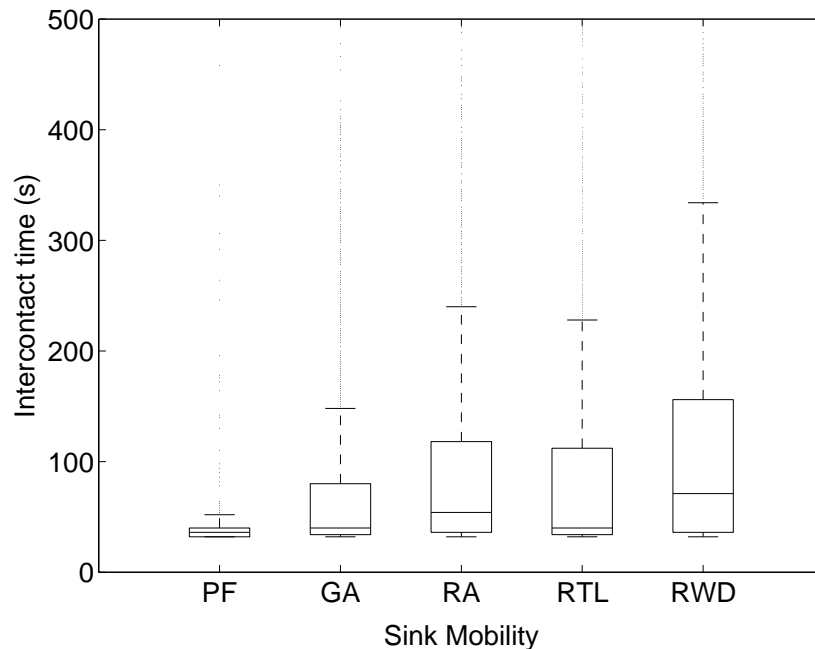
Figure 6.5: Intercontact times of PF, GA, RA, RTL and RWD with confidence bounds.

The performance results of intercontact times with confidence bounds are shown in Fig. 6.5. The results reveal that among the five mobility approaches, PF and GA are the

ones which produce shorter intercontact times while RWD produces the longest intercontact times meaning the worst performance. Longer intercontact times cause mobile sinks to delay communicating with a previously contacted sensor node. Moreover, the intercontact times of PF seem very consistent, so that it is easy for the mobile sinks to estimate the next contact time with a previously contacted sensor node. In particular, consistency in the intercontact times would allow us to find efficient methods for transmission scheduling.

A comparison of the intercontact times of the mobility approaches provided by various numbers of mobile sinks can be seen in Fig. 6.6. For PF, we observe that the number of mobile sinks does not have a significant impact on the intercontact times as the results stay in a constant level from 1 sink up to 10 sinks. Moreover, PF provides the best results for various numbers of mobile sinks. RWD and RTL also do not have very significant decays in the intercontact times with the increasing number of mobile sinks. On the other hand, the intercontact times of the GA and RA approaches become shorter as higher number of sinks operate. Considering the fact that in the case of more mobile sinks, each sink is assigned to a smaller number of grids or roads. Therefore, their chances of encountering the same sensor nodes increase.

We observe that for all transmission ranges (10m, 25m, 50m and 100m), PF, GA and RA provide shorter intercontact times compared to RTL and RWD. As expected, with longer transmission ranges, intercontact times decrease for GA, RA, RTL and RWD. Moreover, the effects of mobile sink positioning approaches are more significant for lower transmission ranges.
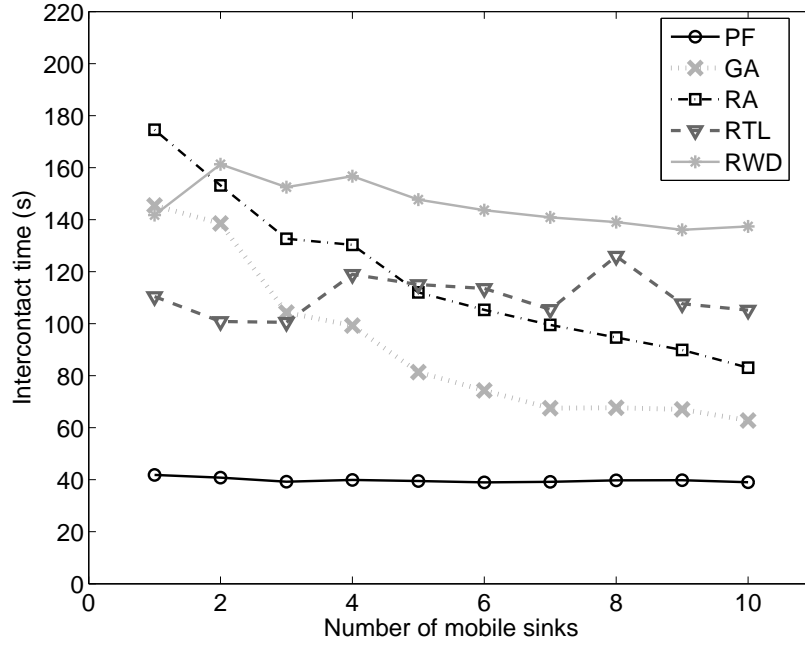
Figure 6.6: Intercontact times of PF, GA, RA, RTL and RWD with 1 to 10 mobile sinks.

6.3.2.2 Recontact rates

While intercontact times metric provides insight into the performance of the network, the intercontact times results do not involve the case which a mobile sink communicates with a sensor node only once during the entire simulation time. Therefore, we analyze the recontact count for each pair of mobile sink and sensor node, which is the number of contacts of the mobile sink and the sensor node after their first encounter. Recontact rate of a mobile sink is its averaged recontact count considering all the sensor nodes that communicated with the mobile sink.
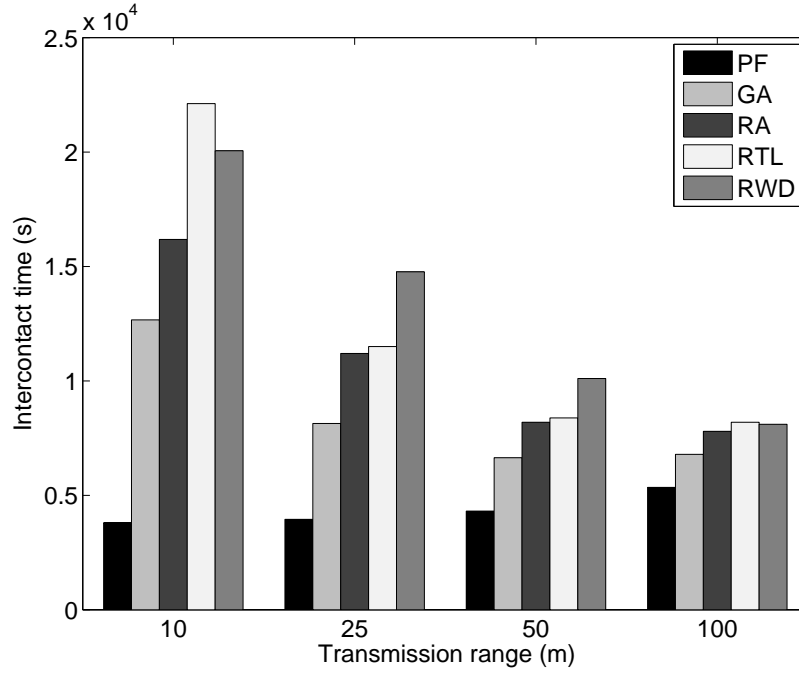
Figure 6.7: Intercontact times of PF, GA, RA, RTL and RWD for 10m, 25m, 50m and 100m transmission ranges.

Figure 6.8 shows the results of average recontact rates with settings ranging from 1 to 10 mobile sinks. The PF approach is the clear winner with an average rate of more than 5.0 due to sinks' behavior of following contacted sensor nodes and sticking with them as much as possible. The decrease in the rates for 3 sinks is caused by the masses of the mobile sinks which restrict them from staying close to each other. For the single mobile sink setting, we observe that recontact rates of GA, RA, RTL and RWD are very low without any significant difference between them. On the other hand, the rate difference becomes significant for multiple sinks. Among these four approaches, GA is the best one reaching the rate of more than 2.0, while RA reaches the rate of approximately 2.0. On the other hand,

the rates of RTL and RWD do not significantly increase with the addition of more mobile sink nodes in the network.
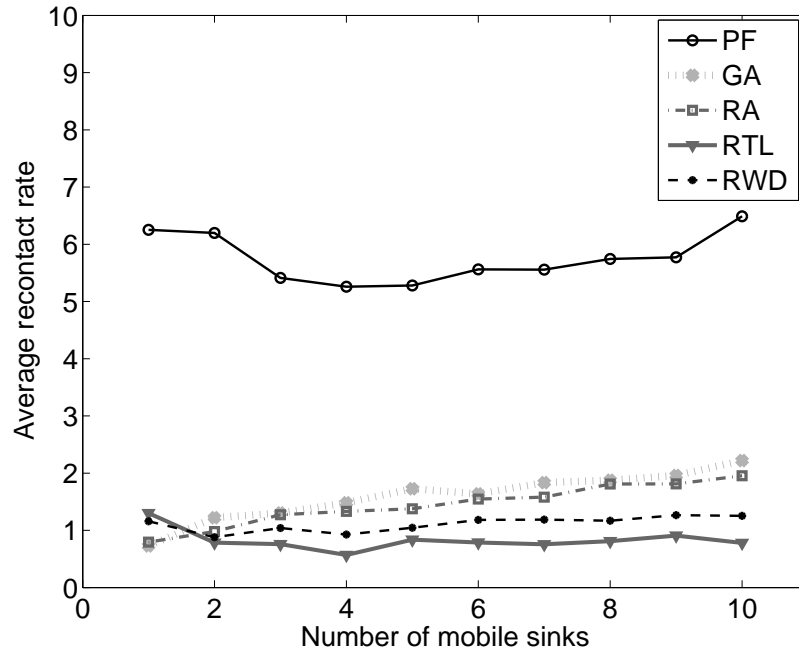
Figure 6.8: Recontact rates of PF, GA, RA, RTL and RWD with 1 to 10 sinks.

As it can be seen on Fig. 6.9, PF produces the best outcome in terms of the recontact rates for 10m, 25m, 50m and 100m transmission ranges. On the other hand, RTL has the worst performance, producing less than half of the recontact rates of PF for all transmission ranges. Moreover, longer transmission ranges provide higher recontact rates for all mobile sink positioning strategies.

Considering intercontact times and recontact rates for analyzing the tracking success of the mobile sinks, we observe that PF is the best strategy. Compared to RTL and RWD,

189

GA and RA are better tracking strategies since they produce shorter intercontact times and higher recontact rates.
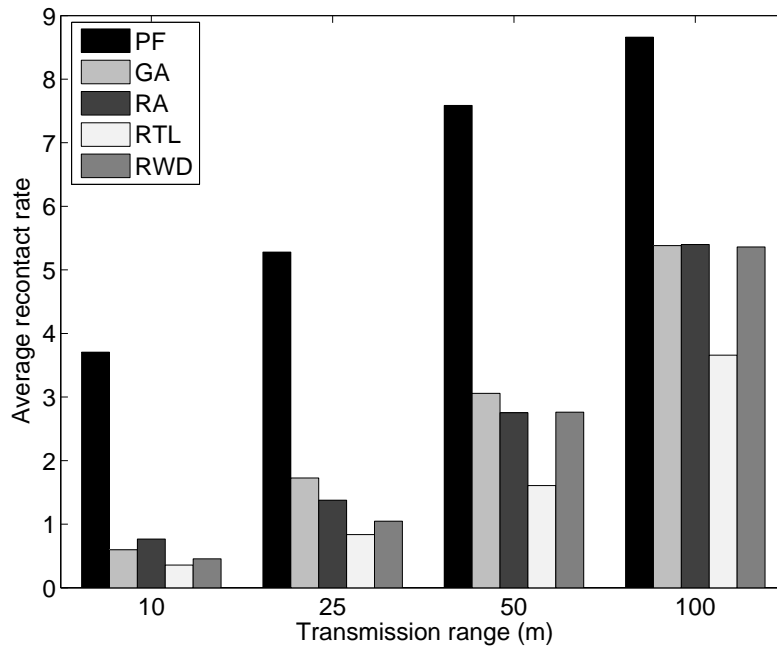
Figure 6.9: Recontact rates of PF, GA, RA, RTL and RWD for 10m, 25m, 50m and 100m transmission ranges.

6.3.2.3 Number of transmissions

The number of transmissions metric represents the wireless communication overhead which leads to the energy consumption of the sensor nodes and the mobile sink nodes. We consider the average number of wireless transmissions of all nodes in the network including the transmissions in successful or failed sessions.

Figure 6.10 shows the results of the approaches with 5 mobile sinks for transmission ranges of 10m, 25m, 50m and 100m. First of all, we observe that increase in transmission range dramatically increases the number of transmissions. This is an expected result and it is caused by the exponential increase in the number of neighbors of a sensor node. In the case of having limited energy resources, a more effective routing protocol may provide better energy preservation for sensor nodes with high transmission ranges. Secondly, the use of PF results more wireless transmissions while the difference is not very significant. This is an expected side effect of the PF strategy since mobile sinks are able to communicate with sensor nodes multiple times and in shorter time periods. Nonetheless, sinks are in limited number and the number of transmissions among sinks and sensor nodes is significantly fewer than the number of transmissions among sensor node pairs. Furthermore, sinks are assumed to have more resources in terms of energy and storage while sensor nodes which are neighbors of the sinks may consume more energy resources.

As an expected outcome of having more mobile sinks, the number of transmissions increase from 1 mobile sink to 10 mobile sinks as shown in Fig. 6.11. However, the increase is not dramatic. From 1 sink to 10 sinks, it is less than 20% for RA, about 15% for PF and less than 15% for the other three approaches. Considering the successful network coverage provided by having multiple mobile sinks, the increases in the number of transmissions are in acceptable amounts.
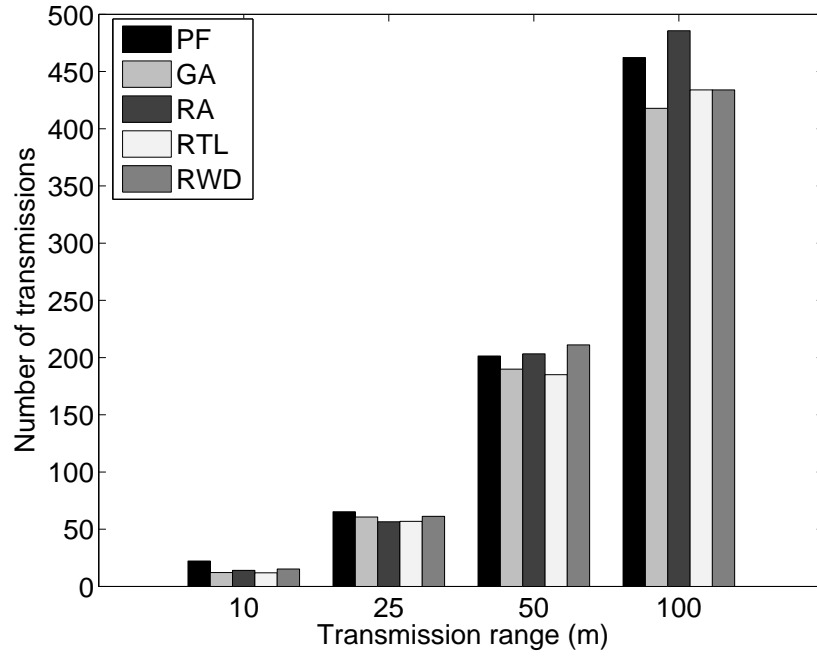
Figure 6.10: Average number of transmissions of PF, GA, RA, RTL and RWD for 10m, 25m, 50m and 100m transmission ranges.
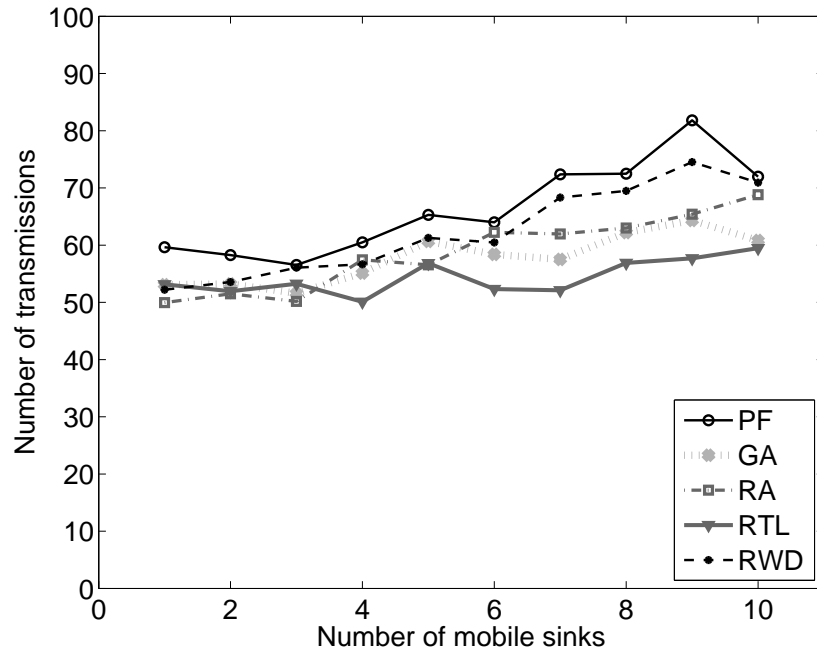
Figure 6.11: Average number of transmissions of PF, GA, RA, RTL and RWD with 1 to 10 mobile sinks.

6.3.2.4 Number of detected sensors

We use the total number of detected sensors metric in our analysis to have better insight into the network's coverage performance. We mean that a sensor is detected when there is a direct communication of the sensor with any mobile sink.

Figure 6.12 reveals the results of the approaches with 10m, 25m, 50m and 100m transmission range values with 5 mobile sinks. Among all the approaches, RA and PF are overall the best ones reaching up to more than 80% of the 200 sensor nodes. RWD also provides a reasonably good coverage of sensor nodes since the mobile sinks mostly choose the popular locations where sensor nodes are also most likely present. With higher transmission ranges, the coverage performance is better for all the approaches. Having 50m or 100m transmission ranges, RA provides the best network coverage such that most sensor nodes encounter with at least one mobile sink along their way.

Figure 6.13 shows the total number of detected sensors of the strategies from 1 to 10 mobile sinks. First, we observe that the number of detected sensors are higher for RA and PF compared to the other three approaches. RTL provides the worst performance, having less number of sensor nodes detected for all cases. Moreover, the increase in the number of mobile sinks brings an increase in the number of detected sensor nodes. In comparison to the single mobile sink setting, the number of detected sensors becomes more than 3 times higher for 10 mobile sinks. Hence, one can say that the network coverage is highly dependent on the number of mobile sinks.
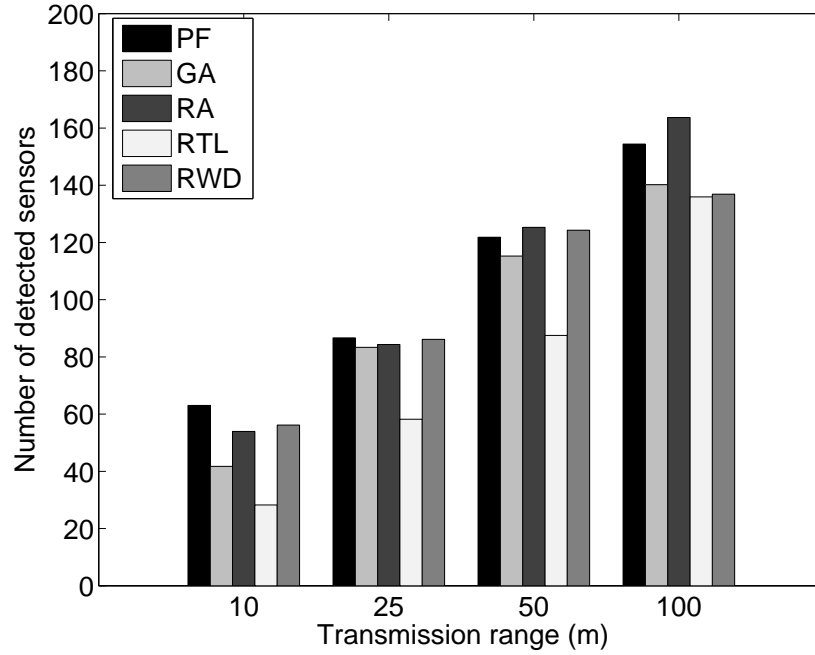
Figure 6.12: Number of detected sensors of PF, GA, RA, RTL and RWD for 10m, 25m, 50m and 100m transmission ranges.

6.3.2.5 Rescue success ratio

Considering the mobile sinks with capability of acting to the emergent events, they should be able to reach the areas where pedestrians in need of help exist. Moreover, the time it takes to reach an emergent event must be short. Thus, we consider the message delay and the travel time for the mobile sink after receiving a message to reach the effected area. According to sum of these two times, we analyze rescue success ratios. We assume a rescue time of 10 minutes, which includes the message delay and the travel time of the mobile sink.
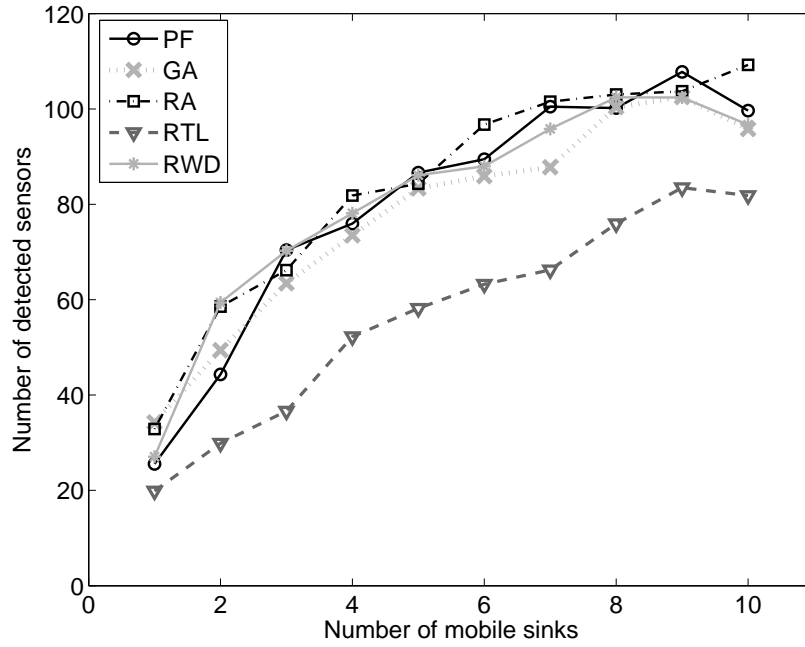
Figure 6.13: Number of detected sensor nodes of PF, GA, RA, RTL and RWD with 1 to 10 mobile sinks.

Figure 6.14 shows the success ratio results of the approaches with 25m transmission range. This figure also reveals the effect of having multiple mobile sinks to rescue success ratios. With 10 mobile sinks, PF reaches more than 70% of the emergent events in less than 10 minutes. For RTL, success ratio increases from 10% to 60% from 1 to 10 mobile sinks while for the other approaches it increases approximately from 30% to 70%.

Overall, the network simulations provide promising results in terms of metrics such as intercontact times, rescue success ratios, number of detected sensor nodes, and average recontact rates. The performance results show that the proposed network model and the approaches can be very useful as a disaster response strategy in environments with limited

196

vehicle use such as theme parks. As an interesting finding of the simulation study, we first observe that having multiple sinks clearly produces better network performance. Moreover, we observe that with the use of 200 sensor nodes, which corresponds to only 2% of the 10,000 pedestrians, the mobile sinks can achieve 70% rescue success. Furthermore, higher rescue success ratios can be achieved with vehicles having higher speeds. Finally, for PF, GA, and RA mobile sink mobility approaches, we find that fewer than or equal to 7 mobile sinks are enough to track most of the pedestrians during their evacuation.
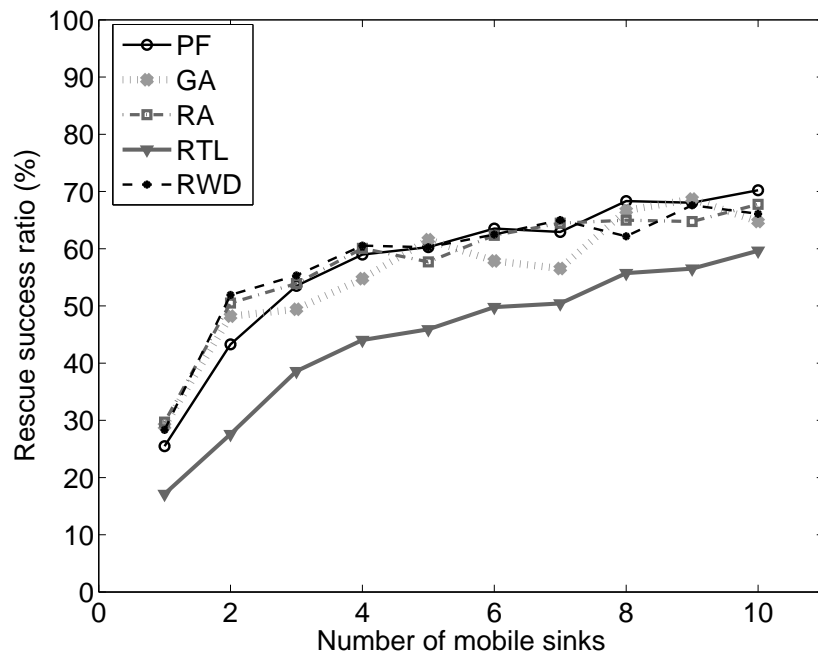
Figure 6.14: Rescue success rates of PF, GA, RA, RTL and RWD with 1 to 10 mobile sinks.

6.4 Concluding Remarks

In this chapter, we proposed an opportunistic network model which involves the use of smartphones and mobile sinks for tracking pedestrians during evacuation from disasters. We consider the use of multiple mobile sinks and propose three sink placement and mobility approaches, which we named *physical force based* (PF), *grid allocation based* (GA) and *road allocation based* (RA) movement strategies. The performances of the proposed network model and the approaches are evaluated in comparison to two random sink mobility models through extensive network and mobility simulations for the theme park scenario. We observed that our approaches produce better results in terms of the network coverage and the rescue success, while they do not bring extra communication overhead to the network. Moreover, it is shown that having multiple mobile sinks in the network has significant advantages over having single mobile sink.

We find that our network model with multiple mobile sinks can be useful as part of emergency evacuation planning in large and crowded areas with limited vehicle use.

CHAPTER 7
CONCLUSIONS AND FUTURE WORK

We introduced a new mobility model, which we named TP, for the movement of visitors in a theme park in Chapter 3. In this model, we combined the non-deterministic behavior of the human walking pattern with the deterministic behavior of attractions in a theme park. We divided the attractions into groups of main rides, medium-sized rides, live shows and restaurants. We used queueing-theoretic models to calculate times spent by visitors at different attractions. We validated the accuracy of our model through extensive simulations using theme park statistics, GPS traces collected in a real theme park and the data generated by simulations of other mobility models. The results show that our model provides a better match to the real-world data compared to SLAW and RWP.

In Chapter 4, we introduced the mobility model, TP-D, of the theme park visitors in disaster scenarios. We used real theme park maps to model the disaster environment. The mobility of the visitors are modeled using the theme park models and the social force model. Through the simulations, our model is evaluated in comparison with the results of TP, SLAW, RWP, and the GPS traces. Moreover, the effects of the unique parameters of the model such as visibility and expected number of red-zones are investigated.

In Chapter 5, a WSN with mobile sinks model is proposed for the event coverage problem in theme parks. A realistic human mobility model for theme parks (TP) is used to simulate the movement of theme park visitors. A dynamic directed graph model representing attractions, mobile sinks and dynamic events with the nodes and movement paths of visitors and sinks with the edges is used to model the environment. New strategies for sink positioning and event handling decision problems are introduced for the event coverage. For mobile sink positioning, crowd density based probability estimation (CDPE) and hot-spot based probability estimation (HSPE) strategies are proposed. For event handling, we introduced fastest responder (FR) and closest sink (CS) strategies for both static and dynamic edge weights in the directed graph model.

The success of the model and strategies are evaluated through extensive simulations of different scenarios using the TP mobility and the SLAW model. Furthermore, it is shown that using multiple mobile sinks has a significant advantage over using a single mobile sink. We found that our model of WSN with multiple mobile sinks can be used for security and emergency applications in theme parks.

The first WSN model proposed in Chapter 5 is extended by considering a connected topology of mobile sinks, which allows direct wireless communications throughout the operation of the network. We applied a *p*-center approach to solve the problem on top of this model. We proposed a new variant, *communication-constrained p-center problem*, and an exact solution algorithm. The positions of the mobile sinks are updated in the theme park using the proposed *p-center positioning* (PcP) and *p-median positioning* (PmP) approaches.

The evaluation of the approaches w.r.t. two other baselines indicated that performance of the mobile sinks in terms of the event handling times and success ratios can be significantly increased.

The second study in Chapter 5 can be extended in the future with addition of a polynomial time heuristic algorithm for the communication-constrained p-center problem. Moreover, simulation study for this model can cover more scenarios such as comparison of the successes of multiple sinks on all three event distributions.

In Chapter 6, we introduced the challenge of visitor tracking and evacuation in disaster areas. For the application scenario of theme parks, the safety of the visitors is a major concern for the operators due to the high volume of visitors and the large area with many physical obstacles. A model of opportunistic network as an infrastructure-independent networked system is considered for solving the problem of visitor tracking. The proposed mobility model for disaster scenarios is used for the simulation of movements of people during their evacuation and the performance evaluation of the network model. The performance of the proposed approach is analyzed with metrics such as evacuation times and the number of successfully monitored people.

As a future work, the proposed approaches can be applied and tested for the crowded environments similar to theme parks where the vehicle use is limited. Airports, shopping malls, state fairs are examples of such scenarios. Furthermore, we believe that the techniques introduced in this dissertation can be used for solving more sophisticated problems such as

modeling mobility of people in urban environments, evacuation planning of metropolitan areas, and event coverage in areas such as city squares with the existence of vehicles.

With the popular usage of smartphones, new approaches can be proposed for urban sensing and crowdsourcing applications in crowded environments such as university campuses or city squares. For the ordinary scenarios such as the daily presence and movement of people, mobile apps can be implemented as internet-based services. For the extreme scenarios such as disasters, there is a need for networked systems that operate autonomously and are resilient to disasters. There is a certain need for more understanding of the disaster scenarios and new approaches for this type of networked systems. Opportunistic communication may be a feasible way of operation for transmitting critical messages to smartphones and raising awareness.

Wireless networks with mobile elements such as electric vehicles can serve as alternative solutions to problems such as crowd management, security, or search an rescue missions. While we proposed new and unconventional systems as possible solutions, there are other problems such as privacy issues due to crowd density detection and monitoring. New approaches could be proposed for these problems.

LIST OF REFERENCES

[1] T. Camp, J. Boleng, and V. Davies, "A survey of mobility models for ad hoc network research," *Wireless Communications and Mobile Computing*, vol. 2, pp. 483–502, September 2002.

[2] I. Akyildiz, W. Su, Y. Sankarasubramaniam, and E. Cayirci, "A survey on sensor networks," *Communications Magazine, IEEE*, vol. 40, pp. 102–114, Aug 2002.

[3] L. Pelusi, A. Passarella, and M. Conti, "Opportunistic networking: data forwarding in disconnected mobile ad hoc networks," *Communications Magazine, IEEE*, vol. 44, no. 11, pp. 134–141, 2006.

[4] K. Lee, S. Hong, S. J. Kim, I. Rhee, and S. Chong, "SLAW: self-similar least-action human walk," *IEEE/ACM Transactions on Networking*, vol. 20, pp. 515–529, April 2012.

[5] V. Vukadinovic and S. Mangold, "Opportunistic wireless communication in theme parks: a study of visitors mobility," in *Proc. of the CHANTS '11*, pp. 3–8, September 2011.

[6] "Report on safety," tech. rep., Walt Disney Resorts and Parks, January 2008.

[7] G. Solmaz, M. Akbas, and D. Turgut, "Modeling visitor movement in theme parks," in *Proc. of the IEEE LCN'12*, pp. 36–45, October 2012.

[8] G. Solmaz, M. Akbas, and D. Turgut, "A mobility model of theme park visitors," *IEEE Transactions on Mobile Computing (TMC)*, vol. 14, December 2015.

[9] G. Solmaz and D. Turgut, "Theme park mobility in disaster scenarios," in *Proceedings of IEEE GC'13*, pp. 399–404, December 2013.

[10] G. Solmaz and D. Turgut, "Pedestrian mobility in theme park disasters," *Communications Magazine, IEEE*, vol. 53, pp. 172–177, July 2015.

[11] G. Solmaz and D. Turgut, "Modeling pedestrian mobility in disaster areas," *To be submitted to IEEE Transactions on Mobile Computing (TMC)*, October 2015.

[12] G. Solmaz and D. Turgut, "Event coverage in theme parks using wireless sensor networks with mobile sinks," in *Proc. of the IEEE ICC'13*, pp. 1522–1526, June 2013.

[13] G. Solmaz and D. Turgut, "Optimizing event coverage in theme parks," *Wireless Networks (WINET) Journal*, vol. 20, pp. 1445–1459, August 2014.

[14] G. Solmaz, K. Akkaya, and D. Turgut, "Communication-constrained p-center problem for event coverage in theme parks," in *Proc. of the IEEE GLOBECOM'14*, pp. 486–491, December 2014.

[15] G. Solmaz and D. Turgut, "Tracking evacuation of pedestrians during disasters," in *Accepted to appear in IEEE GLOBECOM'15*, December 2015.

[16] G. Solmaz and D. Turgut, "Tracking pedestrians and emergent events in disaster areas," *To be submitted to IEEE/ACM Transactions on Networking (ToN)*, October 2015.

[17] G. Solmaz and D. Turgut, "A survey of human mobility models," *To be submitted to Ad Hoc Networks Journal*, October 2015.

[18] D. Brockmann, L. Hufnagel, and T. Geisel, "The scaling laws of human travel," *Nature*, vol. 439, no. 7075, pp. 462–465, 2006.

[19] M. F. Shlesinger, G. M. Zaslavsky, and U. Frisch, "Lévy flights and related topics in physics," in *Levy flights and related topics in Physics*, vol. 450, 1995.

[20] G. M. Viswanathan, V. Afanasyev, S. Buldyrev, E. Murphy, P. Prince, H. E. Stanley, *et al.*, "Lévy flight search patterns of wandering albatrosses," *Nature*, vol. 381, no. 6581, pp. 413–415, 1996.

[21] M. C. González, C. A. Hidalgo, and A.-L. Barabási, "Understanding individual human mobility patterns," *Nature*, vol. 453, pp. 779–782, June 2008.

[22] C. Song, Z. Qu, N. Blumm, and A.-L. Barabási, "Limits of predictability in human mobility," *Science*, vol. 327, pp. 1018–1021, February 2010.

[23] F. P. Tso, J. Teng, W. Jia, and D. Xuan, "Mobility: A double-edged sword for HSPA networks: A large-scale test on hong kong mobile HSPA networks," *IEEE Transactions on Parallel and Distributed Systems*, vol. 23, pp. 1895–1907, October 2012.

[24] S. Wang, Y. Cui, S. Das, W. Li, and J. Wu, "Mobility in IPv6: Whether and how to hierarchize the network?," *IEEE Transactions on Parallel and Distributed Systems*, vol. 22, pp. 1722–1729, October 2011.

[25] H. Nishiyama, T. Ngo, N. Ansari, and N. Kato, "On minimizing the impact of mobility on topology control in mobile ad hoc networks," *IEEE Transactions on Wireless Communications*, vol. 11, pp. 1158–1166, March 2012.

[26] M. I. Akbas, M. R. Brust, and D. Turgut, "SOFROP: Self-organizing and fair routing protocol for wireless networks with mobile sensors and stationary actors," *Computer Communications*, vol. 34, pp. 2135–2146, December 2011.

[27] D. Turgut, B. Turgut, and L. Bölöni, "Stealthy dissemination in intruder tracking sensor networks," in *Proc. of the IEEE LCN'09*, pp. 22–29, October 2009.

[28] D. Turgut and L. Bölöni, "A pragmatic value-of-information approach for intruder tracking sensor networks," in *Proc. of the IEEE ICC'12*, pp. 4931–4936, June 2012.

[29] D. Turgut and L. Bölöni, "IVE: Improving the value of information in energy-constrained intruder tracking sensor networks," in *Proc. of the IEEE ICC'13*, pp. 6360–6364, June 2013.

[30] M. Akbas, R. Avula, M. Bassiouni, and D. Turgut, "Social network generation and friend ranking based on mobile phone data," in *Proc. of the IEEE ICC'13*, pp. 1444–1448, June 2013.

[31] E. Bulut and B. Szymanski, "Exploiting friendship relations for efficient routing in mobile social networks," *IEEE Transactions on Parallel and Distributed Systems*, vol. 23, pp. 2254–2265, December 2012.

[32] S. Kopman, M. Akbas, and D. Turgut, "Epidemicsim: Epidemic simulation system with realistic mobility," in *Proc. of the IEEE P2MNet'12*, pp. 663–669, October 2012.

[33] T. Bhatia, G. Solmaz, D. Turgut, and L. Bölöni, "Two algorithms for the movements of robotic bodyguard teams," in *Proc. of Workshop on Knowledge, Skill, and Behavior Transfer in Autonomous Robots*, pp. 2–8, January 2015.

[34] A. Chaintreau, P. Hui, J. Crowcroft, C. Diot, R. Gass, and J. Scott, "Impact of human mobility on opportunistic forwarding algorithms," *IEEE Transactions on Mobile Computing*, vol. 6, pp. 606–620, June 2007.

[35] S. S. Bacanlı, G. Solmaz, and D. Turgut, "Opportunistic message broadcasting in campus environments," in *Accepted to appear in IEEE GLOBECOM'15*, December 2015.

[36] I. Rhee, M. Shin, S. Hong, K. Lee, S. J. Kim, and S. Chong, "On the Lévy-walk nature of human mobility," *IEEE/ACM Transactions on Networking*, vol. 19, pp. 630–643, June 2011.

[37] S. Wanhill, "Theme parks: Their development and operation," in *Proc. of the CAUTHE'06*, pp. 1889–1921, February 2006.

[38] A. Munjal, T. Camp, and W. C. Navidi, "SMOOTH: a simple way to model human mobility," in *Proceedings of the 14th ACM international conference on Modeling, analysis and simulation of wireless and mobile systems*, pp. 351–360, ACM, 2011.

[39] A. Munjal, T. Camp, and W. C. Navidi, "SMOOTH: a simple way to model human walks," *ACM SIGMOBILE Mobile Computing and Communications Review*, vol. 14, pp. 34–36, November 2010.

[40] J. Yoon, M. Liu, and B. Noble, "Random waypoint considered harmful," in *INFOCOM 2003. twenty-second annual joint conference of the IEEE computer and communications. IEEE societies*, vol. 2, pp. 1312–1321, IEEE, 2003.

[41] M. Schwamborn and N. Aschenbruck, "Introducing geographic restrictions to the slaw human mobility model," in *Proc. of the IEEE MASCOTS'13*, pp. 264–272, Aug 2013.

[42] N. Aschenbruck and M. Schwamborn, "Synthetic map-based mobility traces for the performance evaluation in opportunistic networks," in *Proceedings of the Second International Workshop on Mobile Opportunistic Networking*, pp. 143–146, 2010.

[43] D. Helbing and A. Johansson, "Pedestrian, crowd and evacuation dynamics," *Encyclopedia of Complexity and Systems Science*, vol. 16, no. 4, pp. 6476–6495, 2010.

[44] X. Liu, C. Williamson, and J. Rokne, "Physics-based modeling of skier mobility and avalanche rescue in mountainous terrain," in *Proc. of the IEEE LCN'10*, pp. 645–652, October 2010.

[45] W. Hsu, K. Merchant, H. Shu, C. Hsu, and A. Helmy, "Weighted waypoint mobility model and its impact on ad hoc networks," *ACM SIGMOBILE Mobile Computing and Communications Review*, vol. 9, pp. 59–63, January 2005.

[46] J. Kim, V. Sridhara, and S. Bohacek, "Realistic mobility simulation of urban mesh networks," *Ad Hoc Networks*, vol. 7, pp. 411–430, March 2009.

[47] V. Vukadinovic, F. Dreier, and S. Mangold, "Impact of human mobility on wireless ad hoc networking in entertainment parks," *Ad Hoc Networks*, vol. 12, no. 0, pp. 17 – 34, 2014.

[48] A. Munjal, T. Camp, and N. Aschenbruck, "Changing trends in modeling mobility: a simple way to model human walks," *Journal of Electrical and Computer Engineering*, vol. 2012, pp. 1–16, October 2012.

[49] L. Guo, R. A. Beyah, and Y. Li, "SMITE: A stochastic compressive data collection protocol for mobile wireless sensor networks.," in *Proc. of the IEEE INFOCOM'11*, pp. 1611–1619, April 2011.

[50] R. Pazzi, D. Zhang, A. Boukerche, and L. Mokdad, "E-TRAIL: energy-efficient trail-based data dissemination protocol for wireless sensor networks with mobile sinks," in *Proc. of the IEEE ICC'11*, pp. 1–5, June 2011.

[51] X. Cheng, D.-Z. Du, L. Wang, and B. Xu, "Relay sensor placement in wireless sensor networks," *Wireless Networks*, vol. 14, pp. 347–355, June 2008.

[52] K. Xu, H. Hassanein, G. Takahara, and Q. Wang, "Relay node deployment strategies in heterogeneous wireless sensor networks," *IEEE Transactions on Mobile Computing*, vol. 9, pp. 145 –159, February 2010.

[53] F. M. Al-Turjman, H. S. Hassanein, W. M. Alsalih, and M. Ibnkahla, "Optimized relay placement for wireless sensor networks federation in environmental applications," *Wireless Communications and Mobile Computing*, vol. 11, pp. 1677–1688, December 2011.

[54] R. Sugihara and R. K. Gupta, "Path planning of data mules in sensor networks," *ACM Transactions on Sensor Networks*, vol. 8, pp. 1–27, August 2011.

[55] N. Dimokas, D. Katsaros, L. Tassiulas, and Y. Manolopoulos, "High performance, low complexity cooperative caching for wireless sensor networks," *Wireless Networks*, vol. 17, pp. 717–737, April 2011.

[56] G. Resta and P. Santi, "The fundamental limits of broadcasting in dense wireless mobile networks," *Wireless Networks*, vol. 18, pp. 679–695, August 2012.

[57] S. Basagni, A. Carosi, E. Melachrinoudis, C. Petrioli, and Z. M. Wang, "Controlled sink mobility for prolonging wireless sensor networks lifetime," *Wireless Networks*, vol. 14, no. 6, pp. 831–858, 2008.

[58] S. Basagni, A. Carosi, C. Petrioli, and C. A. Phillips, "Moving multiple sinks through wireless sensor networks for lifetime maximization," in *MASS*, pp. 523–526, Sep.-Oct. 2008.

[59] S. Basagni, A. Carosi, and C. Petrioli, "Heuristics for lifetime maximization in wireless sensor networks with multiple mobile sinks," in *Proc. of the IEEE ICC'09*, pp. 1–6, June 2009.

[60] S. Basagni, A. Carosi, C. Petrioli, and C. A. Phillips, "Coordinated and controlled mobility of multiple sinks for maximizing the lifetime of wireless sensor networks," *Wireless Networks*, vol. 17, pp. 759–778, April 2011.

[61] S. Basagni, M. Nati, C. Petrioli, and R. Petroccia, "ROME: Routing over mobile elements in WSNs," in *Proc. of the IEEE GLOBECOM'2009*, pp. 1 –7, December 2009.

[62] D. Vergados, A. Sgora, D. Vergados, and P. Chatzimisios, "Joint per-flow scheduling and routing in wireless multihop networks," in *Proc. of the ISCC'11*, pp. 213 –217, July 2011.

[63] B. K. Haberman and J. W. Sheppard, "Overlapping particle swarms for energy-efficient routing in sensor networks," *Wireless Networks*, vol. 18, pp. 351–363, May 2012.

[64] J. A. Sanchez, R. Marin-Perez, and P. M. Ruiz, "Beacon-less geographic multicast routing in a real-world wireless sensor network testbed," *Wireless Networks*, vol. 18, pp. 565–578, July 2012.

[65] G. Kadas and P. Chatzimisios, "Collaborative efforts for safety and security in vehicular communication networks," in *Proc. of the PCI'11*, pp. 117 –121, October 2011.

[66] M. Di Francesco, S. K. Das, and G. Anastasi, "Data collection in wireless sensor networks with mobile elements: A survey," *ACM Transactions on Sensor Networks*, vol. 8, pp. 1–31, August 2011.

[67] C. Zhu, L. Shu, T. Hara, L. Wang, S. Nishio, and L. T. Yang, "A survey on communication and data management issues in mobile sensor networks," *Wireless Communications and Mobile Computing*, pp. n/a–n/a, November 2011.

[68] G. Anastasi, E. Borgia, M. Conti, and E. Gregori, "A hybrid adaptive protocol for reliable data delivery in WSNs with multiple mobile sinks," *The Computer Journal*, vol. 54, pp. 213–229, February 2011.

[69] D. Turgut and L. Bölöni, "Three heuristics for transmission scheduling in sensor networks with multiple mobile sinks," in *Proc. of the AAMAS'08 Workshop on Agent Technology for Sensor Networks*, pp. 1–8, May 2008.

[70] D. Turgut and L. Bölöni, "Heuristic approaches for transmission scheduling in sensor networks with multiple mobile sinks," *The Computer Journal*, vol. 54, pp. 332–344, March 2011.

[71] L. Bölöni and D. Turgut, "Should I send now or send later? A decision-theoretic approach to transmission scheduling in sensor networks with mobile sinks," *Wireless Communications and Mobile Computing Journal on Mobility Management and Wireless Access*, vol. 8, pp. 385–403, March 2008.

[72] J. Luo, J. Panchard, M. Pirkowski, M. Grossglauser, and J. pierre Hubaux, "MobiRoute: routing towards a mobile sink for improving lifetime in sensor networks," in *Proc. of the IEEE/ACM DCOSS'06*, pp. 480–497, June 2006.

[73] S. A. Awwad, C. K. Ng, N. K. Noordin, and M. F. Rasid, "Cluster based routing protocol for mobile nodes in wireless sensor network," *Wireless Personal Communications*, vol. 61, pp. 251–281, November 2011.

[74] H. Kanai, Y. Koizumi, H. Ohsaki, and M. Imase, "Gradient-based routing in delay tolerant mobile sensor networks incorporating node mobility," in *Proc. of the CCNC'12*, pp. 235 –239, January 2012.

[75] J.-H. P. W. G. P. Zappi, E. Bales and T. Rosing, "The CitiSense air quality monitoring mobile sensor node," in *Proc. of the IPSN'12 Workshop on Mobile Sensing*, pp. 1–5, April 2012.

[76] M. Akbas, M. Brust, and D. Turgut, "SOFROP: self-organizing and fair routing protocol for wireless networks with mobile sensors and stationary actors," *Computer Communications*, vol. 34, pp. 2135–2146, December 2011.

[77] R. Luo and O. Chen, "Mobile sensor node deployment and asynchronous power management for wireless sensor networks," *IEEE Transactions on Industrial Electronics*, vol. 59, pp. 2377 –2385, May 2012.

[78] M. Akbas, G. Solmaz, and D. Turgut, "Actor positioning based on molecular geometry in aerial sensor networks," in *Proceedings of IEEE ICC'12*, pp. 508–512, June 2012.

[79] M. Akbas, G. Solmaz, and D. Turgut, "Molecular geometry inspired positioning for aerial networks," *Moderate revision for Computer Networks Journal*, August 2015.

[80] J. Xu, G. Solmaz, R. Rahmatizadeh, D. Turgut, and L. Bölöni, "Animal monitoring with unmanned aerial vehicle-aided wireless sensor networks," in *Accepted to appear in IEEE LCN'15*, October 2015.

[81] Z. Sun, I. Akyildiz, and G. Hancke, "Dynamic connectivity in wireless underground sensor networks," *IEEE Transactions on Wireless Communications*, vol. 10, pp. 4334 –4344, December 2011.

[82] M. Erol-Kantarci, S. Oktug, L. Vieira, and M. Gerla, "Performance evaluation of distributed localization techniques for mobile underwater acoustic sensor networks," *Ad Hoc Networks*, vol. 9, pp. 61–72, January 2011.

[83] M. Younis and K. Akkaya, "Strategies and techniques for node placement in wireless sensor networks: a survey," *Ad Hoc Networks*, vol. 6, pp. 621–655, June 2008.

[84] Z. Vincze, K. Fodor, R. Vida, and A. Vidács, "Electrostatic modelling of multiple mobile sinks in wireless sensor networks," in *Proc. of the IFIP Networking Workshop on Performance Control in Wireless Sensor Networks*, pp. 30–37, May 2006.

[85] Y.-C. Wang, F.-J. Wu, and Y.-C. Tseng, "Mobility management algorithms and applications for mobile sensor networks," *Wireless Communications and Mobile Computing*, vol. 12, pp. 7–21, January 2012.

[86] T. Melodia, D. Pompili, and I. F. Akyldiz, "Handling mobility in wireless sensor and actor networks," *IEEE Transactions on Mobile Computing*, vol. 9, pp. 160–173, February 2010.

[87] Z. Vincze, D. Vass, R. Vida, A. Vidács, and A. Telcs, "Adaptive sink mobility in event-driven multi-hop wireless sensor networks," in *Proc. of the InterSense'06*, May 2006.

[88] G. Wang, T. Wang, W. Jia, M. Guo, and J. Li, "Adaptive location updates for mobile sinks in wireless sensor networks," *The Journal of Supercomputing*, vol. 47, pp. 127–145, February 2009.

[89] A. W. Khan, A. H. Abdullah, M. H. Anisi, and J. I. Bangash, "A comprehensive study of data collection schemes using mobile sinks in wireless sensor networks," *Sensors*, vol. 14, no. 2, pp. 2510–2548, 2014.

[90] X. Wang, X. Lin, Q. Wang, and W. Luan, "Mobility increases the connectivity of wireless networks," *IEEE/ACM Transactions on Networking (TON)*, vol. 21, no. 2, pp. 440–454, 2013.

[91] Y. Bi, J. Niu, L. Sun, W. Huangfu, and Y. Sun, "Moving schemes for mobile sinks in wireless sensor networks," in *Performance, Computing, and Communications Conference, 2007. IPCCC 2007. IEEE Internationa*, pp. 101–108, April 2007.

[92] R. Rahmatizadeh, S. Khan, A. Jayasumana, D. Turgut, and L. Bölöni, "Routing towards a mobile sink using virtual coordinates in a wireless sensor network," in *Proc. of the IEEE ICC'14*, pp. 12–17, June 2014.

[93] J. Luo and J.-P. Hubaux, "Joint sink mobility and routing to maximize the lifetime of wireless sensor networks: the case of constrained mobility," *IEEE/ACM Transactions on Networking (TON)*, vol. 18, no. 3, pp. 871–884, 2010.

[94] W. Wang, V. Srinivasan, and K.-C. Chua, "Extending the lifetime of wireless sensor networks through mobile relays," *IEEE/ACM Transactions on Networking (TON)*, vol. 16, pp. 1108–1120, Oct. 2008.

[95] C.-M. Angelopoulos, S. Nikoletseas, D. Patroumpa, and J. Rolim, "Coverage-adaptive random walks for fast sensory data collection," in *Proc. of the ADHOC-NOW'10*, pp. 81–94, August 2010.

[96] T. Hara, "Quantifying impact of mobility on data availability in mobile ad hoc networks," *IEEE Transactions on Mobile Computing*, vol. 9, pp. 241–258, February 2010.

[97] G. Carofiglio, C. Chiasserini, M. Garetto, and E. Leonardi, "Route stability in manets under the random direction mobility model," *IEEE Transactions on Mobile Computing*, vol. 8, pp. 1167–1179, September 2009.

[98] R. La, "Distributional convergence of intermeeting times under the generalized hybrid random walk mobility model," *IEEE Transactions on Mobile Computing*, vol. 9, pp. 1201–1211, September 2010.

[99] O. Kariv and S. L. Hakimi, "An algorithmic approach to network location problems. i: The p-centers," *SIAM Journal on Applied Mathematics*, vol. 37, no. 3, pp. 513–538, 1979.

[100] O. Kariv and S. L. Hakimi, "An algorithmic approach to network location problems. i: The p-medians," *SIAM Journal on Applied Mathematics*, vol. 37, no. 3, pp. 539–560, 1979.

[101] M. G. Resende and R. F. Werneck, "A hybrid heuristic for the p-median problem," *Journal of Heuristics*, vol. 10, no. 1, pp. 59–88, 2004.

[102] F. Aykut Özsoy and M. Ç. Pınar, "An exact algorithm for the capacitated vertex p-center problem," *Computers & Operations Research*, vol. 33, pp. 1420–1436, December 2006.

[103] J. Reese, "Solution methods for the p-median problem: An annotated bibliography," *Networks*, vol. 48, pp. 125–142, October 2006.

[104] W. C.-K. Yen, "The connected p-center problem on block graphs with forbidden vertices," *Theoretical Computer Science*, vol. 426, pp. 13–24, April 2012.

[105] W. C.-K. Yen and C.-T. Chen, "The connected p-center problem with extension," in *Proc. of the JCIS'06*, October 2006.

[106] W. C.-K. Yen and C.-T. Chen, "The *p*-center problem with connectivity constraint.," *Applied Mathematical Sciences*, vol. 1, no. 27, pp. 1311–1324, 2007.

[107] D. Zhou and J. Gao, "Maintaining approximate minimum steiner tree and k-center for mobile agents in a sensor network," in *Proc. of the IEEE INFOCOM'10*, pp. 511–515, March 2010.

[108] K. Akkaya and M. F. Younis, "COLA: A coverage and latency aware actor placement for wireless sensor and actor networks," in *VTC Fall*, pp. 1–5, February 2006.

[109] N. Shiwakoti, M. Sarvi, G. Rose, and M. Burd, "Enhancing the safety of pedestrians during emergency egress," *Transportation Research Record: Journal of the Transportation Research Board*, vol. 2137, no. 1, pp. 31–37, 2009.

[110] I. G. Georgoudas, G. C. Sirakoulis, and I. T. Andreadis, "An anticipative crowd management system preventing clogging in exits during pedestrian evacuation processes," *Systems Journal, IEEE*, vol. 5, no. 1, pp. 129–141, 2011.

[111] C. Papageorgiou, K. Birkos, T. Dagiuklas, and S. Kotsopoulos, "Modeling human mobility in obstacle-constrained ad hoc networks," *Ad Hoc Networks*, vol. 10, pp. 421 – 434, May 2012.

[112] C. Papageorgiou, K. Birkos, T. Dagiuklas, and S. Kotsopoulos, "An obstacle-aware human mobility model for ad hoc networks," in *Proc. of the IEEE MASCOTS '09*, pp. 1–9, Sept 2009.

[113] N. Aschenbruck, E. Gerhards-Padilla, M. Gerharz, M. Frank, and P. Martini, "Modelling mobility in disaster area scenarios," in *Proc. of the ACM MSWiM'07*, pp. 4–12, October 2007.

[114] N. Aschenbruck, E. Gerhards-Padilla, and P. Martini, "Modeling mobility in disaster area scenarios," *Performance Evaluation*, vol. 66, no. 12, pp. 773–790, 2009.

[115] N. Aschenbruck, M. Frank, P. Martini, and J. Tolle, "Human mobility in manet disaster area simulation - a realistic approach," in *Local Computer Networks, 2004. 29th Annual IEEE International Conference on*, pp. 668–675, Nov 2004.

[116] T. Yamada, "A network flow approach to a city emergency evacuation planning," *International Journal of Systems Science*, vol. 27, pp. 931–936, May 1996.

[117] N. Zou, S.-T. Yeh, G.-L. Chang, A. Marquess, and M. Zezeski, "Simulation-based emergency evacuation system for Ocean City, Maryland, during hurricanes," *Transportation Research Record: Journal of the Transportation Research Board*, vol. 1922, no. 1, pp. 138–148, 2005.

[118] Y. S. Park, E. Manli, M. Hope, V. Sokolov, and H. Ley, "Fuzzy rule-based approach for evacuation trip demand modeling," in *Transportation Research Board 89th Annual Meeting*, no. 10-2635, 2010.

[119] X. Chen and F. B. Zhan, "Agent-based modelling and simulation of urban evacuation: relative effectiveness of simultaneous and staged evacuation strategies," *Journal of the Operational Research Society*, vol. 59, pp. 25 – 33, 2008.

[120] A. Kirchner and A. Schadschneider, "Simulation of evacuation processes using a bionics-inspired cellular automaton model for pedestrian dynamics," *Physica A: Statistical Mechanics and its Applications*, vol. 312, no. 12, pp. 260 – 276, 2002.

[121] E. Kwon and S. Pitt, "Evaluation of emergency evacuation strategies for downtown event traffic using a dynamic network model," *Transportation Research Record: Journal of the Transportation Research Board*, vol. 1922, pp. 149–155, 2005.

[122] A. Fujihara and H. Miwa, "Real-time disaster evacuation guidance using opportunistic communications," in *Proc. of the IEEE/IPSJ SAINT'12*, pp. 326–331, July 2012.

[123] A. T. El-Sergany and S. Alam, "Trip distribution model for flood disaster evacuation operation," *ITE Journal*, vol. 82, pp. 42–47, October 2012.

[124] Y. Iizuka, K. Yoshida, and K. Iizuka, "An effective disaster evacuation assist system utilized by an ad-hoc network," in *HCI International 2011 Posters Extended Abstracts*, vol. 174 of *Communications in Computer and Information Science*, pp. 31–35, 2011.

[125] N. Kamiyama, N. Katoh, and A. Takizawa, "An efficient algorithm for the evacuation problem in a certain class of a network with uniform path-lengths (algorithmic aspects in information and management)," *Lecture notes in computer science*, vol. 4508, pp. 178–190, 2008.

[126] Ó. Helgason, S. T. Kouyoumdjieva, and G. Karlsson, "Opportunistic communication and human mobility," *Mobile Computing, IEEE Transactions on*, vol. 13, no. 7, pp. 1597–1610, 2014.

[127] J. Qing-Shan and G. Ying, "Event-based evacuation in outdoor environment," in *Proc. of the CCDC'12*, pp. 33–38, 2012.

[128] A. Clementi, F. Pasquale, and R. Silvestri, "Opportunistic MANETs: mobility can make up for low transmission power," *IEEE/ACM Transactions on Networking (TON)*, vol. 21, no. 2, pp. 610–620, 2013.

[129] E. Rozner, M. K. Han, L. Qiu, and Y. Zhang, "Model-driven optimization of opportunistic routing," *Networking, IEEE/ACM Transactions on*, vol. 21, no. 2, pp. 594–609, 2013.

[130] S. Winter, K.-F. Richter, M. Shi, and H.-S. Gan, "Get me out of here: collaborative evacuation based on local knowledge," in *Proc. of the IWCTS'11*, pp. 35–42, November 2011.

[131] M. Uddin, D. Nicol, T. Abdelzaher, and R. Kravets, "A post-disaster mobility model for delay tolerant networking," in *Proc. of the WSC'09*, pp. 2785 –2796, December 2009.

[132] M. Uddin, H. Ahmadi, T. Abdelzaher, and R. Kravets, "Intercontact routing for energy constrained disaster response networks," *Mobile Computing, IEEE Transactions on*, vol. 12, pp. 1986–1998, Oct 2013.

[133] W. Gao, G. Cao, A. Iyengar, and M. Srivatsa, "Cooperative caching for efficient data access in disruption tolerant networks," *Mobile Computing, IEEE Transactions on*, vol. 13, no. 3, pp. 611–625, 2014.

[134] E. Ayday and F. Fekri, "An iterative algorithm for trust management and adversary detection for delay-tolerant networks," *Mobile Computing, IEEE Transactions on*, vol. 11, no. 9, pp. 1514–1531, 2012.

[135] O. V. Drugan, T. Plagemann, and E. Munthe-Kaas, "Detecting communities in sparse manets," *IEEE/ACM Transactions on Networking (TON)*, vol. 19, no. 5, pp. 1434–1447, 2011.

[136] N. Palmer, R. Kemp, T. Kielmann, and H. Bal, "Raven: Using smartphones for collaborative disaster data collection," *Proceedings of ISCRAM*, 2012.

[137] T. Fujiwara, H. Makie, and T. Watanabe, "A framework for data collection system with sensor networks in disaster circumstances," in *Wireless Ad-Hoc Networks, 2004 International Workshop on*, pp. 94–98, IEEE, 2004.

[138] G. Tuna, V. C. Gungor, and K. Gulez, "An autonomous wireless sensor network deployment system using mobile robots for human existence detection in case of disasters," *Ad Hoc Networks*, vol. 13, pp. 54–68, 2014.

[139] J. Patrix, A.-I. Mouaddib, and S. Gatepaille, "Detection of primitive collective behaviours in a crowd panic simulation based on multi-agent approach.," *International Journal of Swarm Intelligence Research*, vol. 3, pp. 50–65, June 2012.

[140] S. C. Nelson, A. F. Harris, III, and R. Kravets, "Event-driven, role-based mobility in disaster recovery networks," in *Proc. of the ACM CHANTS'07*, pp. 27–34, September 2007.

[141] A.-L. B. James P. Bagrow, Dashun Wang, "Collective response of human populations to large-scale emergencies," *PLoS ONE*, vol. 6, March 2011.

[142] O. Patterson, F. Weil, and K. Patel, "The role of community in disaster response: Conceptual models," *Population Research and Policy Review*, vol. 29, pp. 127–141, April 2010.

[143] J. Kirchhoff, J. Bauer, R. Ernst, C. Fuchs, S. Jopen, and N. Aschenbruck, "Extending odmrp for on-site deployments in disaster area scenarios," in *Proc. of the IEEE IPCCC'13*, pp. 1–10, December 2013.

[144] J. Broch, D. A. Maltz, D. B. Johnson, Y.-C. Hu, and J. Jetcheva, "A performance comparison of multi-hop wireless ad hoc network routing protocols," in *Proc. of the MobiCom'98*, pp. 85–97, October 1998.

[145] R. Groenevelt, E. Altman, and P. Nain, "Relaying in mobile ad hoc networks: The brownian motion mobility model," *Wireless Networks*, vol. 12, pp. 561–571, September 2006.

[146] I. Rhee, K. Lee, S. Hong, S. J. Kim, and S. Chong, "Demystifying the levy-walk nature of human walks," tech. rep., CSC, NCSU, 2008.

[147] M. Ester, H. P. Kriegel, J. Sander, and X. Xu, "A density-based algorithm for discovering clusters in large spatial databases with noise," in *Proc. of the ACM SIGKDD'96*, pp. 226–231, August 1996.

[148] M. Haklay and P. Weber, "OpenStreetMap: User-generated street maps.," *Pervasive Computing*, vol. 7, pp. 12–18, December 2008.

[149] I. Rhee, M. Shin, S. Hong, K. Lee, S. Kim, and S. Chong, "CRAW-DAD data set ncsu/mobilitymodels (v. 2009-07-23)." Downloaded from http://crawdad.org/ncsu/mobilitymodels/, July 2009.

[150] M. Kim, D. Kotz, and S. Kim, "Extracting a mobility model from real user traces.," in *Proc. of the IEEE INFOCOM'06*, vol. 6, pp. 1–13, 2006.

[151] I. Rhee, M. Shin, S. Hong, K. Lee, and S. Chong, "On the levy-walk nature of human mobility," in *Proc. of the IEEE INFOCOM'08*, pp. 1597–1605, April 2008.

[152] "Theme index: Global attractions attendance report," tech. rep., Themed Entertainment Association (TEA), 2013.

[153] M. K. Van Aalst, "The impacts of climate change on the risk of natural disasters," *Disasters*, vol. 30, no. 1, pp. 5–18, 2006.

[154] A. Boukerche, B. Turgut, N. Aydin, M. Ahmad, L. Bölöni, and D. Turgut, "Routing protocols in ad hoc networks: a survey," *Computer Networks (Elsevier)*, vol. 55, pp. 3032–3080, September 2011.

[155] "SEGWAY." http://www.segway.com.

[156] D. Avis and K. Fukuda, "Reverse search for enumeration," *Discrete Applied Mathematics*, vol. 65, no. 13, pp. 21 – 46, 1996.

[157] S. Hallegatte, "Trends in hazards and the role of climate change," in *Natural Disasters and Climate Change*, pp. 77–97, 2014.

[158] A. Vahdat and D. Becker, "Epidemic routing for partially connected ad hoc networks," tech. rep., Technical Report CS-200006, Duke University, 2000.